Modulation of auxin transport via ZF proteins adjust plant response to high ambient temperature

by

Christina Artner

August, 2022

A thesis submitted to the

Graduate School of the Institute of Science and Technology Austria

in partial fulfillment of the requirements

for the degree of

Doctor of Philosophy

Committee in charge:

Beatriz Vicoso, Chair

Eva Benkova

Jiri Friml

Jürgen Kleine-Vehn

The dissertation of Christina Artner, titled Modulation of auxin transport via ZF proteins adjust plant response to high ambient temperature, is approved by:

Supervisor: Prof Eva Benková, ISTA, Klosterneuburg, Austria

Signature: _____

Committee Member: Prof. Jiří Friml, ISTA, Klosterneuburg, Austria

Signature: _____

Committee Member: Prof. Jürgen Kleine-Vehn, Albert-Ludwigs-Universität Freiburg, Germany

Signature: _____

Exam Chair: Prof. Beatriz Vicoso, ISTA, Klosterneuburg, Austria

Signature: _____

signed page is on file

ISTA Thesis, ISSN: 2663-337X, ISBN: 978-3-99078-022-0

I hereby declare that this dissertation is my own work and that it does not contain other people's work without this being so stated; this thesis does not contain my previous work without this being stated, and the bibliography contains all the literature that I used in writing the dissertation.

I declare that this is a true copy of my thesis, including any final revisions, as approved by my thesis committee, and that this thesis has not been submitted for a higher degree to any other university or institution.

I certify that any republication of materials presented in this thesis has been approved by the relevant publishers and co-author

Signature _____

Christina Artner

August, 2022

signed page is on file

Abstract

As the overall global mean surface temperature is increasing due to climate change, plant adaptation to those stressful conditions is of utmost importance for their survival. Plants are sessile organisms, thus to compensate for their lack of mobility, they evolved a variety of mechanisms enabling them to flexibly adjust their physiological, growth and developmental processes to fluctuating temperatures and to survive in harsh environments. While these unique adaptation abilities provide an important evolutionary advantage, overall modulation of plant growth and developmental program due to non-optimal temperature negatively affects biomass production, crop productivity or sensitivity to pathogens. Thus, understanding molecular processes underlying plant adaptation to increased temperature can provide important resources for breeding strategies to ensure sufficient agricultural food production.

An increase in ambient temperature by a few degrees leads to profound changes in organ growth including enhanced hypocotyl elongation, expansion of petioles, hyponastic growth of leaves and cotyledons, collectively named thermomorphogenesis (Casal & Balasubramanian, 2019). Auxin, one of the best-studied growth hormones, plays an essential role in this process by direct activation of transcriptional and non-transcriptional processes resulting in elongation growth (Majda & Robert, 2018).To modulate hypocotyl growth in response to high ambient temperature (hAT), auxin needs to be redistributed accordingly. PINs, auxin efflux transporters, are key components of the polar auxin transport (PAT) machinery, which controls the amount and direction of auxin translocated in the plant tissues and organs(Adamowski & Friml, 2015). Hence, PIN-mediated transport is tightly linked with thermo-morphogenesis, and interference with PAT through either chemical or genetic means dramatically affecting the adaptive responses to hAT. Intriguingly, despite the key role of PIN mediated transport in growth response to hAT, whether and how *PINs* at the level of expression adapt to fluctuation in temperature is scarcely understood.

With genetic, molecular and advanced bio-imaging approaches, we demonstrate the role of PIN auxin transporters in the regulation of hypocotyl growth in response to hAT. We show that via adjustment of *PIN3*, *PIN4* and *PIN7* expression in cotyledons and hypocotyls, auxin distribution is

modulated thereby determining elongation pattern of epidermal cells at hAT. Furthermore, we identified three Zinc-Finger (ZF) transcription factors as novel molecular components of the thermo-regulatory network, which through negative regulation of *PIN* transcription adjust the transport of auxin at hAT. Our results suggest that the ZF-PIN module might be a part of the negative feedback loop attenuating the activity of the thermo-sensing pathway to restrain exaggerated growth and developmental responses to hAT.

Acknowledgements

First I would like to thank my supervisor, Eva Benkova for giving me the chance to work on my project and the freedom to develop it in unexpected directions throughout my PhD. I greatly appreciate her motivating and supporting attitude and the attention she gives to create a cohesive and friendly environment in the group. In addition I want to thank my committee member, Jiri Friml for his honest and constructive feedback and discussion.

I would like to acknowledge ISTA and all the people from the Scientific Service Units and at ISTA, in particular Dorota Jaworska for excellent technical and scientific support as well as ÖAW for funding my research for over 3 years (DOC ÖAW Fellowship PR1022OEAW02).

Additionally I thank all my colleagues from Benkova and Friml lab which accompanied and guided me through my years at ISTA. Special thanks goes to Karolina and Tereza for technical and scientific assistance as well as critical discussions.

Last but not least I would like to thank my family for their mental and emotional support and the time they spend on listening to my scientific as well as non-scientific anecdotes. Last I want to thank Markus for encouraging me to follow my ambitions and reminding me that, despite of science, there are other important things in life still waiting to be explored.

About the Author

Christina Artner completed her BSc in Food and Biotechnology and MSc in Biotechnology at the University of Natural Resources and Life Sciences, Vienna. She joined IST in September 2016 and affiliated with Eva Benkova's Lab in summer 2017. During her PhD, she investigate the question how plants modify their auxin transport system to ensure appropriate cell and tissue growth during high ambient temperature response. In particular, she focused on the role of ZF proteins, upstream regulators of auxin transport proteins, and their role in modulating auxin distribution and subsequent cell elongation in thermomorphogenic responses.

Table of Content

Abbreviations

ARF6	AUXIN RESPONSE FACTOR 6
Asp	aspartic acid
BRs	Brassinosteroids
BZR1	BRASSINAZOLE RESISTANT 1
CAA1	CIRCADIAN CLOCK ASSOCIATED 1
CRY1	CRYPTOCHROME1
D6PK	D6 PROTEIN KINASE
EAR motif	Ethylene-responsive element binding-factor-associated amphiphilic repression motif
EC	Evening Complex
ELF3	EARLY FLOWERING 3
EXP	EXPANSIN
GA	Gibberellin
Glu	glutamate
hAT	high ambient temperature
IAA19	*INDOLE ACETIC ACID INDUCIBLE 19*
LUX	LUX ARRHYTHMO
NAA	naphthalene-1-acetic acid
NPA	Naphthylphthalamic acid
oAT	optimal ambient temperature
PAT	polar auxin transport
phyB	phytochrome B

PIFs	PHYTOCHROME INTERACTING FACTORs
PINs	PIN-FORMED proteins
SAURs	SMALL AUXIN UP RNAs
SHB1	SHORT HYPOCOTYL UNDER BLUE LIGHT 1
TAA1	TRYPTOPHAN AMINOTRANSFERASE OF ARABIDOPSIS1
TIR1/AFB	TRANSPORT INHIBITOR RESPONSE 1/AUXIN-RELATED F-BOX
TOC1	TIMING OF CAB EXPRESSION 1
TOT3	MITOGEN-ACTIVATED PROTEIN KINASE KINASE KINASE KINASE4 (MAP4K4)/TARGET OF TEMPERATURE3
Trp	Tryptophan
UV-B	ultraviolet-B light photoreceptor
UVR8	UV RESISTANT LOCUS 8
XTR7	XYLOGLUCAN ENDOTRANSGLYCOSYLASE-RELATED PROTEIN 7
YUC	YUCCA
ZFP	Zinc Finger proteins
ZTL	ZEITLUPE

Part 1: *Arabidopsis* response to hAT

Introduction

Plants are exposed to different unfavorable conditions throughout their lifetime, which limits their development and growth. These stressful conditions can be classified into biotic and abiotic stresses. Biotic stress is caused by pathogen attacks such as bacteria, fungi, nematodes and insects (Gull, 2019). In contrast, abiotic stress includes radiation, salinity, floods, drought, extremes in temperature and heavy metals (Gull, 2019). In the context of climate change, elevated temperature is a predominant problem for crop plants in agriculture (Chuang et al., 2017).

Thermomorphogenesis

Plants respond to a wide range of temperatures by adjusting their development. The model plant *Arabidopsis thaliana* shows optimal growth between 20-23°C, at so called optimal ambient temperature (oAT) (Rivero et al., 2014). With rising temperature between 23-30°C, plants experience high ambient temperature (hAT) conditions, while temperatures above approximately 35°C cause severe heat stress response leading to cell death (Zhao, Lu, Wang, & Jin, 2020). Typical developmental responses at hAT include enhanced hypocotyl growth, hyponastic leaf movement, narrowing of leaves and early flowering (Casal & Balasubramanian, 2019). These morphological adjustments during hAT are collectively known as thermo-morphogenesis (Casal & Balasubramanian, 2019) and they are believed to help plants to cope with unfavorable hAT conditions.

Under optimal conditions, leaves are placed in horizontal position to enable ideal exposure to the light for photosynthesis. With increasing temperature plants elongate their petioles and move leaves to a more vertical position allowing efficient distancing between the true leaves for cooling and reduction of light capture (Gray, Östin, Sandberg, Romano, & Estelle, 1998; van Zanten, Pons, Janssen, Voesenek, & Peeters, 2010). Induced hypocotyl elongation during hAT response is hypothesized to protect the shoot by enabling its movement away from the heat absorbing soil (Gray et al., 1998; van Zanten et al., 2010). In fact, hAT induced phenotypic

responses positively affect transpiration rate and leaf cooling in *Arabidopsis* (Crawford, McLachlan, Hetherington, & Franklin, 2012). When seedlings experience reduced light intensity and red to far red light ratio due to neighboring competition for the limited light source, shade avoidance response (SAR) is activated, exhibiting similar developmental adaptations as those to hAT (Xu, Chen, & Tao, 2021). Thus, partially shared perception and downstream signaling mechanisms can be acting for hAT and SAR.

Mechanisms for temperature sensing

From the phytochrome family, phytochrome B (phyB) is one of the best studied light receptors in plants. It consists of two apoproteins harboring a chromophore each (Rockwell & Lagarias, 2006). When exposed to light, phyB confirmation is reversibly changed from the inactive Pr to its active Pfr form before translocated to the nucleus to activate downstream signaling (Pham, Kathare, & Huq, 2018). The conversion back to its inactive Pfr form is light and temperature dependent. Higher temperature promote this process called dark or thermal conversion, resulting in accumulation of inactive phyB (Jae-Hoon et al., 2016). Phototropins are blue light receptors which regulate chloroplast positioning in a light and temperature dependent manner. They consist of two LOV (light, oxygen or voltage) domains which covalently bind flavin-mononucleotide upon blue light absorption resulting in activation of phototropin (Hart & Gardner, 2021). Higher temperature negatively affects the stability of active phototropins, thus reduces chloroplast movement towards the cell surface (Yuta et al., 2017). Additionally, the blue light receptor CRYPTOCHROME1 (CRY1) and ZEUTLUPE (ZTL) as well as ultraviolet-B light photoreceptor (UV-B) UV RESISTANT LOCUS 8 (UVR8) are involved in hAT induced hypocotyl growth (Hayes et al., 2017; D. Ma et al., 2016).

In parallel to the mentioned temperature sensitive light receptors, which are able to sense both environmental signals, other molecular mechanisms have been reported, which so far were only shown to perceive temperature cues. Temperature can affect the level and occupancy of nucleosome by H2A.Z histones, thus enabling adaptation of gene expression (Cortijo et al., 2017). In addition, temperature dependent formation of an RNA hairpin within the PIF7 5’ UTR can adjust alternative RNA formation resulting in enhanced protein translation (Chung et al., 2020)

PIFs as the main players during hAT response

PHYTOCHROME INTERACTING FACTORs (PIFs) belong to the basic helix-loop-helix family of transcription factors and represent a central hub for integration of light and temperature signals (Balcerowicz, 2020). In the absence of light, PIFs activate transcription of downstream genes involved in skotomorphogenesis (de Lucas & Prat, 2014). Light activated phyB is translocated to the nucleus where it affects different downstream regulators including PIFs (Huq, Al-Sady, & Quail, 2003). Direct binding and phosphorylation by active Pfr phyB trigger subsequent ubiquitination and degradation of PIFs via proteasomal degradation pathway, thus switching from skotomorphogenesis to photomorphogenic development (Leivar & Quail, 2011). In addition to the light dependent regulation of PIF proteins, PIF1, PIF4, PIF5 and PF7 have been implicated in thermomorphogenesis (Fiorucci et al., 2020; Koini et al., 2009; Stavang et al., 2009). Due to the strongest reduction of hypocotyl growth in *pif4* during hAT compared to other *pif* single mutants, PIF4 is believed to be the main player during hAT response (Koini et al., 2009). At hAT temperature, phyB is inactivated and as result PIFs accumulate and activate transcription of downstream genes including cell wall-modifying enzymes such as *XYLOGLUCAN ENDOTRANSGLYCOSYLASE-RELATED PROTEIN 7* (*XTR7*) and *EXPANSIN 8* (*EXP8*), auxin biosynthesis and signaling genes such as *YUCCA8* (*YUC8*), *YUC9*, *INDOLE ACETIC ACID INDUCIBLE 19* (*IAA19*), *IAA29* as well as some auxin responsive *SMALL AUXIN UP RNAs* (*SAURs*) (reviewed in Balcerowicz, 2020). Hence, both auxin synthesis and signaling are controlled by PIF4 at hAT.

Auxin regulates cell growth at oAT and hAT

Auxin represents one of the well-known growth promoting hormones. By direct binding to TRANSPORT INHIBITOR RESPONSE 1/AUXIN-RELATED F-BOX (TIR1/AFB) family of F-box proteins auxin activates a cascade leading to ubiquitination and subsequent degradation of the negative regulators AUX/IAA and release of auxin response factors (ARFs) enabling auxin responsive gene expression (Leyser, 2018). When exogenously applied or endogenously induced, auxin can promote hypocotyl growth (Chapman et al., 2012; Munguía-Rodríguez et al., 2020). Under warm temperatures, auxin insensitive mutants *axr1-12* and *tir1-1* fail to elongate their hypocotyl and consequently exhibit reduced mean epidermal cell length (Gray et al., 1998).

During hAT, auxin biosynthesis is directly modulated via PIF4 mediated transcriptional regulation. Two main mechanisms for indole-3-acetic acid (IAA) synthesis have been proposed, including the tryptophan dependent and the tryptophan independent pathway (Di, Zhang, Luo, An, & Guo, 2016). Upon hAT, tryptophan dependent auxin biosynthesis is upregulated via *PIF4* mediated enhancement of *YUC8* and *YUC9* expression (J. Sun, Qi, Li, Chu, & Li, 2012) Together with TRYPTOPHAN AMINOTRANSFERASE OF ARABIDOPSIS1 (TAA1), YUCs are responsible for converting Tryptophan to IAA (Di et al., 2016).

At oAT, *YUC8* and *YUC9* genes are generally expressed in cotyledon in a diffuse pattern with the maximum on the leaf margins and partially neighboring vasculature, suggesting that auxin production is taking place in almost the whole cotyledon (Müller-Moulé et al., 2016). Since typical auxin signaling response is mainly restricted to the cotyledon tip, the importance of auxin transport mechanisms facilitating auxin relocation towards the tip is hypothesized (Bai & DeMason, 2008; Munguía-Rodríguez et al., 2020). With increasing temperature, *PIF4* expression is enhanced in the cotyledon vasculature and overall epidermis (S. Kim et al., 2020). Thus, PIF4 dependent induction of *YUC8* and *YUC9* transcription upon hAT is suggested to trigger auxin synthesis all over the cotyledon tissue. Similar as SAR, hAT induce auxin signaling mainly around the cotyledon tip and partially blade margin (Tao et al., 2008,Figure 4E). Consequently, specific adjustment of auxin transport within the cotyledon during hAT is particularly important to ensure efficient relocation of high auxin levels towards cotyledon tip. In addition, cotyledon derived auxin needs to be further transported towards the petiole and hypocotyl to enable local cell elongation and subsequent organ growth (Bellstaedt et al., 2019; Park et al., 2019).

PIN dependent modulation of auxin transport during hAT in cotyledon

The PIN-FORMED (PIN) proteins are family of auxin efflux carriers, which facilitate PATbased on their asymmetrical localization within the cells (Křeček et al., 2009). In accordance with their specific protein localization in different plant organs, they have been implicated in almost all plant developmental processes (Adamowski & Friml, 2015). Chemical blocking of PIN activity in the cotyledon results in diffused auxin response, suggesting their importance in focusing auxin allocation to the cotyledon tip (Munguía-Rodríguez et al., 2020). During hAT, auxin synthesis and

further accumulation in the cotyledon is strongly enhanced via PIF4 (Franklin et al., 2011). To ensure optimal auxin relocation towards the cotyledon tip during hAT response, adjustment of PIN proteins is suggested. However, the specific functions of PIN proteins in this process still remains unclear.

For further re-location across different plant organs, accumulated auxin at the tip of the cotyledon needs to be further loaded onto cotyledon vasculature, enabling directed transport towards petiole, hypocotyl and root. Exogenous application of auxin on the cotyledon tip results in enhanced auxin signaling response mostly in the cotyledon vasculature towards the petiole (Lewis, Wu, Ljung, & Spalding, 2009). However, when PIN protein activity is blocked by local application of NPA on the cotyledon blade in parallel with auxin application on the cotyledon tip, auxin signaling is abolished in cotyledon and petiole vasculature, resulting in reduced hyponastic leaf movement (Michaud, Fiorucci, Xenarios, & Fankhauser, 2017). Consequently, auxin transport in cotyledon and petiole vasculature is partially PIN protein dependent. PIN1, PIN3 and PIN4 are specifically expressed in the cotyledon vasculature, suggesting their potential local involvement in hAT response triggered auxin redistribution (Friml, Wiśniewska, Benková, Mendgen, & Palme, 2002; Sassi et al., 2012). In addition, some PINs, including PIN3 and PIN7, are localized to cotyledon pavement cells (Le et al., 2014). How *PIN* expression and protein localization in cotyledon vasculature and pavement cells is modulated during hAT response, to ensure auxin transport along the vasculature, still remains scarcely understood.

Auxin transport dependent elongation growth at hAT

Once arrived to the petiole vasculature, polar transport of auxin towards the epidermis is facilitated by PIN proteins. Within the petiole, PIN3 and PIN7 are localized in different cell layers. While PIN3 is restricted to the endodermis and epidermis, PIN7 expression was mainly found in the outer cell layers (Park et al., 2019; Sassi et al., 2012). Upon hAT, PIN3 protein polarization towards the lateral endodermal membrane is enhanced via PIF4 dependent induction of PINOID (PID) expression on the abaxial (lower) versus adaxial (upper) side of the petiole, driving enhanced auxin transport towards the abaxial epidermis (Park et al., 2019). Elevated auxin accumulation in the abaxial epidermis triggers expression of auxin responsive genes, including

SAUR19 and *SAUR22,* enabling local cell elongation resulting in hyponastic leaf movement (Park et al., 2019). Accordingly, *pin3* mutant exhibits reduced leaf hyponastic movement and reduced *SAUR* expression at hAT (Park et al., 2019).

In parallel to PIN dependent auxin transport, an alternative mechanism has been demonstrated to adjust auxin allocation between cotyledon and petiole. It has been reported, that epidermal cells layering the vasculature tissues in the midrib and petiole organs exhibit significantly higher plasmodesmata permeability for auxin in the longitudinal direction, thus playing an important role during leaf hyponasty (Gao et al., 2020). If this mechanism actively transports auxin towards the petiole and the hypocotyl during hAT response remains unclear.

To enable enhancement of hypocotyl cell elongation during hAT response, local auxin signaling in the hypocotyl epidermis is essential (S. Kim et al., 2020). Consequently, auxin redirection from the hypocotyl vasculature towards the epidermis is required. During phototropism, adjustment of PIN3 localization to the lateral membrane in the hypocotyl endodermis leads to modulation of temporal auxin distribution, subsequent cell growth and hypocotyl bending towards the light source (Liscum et al., 2014). Plants exposed to shade enhance *PIN3* expression and lateral protein abundance in the hypocotyl endodermis, resulting in elevated auxin transport towards the hypocotyl epidermis (Keuskamp, Pollmann, Voesenek, Peeters, & Pierik, 2010). Analysis of *pin* mutants revealed reduced *pin3* hypocotyl growth upon shade treatment, while *pin4* and *pin7* remained unaffected (Keuskamp et al., 2010). Due to shared signaling components, hAT was suggested, but still not proven, to affect *PIN* expression and protein abundance in a similar manner as shade to modulate auxin distribution (Franklin, Toledo-Ortiz, Pyott, & Halliday, 2014; Park, Kim, Lee, Han, & Park, 2021).

Auxin crosstalk with other hormones during hAT response

During hAT response, different plant hormones such as Brassinosteroids (BRs) and Gibberellins (GAs) are implicated in auxin dependent expression of growth promoting genes (Lu, Wang, Wang, & Liu, 2021). Warm temperatures promote accumulation of BRs, which subsequently lead to activation of transcription factor BRASSINAZOLE RESISTANT 1 (BZR1) (T.-W. Kim et al., 2009). BRZ1 and PIF4 can coordinately induce expression of growth promoting genes, thus adjusting

hypocotyl growth during hAT response (Oh, Zhu, & Wang, 2012). In addition, ARF6 has been shown to interact with PIF4 and BRZ1 forming the BRZ1/ARF6/PIF4 (BAP) module (Bouré, Kumar, & Arnaud, 2019). They share a high number of target genes implicated in cell growth, including *SAURs*, *AUX/IAAs* and *EXPs* (Oh et al., 2014). Thus, the BR and auxin signaling pathways are interconnected with the light and temperature sensitive PIF4 transcriptional regulator through the BAP module components.

Beside auxin and BRs, GAs are crucial regulators of plant growth, controlling both cell division and cell expansion (T. Sun & Gubler, 2004). Recent studies demonstrated involvement of GAs in hAT triggered hypocotyl growth (Stavang et al., 2009). Warm temperatures promote GA synthesis and conformational adjustment leading to inhibition of DELLA proteins (Lu et al., 2021). DELLA proteins are transcriptional regulators, which restrict cell growth by preventing PIF4 and BZR1 binding to the DNA via directly interacting with and inhibiting ARF6 (Lu et al., 2021). Consequently, GAs affect BAP module activity through the negative regulation of DELLAs.

Effect of circadian clock on hAT triggered auxin response

The circadian clock represents an internal timekeeper to adapt plant growth and development under changing environmental conditions. It resembles an oscillating multilayer regulatory mechanism. The central oscillator is composed of a series of sequential transcriptional regulatory loops of genes, which are expressed during different time points of the diurnal cycle (C R McClung, 2019). In this oscillatory process, specific morning expressed genes repress the expression of evening expressed genes and the other way round. EARLY FLOWERING 3 (ELF3) together with ELF4 and LUX ARRHYTHMO (LUX) resemble the Evening Complex (EC), which is active during dark period to modulate clock gene expression (Zhang, Luo, Davis, & Liu, 2021). In addition, EC has been shown to directly inhibit PIF4 expression and protein stability resulting in reduced PIF4 overall activity during night periods (Zhang et al., 2021). Under hAT conditions, EC dependent PIF4 repression is slightly reduced, which lead to PIF4 mediated enhancement of auxin synthesis and signaling, triggering elevated hypocotyl growth at warmer temperatures during dark periods (Lu et al., 2021). CIRCADIAN CLOCK ASSOCIATED 1 (CCA1), a component of the central oscillator being active during the day, and SHORT HYPOCOTYL UNDER BLUE LIGHT 1

(SHB1) coordinately activate *PIF4* expression at dawn, thus driving thermomorphogenic growth during the day (Q. Sun et al., 2019). The evening expressed circadian clock protein TIMING OF CAB EXPRESSION 1 (TOC1) negatively adjust PIF4 transcriptional activity during night period, thus represses thermomorphogenesis during dark (Zhu, Oh, Wang, & Wang, 2016). Consequently, different components of the circadian clock modulate thermomorphogenesis by direct or indirect adjustment of PIF4 dependent auxin synthesis and signaling.

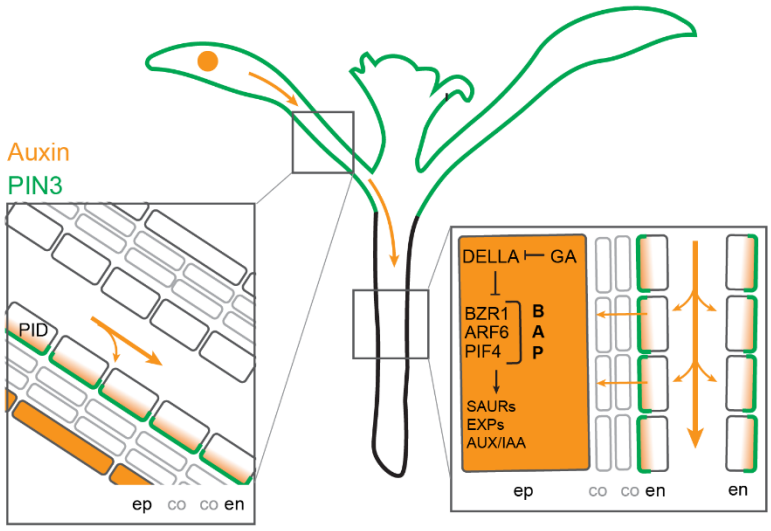

Figure 1: ***Schematic representation of auxin transport dependent hAT response.*** *Upon hAT, auxin synthesis is enhanced in cotyledon and is subsequently transported along the vasculature towards the petiole, where PIF4 induced PID facilitate lateralization of endodermal PIN3 on the abaxial side to redirect auxin flow towards the abaxial epidermis. In the hypocotyl, lateralized endodermal PIN3 drives auxin transport towards the epidermis, where it activates expression of cell growth promoting genes (SAURs, EXPs, AUX/IAAs) via regulation of the BAP module. Orange color represent auxin gradient, green color in the hypocotyl and petiole cells mark PIN3 localization, GA (Gibberillin), BZR1(BRASSINAZOLE RESISTANT 1), ARF6 (AUXIN RESPONSE FACTOR6), PIF4 (PHYTOCHROME INTERACTING FACTOR 4), SAURs (SMALL AUXIN UP RNAs), EXPs (EXPANSINs), AUX/IAA (auxin/indole-3-acetic acid)*

Results

hAT promotes hypocotyl growth in *Arabidopsis* seedlings

Arabidopsis exhibits optimal growth and performance in the temperature range of 20-22°C (Rivero et al., 2014). With increasing temperature up to 28-29°C, *Arabidopsis* seedlings adapt their growth and development by enhanced hypocotyl and petiole growth, formation of smaller and thinner true leaves as well as increased leaf hyponastic movement (Casal & Balasubramanian, 2019). All mentioned growth and developmental alterations caused by increase of the ambient temperature from optimal to high (29°C) are categorized as thermos-morphogenic responses (Casal & Balasubramanian, 2019). The positive effect of hAT on hypocotyl growth has been reported (Fiorucci et al., 2020), however, dynamics of hypocotyl growth response to increase of ambient temperature over a time frame longer than 4 days has not been investigated. For our experimental setup, we chose 21°C as optimal ambient temperature (oAT) and 28°C for high ambient temperature (hAT) treatment. Col-0 wild type (wt) seedlings grown at oAT for 5 days, were transferred to either hAT or oAT at Zeitgeber 2 (Zeitgeber represents the starting time of the light period) and monitored daily. Measurements of hypocotyl length revealed that hypocotyl growth was significantly accelerated starting from day 1 of hAT when compared to seedlings at oAT (Figure 2D). During first three days at hAT, we observed significantly enhanced hypocotyl growth over time (Figure 2A). From day 4 on, no significant increase in hypocotyl length was detected (Figure 2A), suggesting that, in our experimental conditions, hypocotyls reach their maximal length. Accordingly, evaluation of the hypocotyl growth rate confirmed significantly faster elongation at day 1 and 2 after transfer to hAT, when compared to oAT, whereas at day 3, hypocotyl growth rate at hAT was comparable to that at oAT (Figure 2C). These results demonstrate that in response to hAT hypocotyls undergo phase of accelerated elongation growth lasting for about 3 days. Afterwards, elongation ceases, presumably through activation of feedback mechanisms restraining exaggerated growth response.

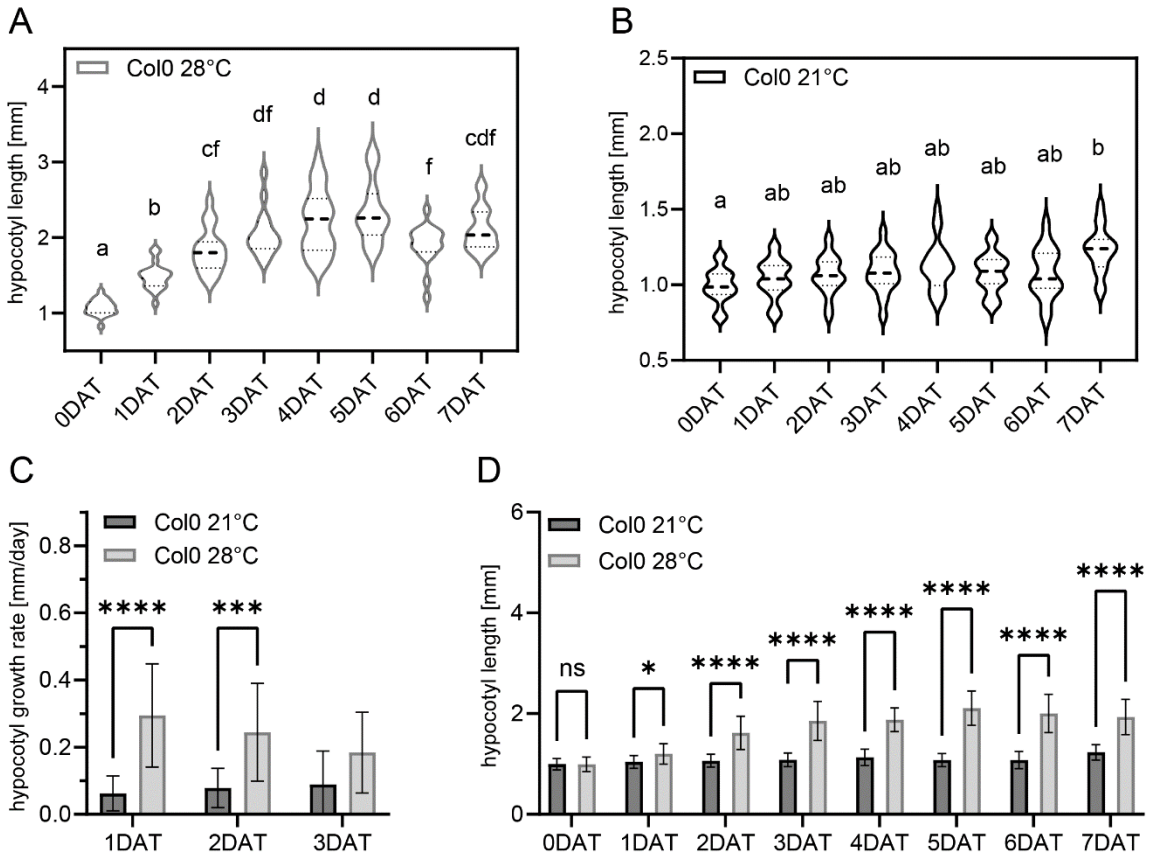

Figure 2: ***Arabidopsis seedlings exhibit hAT driven 2-phase hypocotyl growth response****. 5 day old wt seedlings were transferred to 28°C (hAT) versus 21°C (oAT)* ***(A-B)*** *Hypocotyl length of treated seedlings after 1 till 7 days. Violin plot represents median as dashed lines and quartiles as dotted lines. 2-way ANOVA for statistics, n>15 hypocotyls* ***(C)*** *Hypocotyl growth rate at oAT and hAT monitored over three days, the bars represent mean +- s.d., n > 20 hypocotyls* ***(D)*** *Hypocotyl length of hAT versus oAT treated seedlings. Students t-test for statistical comparison of hAT versus oAT, n>20 hypocotyls, **** = p < 0.0001 *** = p < 0.001, * = p < 0.05 by Student's t-test*

hAT triggers epidermal cell elongation in the hypocotyl

Generally, plant organ growth is dependent on cell division and elongation. It has been shown that hypocotyl growth at hAT is mainly driven by cell elongation rather than additional cell divisions (Gray et al., 1998). Bellsteadt and co-workers showed that after 4 days at hAT, cortex cells were significantly longer in the middle part and apex of the hypocotyl compared to those at 20°C (Bellstaedt et al., 2019). They observed a slight, but not significant increase in the hypocotyl cortex cell number after 4 days of hAT compared to 20°C, which is in accordance with the hypothesis that cell elongation is the main driving force for hypocotyl growth at hAT (Bellstaedt et al., 2019).

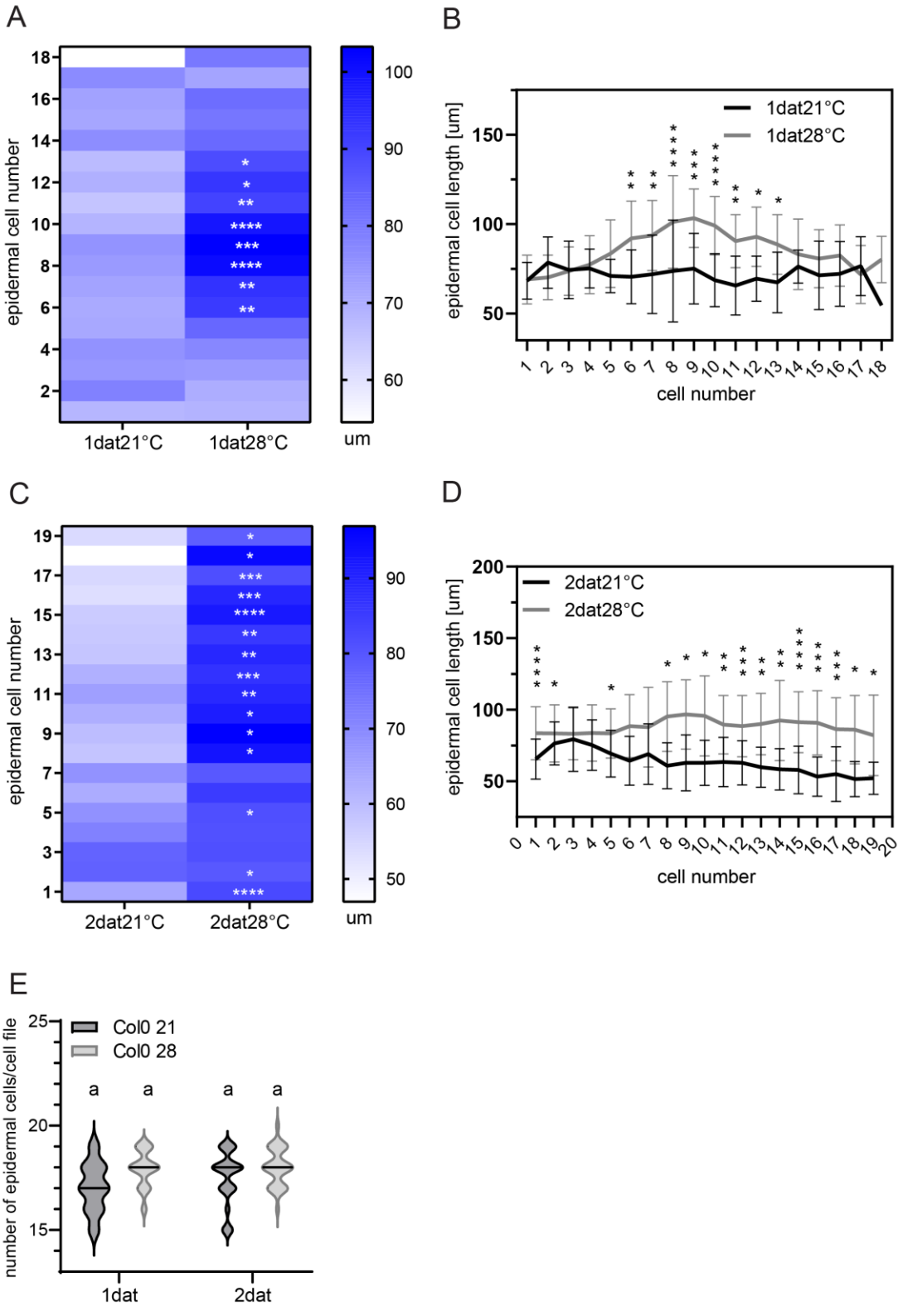
A
epidermal cell number
1dat21°C
1dat28°C
um
B
epidermal cell length [um]
1dat21°C
1dat28°C
cell number
C
epidermal cell number
2dat21°C
2dat28°C
um
D
epidermal cell length [um]
2dat21°C
2dat28°C
cell number
E
number of epidermal cells/cell file
Col0 21
Col0 28
1dat
2dat

Figure 3: ***Temporal adjustment of hypocotyl epidermal cell length pattern during hAT response*** *5 day old wt seedlings were transferred to 28°C (hAT) versus 21°C (oAT) and subsequently stained with Propidium iodid and analyzed by confocal microscopy. Length of epidermal cells was measured and plotted according to the position along the hypocotyl growth axis, where cell1 and 19 are the most bottom and top, respectively.* ***(A,B)*** *Epidermal cell length after 1 day of hAT versus oAT, n > 8 hypocotyls* ***(C,D)*** *Epidermal cell length after 2 days of hAT versus oT.* ***(A,C)*** *Heat maps represent the mean epidermal cell length.* ***(B,D)*** *Line graph represents mean cell length +- s.d. Students t-test was performed for Statistics, n > 8 hypocotyls, **** = p < 0.0001 *** = p < 0.001, ** = p < 0.01, * = p < 0.05* ***(E)*** *Average number of epidermal cells per hypocotyl epidermal cell file at hAT versus oAT. Violin plot represents median as dashed lines and quartiles as dotted lines shows, 2-way ANOVA for statistics, n > 8 hypocotyls, n = 2 cell files per hypocotyl*

We found that hypocotyls exposed to hAT rapidly elongate until they reach the maximal length at day 3-4 (Figure 2A). However, spatio-temporal pattern of epidermal cell elongation underlying acceleration of hypocotyl growth during the first phase (1 to 2days) of response to hAT has not been examined.

In order to track the early hypocotyl response on the cellular level, we measured epidermal cell length after 1 and 2 days of incubation at hAT versus oAT. After 1 day of transfer to hAT, epidermal cells positioned in the middle part of hypocotyl (5^{th} to 13^{th} cell from the root – hypocotyl junction) underwent elongation and they were significantly longer than cells at the hypocotyl base and apex (Figure 3A-B). 2 days after transfer, major cell expansion at the upper part of hypocotyls was detected (Figure 3C-D). As result, all hypocotyl epidermal cells reached the same length and no significant difference in their length was detected when cells were compared to each other (Figure 3C-D). In addition, we could not detect any significant changes in the number of epidermal cells after 1 or 2 days of hAT treatment compared to oAT (Figure 3E). Hence, accelerated growth of hypocotyls triggered by hAT is a spatio-temporally controlled process, characterized by gradual elongation of epidermal cells starting from the cells positioned in the middle part of hypocotyl followed by expansion of cells in the upper hypocotyl zone. Since we did not detected any significant changes in the number of hypocotyl epidermal cells after 1 or 2 days at hAT when compared to oAT, we conclude that divisions of epidermal cells do not significantly contribute to hypocotyl growth adaptation to hAT.

Effect of hAT on auxin synthesis and metabolism in cotyledons and hypocotyls

Auxin is well-established hormonal player in hAT induced hypocotyl growth (Gray et al., 1998), even though, the mechanism behind is no fully resolved yet.

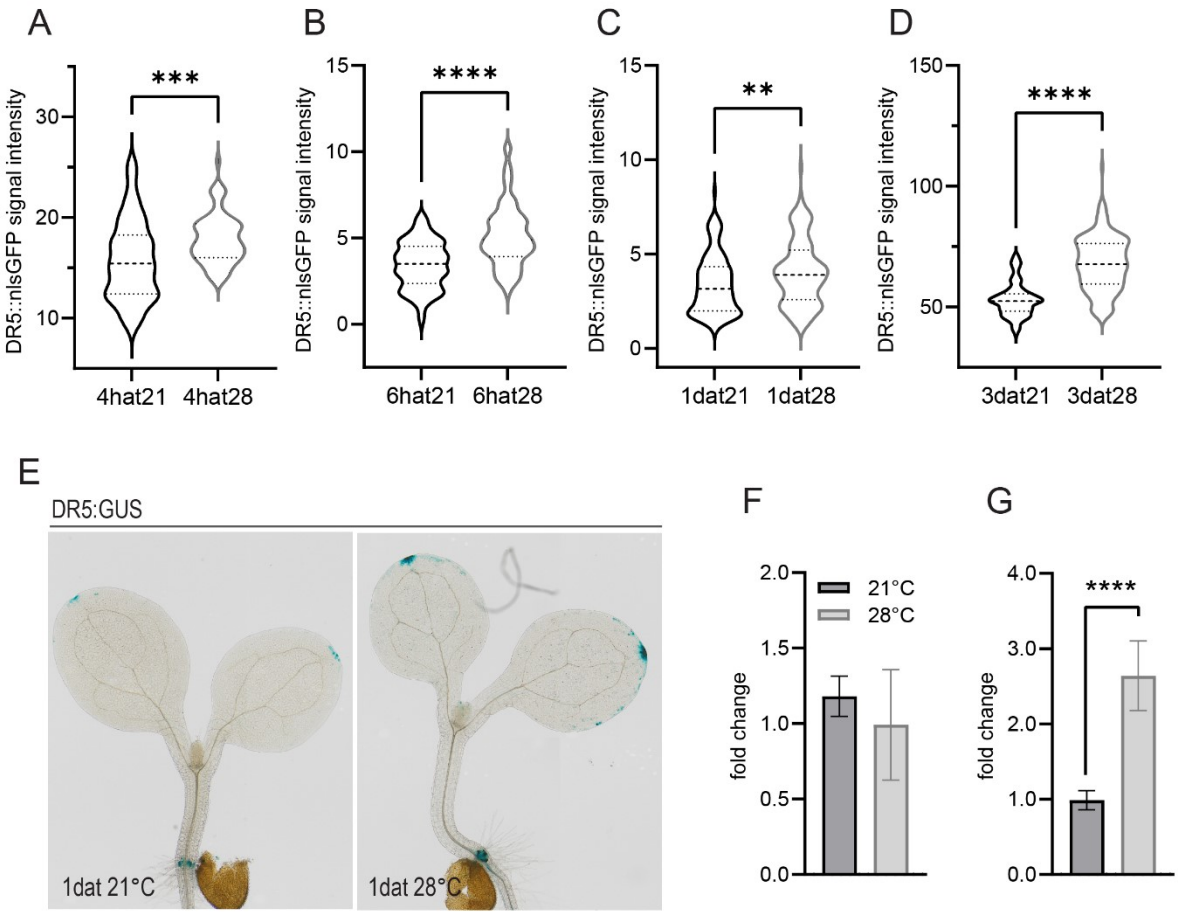

Figure 4: ***Auxin synthesis and signaling in cotyledon is adjusted during hAT response****. 5 day old seedlings were transferred to 21°C (oAT) versus 28°C (hAT) for different time frame.* ***(A-D)*** *DR5:nlsGFP signal detected by confocal microscopy. The GFP nuclear signal intensity measured in in pavement cells at adaxial side represented in violin plot with median as dashed lines and quartiles as dotted lines. Students t-test for statistics , n > 10 cotyledons, n > 5 cells per cotyledon* ***(E)*** *DR5:GUS analysis by light microscopy after 1 day at hAT versus oAT.* ***(F-G)*** *qPCR analysis of YUCCA8 expression in cotyledons after* ***(F)*** *6h and* ***(G)*** *1 day of treatment. Bars represent mean +- s.d. Students t-test for statistics, n=3 biological replicates, **** = p < 0.0001 *** = p < 0.001, ** = p < 0.01*

In general, young leaves and cotyledons represent the main source of auxin production (Teale, Paponov, & Palme, 2006). With increasing temperature, auxin synthesis genes as YUC8 and YUC9 are strongly induced mainly in the cotyledons of seedlings, thus accelerating local auxin production and subsequent response (Bellstaedt et al., 2019; Stavang et al., 2009). However, detailed information about the effect of hAT on auxin metabolism and signaling in the cotyledons versus hypocotyl is missing.

To monitor expression of auxin biosynthesis genes, we separately harvested and analyzed cotyledons after 6h (afternoon) and 1 day (next day morning) of hAT treatment versus oAT. While *YUC8* transcript level was not affected after 6h of hAT, we observed significant enhancement by

2,5 fold after 1 day at hAT versus oAT (Figure 4F,G). It has been reported that the circadian clock affects hAT response. During dark period the evening complex represses PIF4 resulting in reduced thermomorphogenic response (Box et al., 2015), which presumably interferes with PIF4-dependent enhancement of auxin synthesis genes.

To obtain further insights into how hAT affects auxin metabolism, we performed measurements of auxin and auxin related metabolites. Auxin is proposed to be mainly synthesized by Tryptophan dependent pathway. Chorismate, as the final product of the shikimate pathway, is used as precursor for L-Tryptophan (L-Trp) production. Tryptophan itself acts as precursor for different downstream pathways including INDOLE-3-ACETALDOXIME (IAOx) PATHWAY, the INDOLE-3-ACETAMIDE (IAM) PATHWAY the INDOLE-3-PYRUVIC ACID (IPyA) PATHWAY and the TRYPTAMINE (TRA) PATHWAY, which contribute to IAA formation (Di et al., 2016). Within the IPyA pathway, tryptophan aminotransferase TAA1 and its homologues actively convert L-Tryp to IPyA, which is afterwards turned into IAA by YUCCA enzymes (Di et al., 2016). To quickly reduce levels of the biologically active auxin, amino acids and sugars can be attached resulting in formation of different IAA conjugates (Ludwig-Müller, 2011). While attachment of most amino acids to IAA is reversible, enabling temporal auxin storage, conjugation with aspartic acid (Asp) and glutamate (Glu) represent the only so far known irreversible amino acid conjugation resulting in IAA catabolism (Ludwig-Müller, 2011). In addition, auxin can be targeted for degradation via oxidation (oxIAA) and subsequent conjugation to glucose (oxIAA-Glc) (Casanova-Sáez & Voß, 2019). In our experimental setup we transferred 6-day old seedlings to hAT versus oAT and analyzed their auxin metabolites in cotyledons and hypocotyls without shoot apical meristem separately after 1 day of incubation.

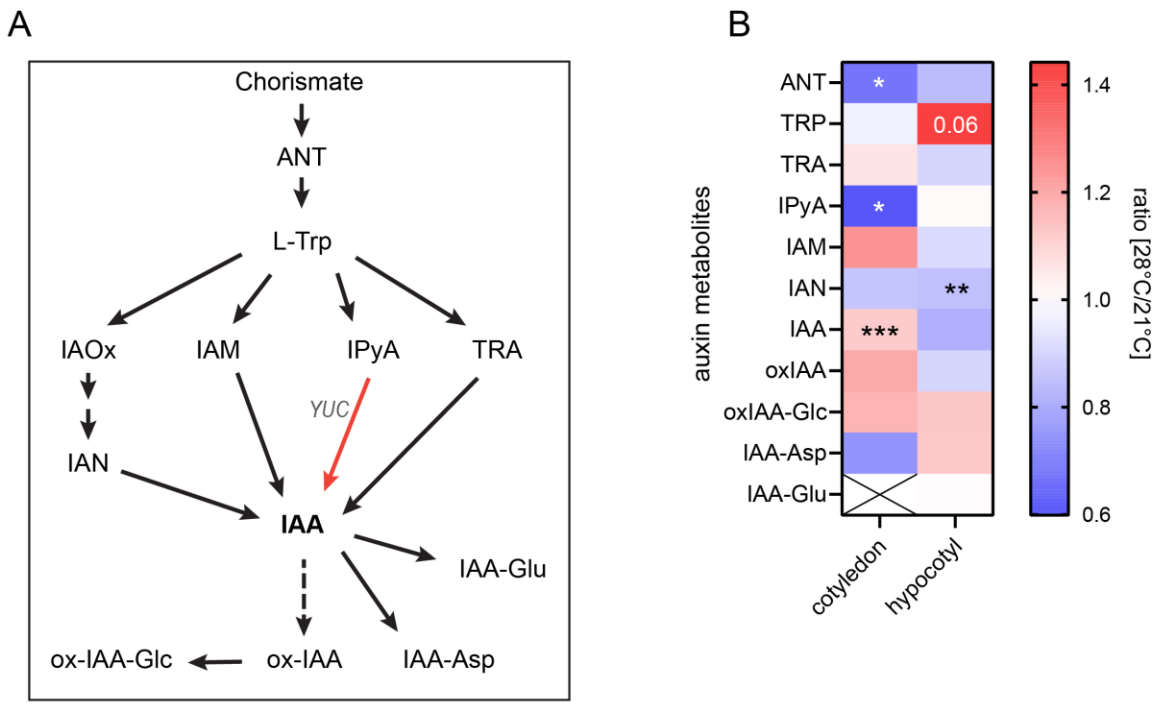

Figure 5: ***Auxin metabolites are affected by hAT****. **(A)** Schematic representation of auxin synthesis pathway. Anthranilate (ANT),L-tryptophane (L-Trp), indole-3-acetaldoxime (IAOx), indole-3-acetamide (IAM), indole-3-pyruvic acid (IPyA), tryptophan aminotransferases (TRA), indole-3-acetonitrile (IAN), indole-3-acetic acid (IAA),* ***(B)*** *Seedlings were grown for 6 days prior transfer to oAT versus hAT. After 1 day of treatment cotyledons and hypocotyls were dissected and their auxin metabolites were analyzed separately. Ratio of ug metabolite between hAT and oAT was calculated and their mean was visualized by heat map. Students t-test to oAT samples for statistics, *** = p < 0.001, ** = p < 0.01, * = p < 0.05*

In cotyledons of seedlings exposed to hAT, we detected significant increase in auxin levels, which correlated with reduction of auxin precursors including ANT, TRP and IPyA compared to oAT (Figure 5B). This suggests that TAA1, YUC-mediated pathway is primarily involved in hAT triggered enhancement of auxin synthesis. While auxin level was significantly enhanced in the cotyledons after hAT treatment, we could not detect any significant alterations in auxin levels, biosynthetic precursors, conjugates or degradation metabolites compared to oAT (Figure 5B). Due to relatively low amount of free auxin found in hypocotyl (17 fmol/hypocotyl) versus cotyledon (42 fmol/cotyledon), we suggest to increase amount of material for further hypocotyl analysis to enable efficient measurement of auxin metabolite changes upon hAT.

In conclusion, hAT induced IAA synthesis mostly via enhancement of YUC-dependent conversion of IPyA in cotyledons.

Local auxin signaling response in the cotyledons and hypocotyl upon hAT

Next, we monitored auxin signaling response using *DR5:nlsGFP* auxin sensitive reporter in cotyledons after 4h, 6h, 1day and 3days of hAT treatment by confocal microscopy. Exposure to hAT resulted in significant increase of GFP signal in cotyledon epidermal cells at all four different time points compared to oAT (Figure 4A-D). Analysis of *DR5:GUS* transcriptional reporter line revealed increased staining in the cotyledon tips after 1 day at hAT (Figure 4E), similarly to previous report (Wang et al., 2016), while signal in epidermal cells was under detection limit. Thus, consistently with enhanced biosynthesis and accumulation of auxin exposed to hAT, auxin signaling pathway in cotyledons is activated.

At hAT, Zheng and co-workers observed strong induction of auxin signal response in the hypocotyl few days after transfer from 22°C to 29°C (Zheng et al., 2016). However, detailed spatial temporal monitoring of auxin signaling in the hypocotyl during adaptation to hAT has not been performed. We used *DR5:nlsGFP* auxin sensitive reporter to monitor auxin signaling in the hypocotyl epidermis, the tissue responding to hAT by cell elongation (Figure 3). We measured the nuclear signal of *DR5:nlsGFP* in the individual epidermal cells along the hypocotyl growth axis. To simplify the data, we calculated average signal of cells grouped according to the position as indicated in the graphs. At oAT, we observed a non-homogenous auxin response along the hypocotyl epidermal cell file (Figure 6A). Those epidermal cells, which are closer to the hypocotyl-root junction (cells1-2), showed increased *DR5:nlsGFP* expression compared to all other cells in the hypocotyl. The lowest signal was found in the cells localized in the middle part of the hypocotyl (Figure 6A). The auxin response in the cells close to the apex (cells16-20) showed moderate strength of nlsGFP signal (Figure 6A). After 5h of hAT treatment, we observed a significant increase in the auxin signaling reporter expression in epidermal cells close to hypocotyl apex when compared to oAT (Figure 6B). Exposure to hAT for 1 day enhanced auxin signaling response in the whole epidermis when compared to oAT (Figure 6C). *DR5:nlsGFP* expression stayed elevated in all epidermal cells for the following two more days (Figure 6D-E).

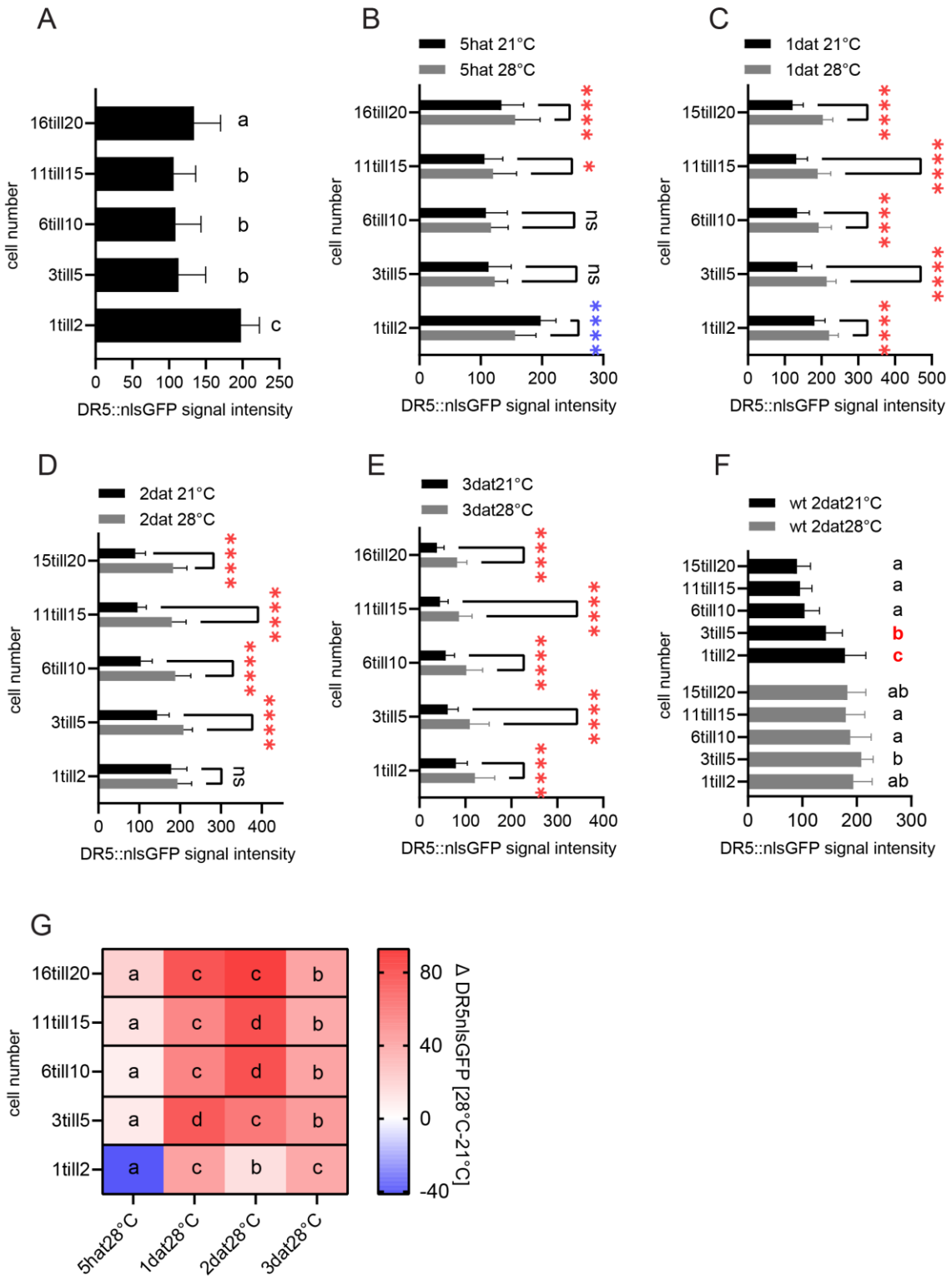
A
16till20
11till15
6till10
3till5
1till2
a
b
b
b
c
cell number
0 50 100 150 200 250
DR5::nlsGFP signal intensity
B
5hat 21°C
5hat 28°C
ns
ns
0 100 200 300
C
1dat 21°C
1dat 28°C
15till20
0 100 200 300 400 500
D
2dat 21°C
2dat 28°C
0 100 200 300 400
E
3dat21°C
3dat28°C
F
wt 2dat21°C
wt 2dat28°C
ab
G
5hat28°C
1dat28°C
2dat28°C
3dat28°C
80
40
0
-40
Δ DR5nlsGFP [28°C-21°C]

Figure 6: ***Auxin signaling in hypocotyl epidermis at hAT****.* ***(A-F)*** *Analysis of auxin signaling response in epidermal cells of 5 day old DR5:nlsGFP seedlings at 21°C (oAT)* ***(A)****, transferred to 21°C (oAT) and 28°C (hAT) for different time frames as indicated* ***(B-F)****. Nuclear GFP signal in the hypocotyl epidermal cells was analyzed by multiphoton microscopy, measured and grouped according to their position within the hypocotyl* ***(B-F).*** *Students t-test was performed for statistics, Blue and red asterisk mark significant down and upregulation of nuclear GFP signal respectively, n > 4 hypocotyls, **** = p < 0.0001, * = p < 0.05, ns = p > 0.05 (B-F), 2 way ANOVA for statistical comparison of DR5:nlsGFP within the group of cells, n > 4 hypocotyls (A,F).* ***(G)*** *Analysis of average difference in DR5:nlsGFP signal intensity between oAT and hAT, 2-way ANOVA for statistical comparison between the different time points.*

For further comparison of auxin signaling response over time, we calculated the difference of *DR5:nlsGFP* signal between hAT and oAT in epidermal hypocotyl cells (ΔDR5:nlsGFP, hAT-oAT) and performed statistics to evaluate significant changes. This analyses show that major enhancement of auxin response in epidermis occurs within first two days after exposure to hAT, which correlates with phase of accelerated hypocotyl growth (Figure 6G, Figure 2A). Lower *ΔDR5:nlsGFP* at day 3 from transfer to hAT correlates with phase of decelerating growth (Figure 6E, Figure 2A) and hints at activation of feedback mechanisms that constrain further enhancement in auxin signaling.

In summary, under oAT we detected a gradual distribution of auxin signaling response in the hypocotyl epidermal cells with the maximum at the hypocotyl base. During accelerated phase of hypocotyl growth triggered by hAT, auxin response in epidermal cells increases and equalizes along the hypocotyl growth axis. Transition of hypocotyl growth to steady state correlates with decrease in auxin response.

Auxin transported from cotyledons enhances hypocotyl growth

Auxin can induce hypocotyl elongation when applied exogenously at oAT (Chapman et al., 2012). or when its endogenous levels are increased via constitutive overexpression of auxin synthesis genes e.g. *YUC4* (Munguía-Rodríguez et al., 2020). At hAT, auxin synthesis is significantly enhanced in cotyledon tissue (Bellstaedt et al., 2019; Stavang et al., 2009; Figure 4G). If auxin transport is repressed by NPA application in *YUC4* overexpressing seedlings, hypocotyl growth is reduced (Munguía-Rodríguez et al., 2020). If cotyledons are dissected from the hypocotyl before transfer to higher temperature or NPA was applied on petiole, hypocotyl elongation was abolished (Bellstaedt et al., 2019).

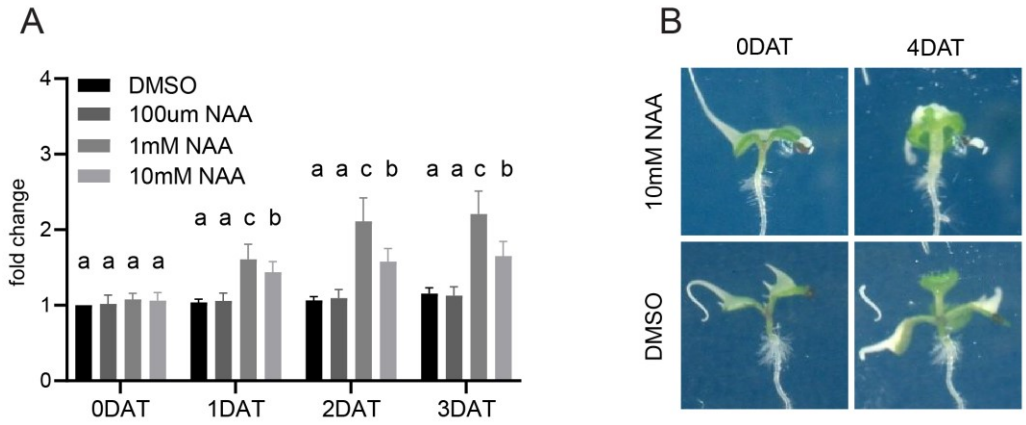

Figure 7: ***Auxin application on the cotyledon triggers hypocotyl growth****.* ***(A)*** *Relative hypocotyl length after different time points of treatment. Bars show mean +- s.d., 2-way ANOVA for statistics n> 20 hypocotyls.* ***(B)*** *Representative images of Col0 shoot after 0 and 4 days of treatment with NAA versus DMSO at oAT. 5 day old Col0 seedlings were treated with 100uM, 1mM or 10mM NAA-lanolin or DMSO-lanolin on the cotyledon at oAT (A,B)*

Even though auxin synthesis is slightly induced in the hypocotyl after hAT as well (Stavang et al., 2009), hypocotyl growth seems to be mainly dependent on cotyledon derived auxin (Bellstaedt et al., 2019; Zheng et al., 2016). All these results support a model, in which auxin transport from the cotyledon towards the hypocotyl is necessary to promote hAT induced hypocotyl growth.

To explore temporal aspects of hypocotyl response to auxin, we applied auxin locally on cotyledons and monitored hypocotyl elongation. To ensure local application of the treatment we mixed the synthetic auxin naphthalene-1-acetic acid (NAA) solution with lanolin paste. The high viscosity of lanolin prevents spreading of the treatment to neighboring organs. We did not observe any significant alterations in hypocotyl length after application of 100uM NAA (Figure 7A). Application of 1mM and 10mM NAA significantly induced hypocotyl growth already after 1 day (Figure 7A). Treatment with 1mM NAA and 10mM NAA resulted in 2.3 and 1.8 fold change increased in hypocotyl length, respectively (Figure 7A). Thus, positive effect of locally applied auxin on hypocotyl growth is concentration dependent.

To examine the role of auxin transport during hAT promoted hypocotyl growth, we locally repressed auxin transport by application of Naphthylphthalamic acid (NPA) on the cotyledon or hypocotyl prior transfer to hAT. NPA was shown to associate and inhibit PIN auxin efflux transporters (Abas et al., 2021).

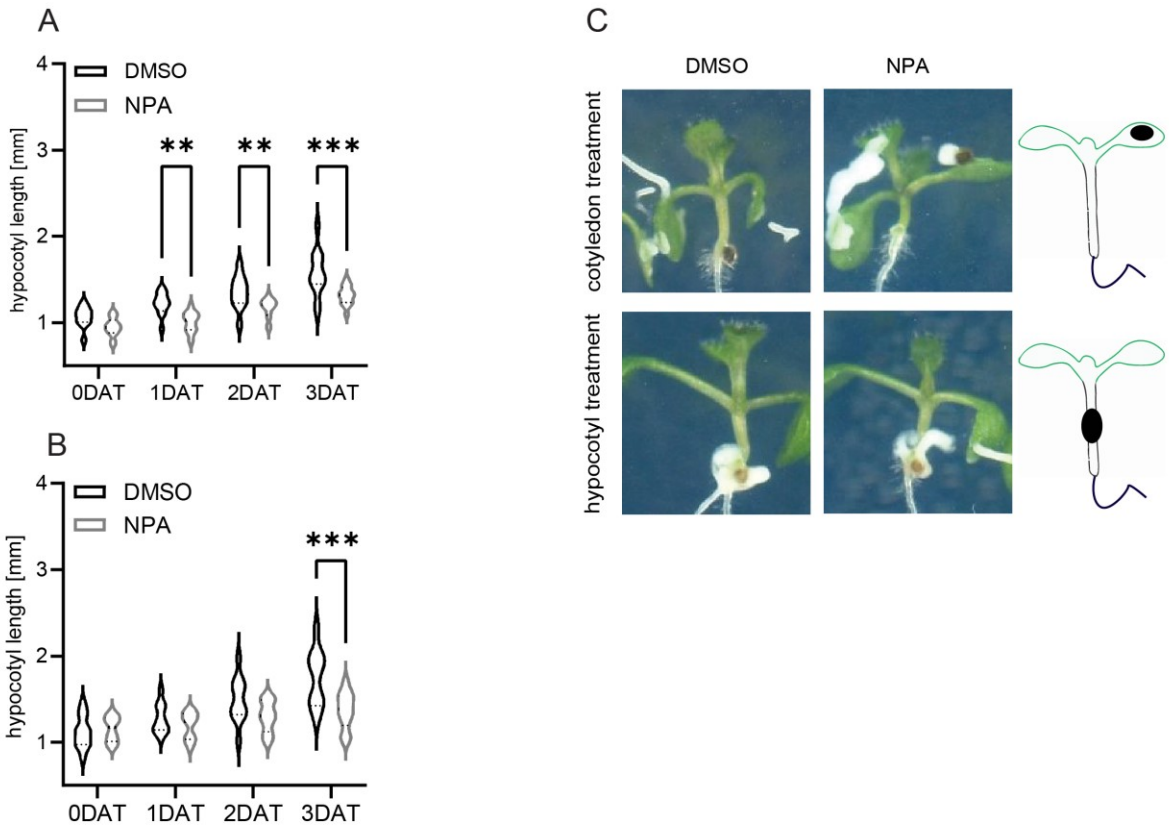

Figure 8: ***Local inhibition of auxin transport represses hAT triggered hypocotyl growth****. 5 day old Col0 seedlings were treated with 100uM NPA-lanolin versus DMSO-lanolin on* ***(A)*** *cotyledon or* ***(B)*** *hypocotyl and transferred to 28°C (hAT). Violin plot represents median as dashed lines and quartiles as dotted lines, n>15 hypocotyls, Students t-test for statistics, *** = p < 0.001, ** = p < 0.01* ***(C)*** *Representative images of Col0 shoot after 3 days of treatment with NPA versus DMSO applied either on cotyledon or hypocotyl at hAT.*

Seedlings, whose cotyledons were treated with NPA, showed significantly less accelerated hypocotyl growth after 1 day at hAT compared to those on DMSO (Figure 8A). Notably, NPA applied on the hypocotyl attenuated elongation response to hAT only after 3 days (Figure 8B).

Altogether, auxin applied on cotyledons at oAT accelerates hypocotyl elongation growth already within 1 day. When simultaneously with increased temperature auxin transport from cotyledons is locally inhibited by application of NPA, the hypocotyl growth response is significantly attenuated. Interestingly, when auxin transport at hAT is inhibited by NPA treatment on hypocotyls impact on elongation growth is less profound.

PIN-mediated auxin transport is required for hypocotyl elongation response to hAT

PIN-FORMED (PIN) proteins are key components of the polar auxin transport machinery in plants. Among the family of PIN proteins, PIN3, PIN4 and PIN7 were shown to be involved in shade triggered hypocotyl growth (Keuskamp et al., 2010) and hAT induced hyponastic leaf movement (Park et al., 2019). However, detailed analyses of the individual PIN genes contribution to regulation of hypocotyl growth response to hAT are missing. To investigate function of PIN genes in hAT driven hypocotyl growth we monitored *pin3*, *pin4*, *pin7* and *pin3/4/7* mutant at hAT versus oAT.

Under oAT, we observed shorter hypocotyl in the *pin3/4/7* triple mutant, while single *pin* mutants showed no significant difference compared to wt (Figure 9A). However, at hAT hypocotyl growth of *pin3*, *pin4* and *pin3/4/7* was enhanced significantly less when compared to wt (Figure 9C). Hypocotyl growth of *pin7* was similar to wt after 1 and 2 days of exposure to hAT (Figure 9C). To determine if *pin* mutants could reach wt hypocotyl length at later time points, we analyzed hypocotyl growth response up to 7 days after transfer to hAT. *pin3*, *pin4* as well as *pin3/4/7* showed reduced hypocotyl growth from 1 day until 7 days after transfer to hAT. Interestingly, at later time points we noticed increased hypocotyl length of *pin7* mutant at oAT and partly also at hAT when compared to wt, suggesting that PIN7 might play a distinct role in regulation of hypocotyl growth when compared to PIN3 and PIN4 (Figure 9D). To test whether auxin enhancing effects on hypocotyl growth is dependent on the PIN-mediated transport, we applied auxin on cotyledons of the respective *pin* mutants and grew them at oAT for additional 4 days (Figure 9E). While *pin3* treated with 1mM NAA exhibited similar hypocotyl growth rate as wt, the response was severely attenuated in *pin3/4/7* (Figure 9E). Interestingly, hypocotyl growth rate after 1mM NAA application was significantly increased in *pin7* mutant compared to wt, and modest enhancement was detected also in *pin4* (Figure 9E).

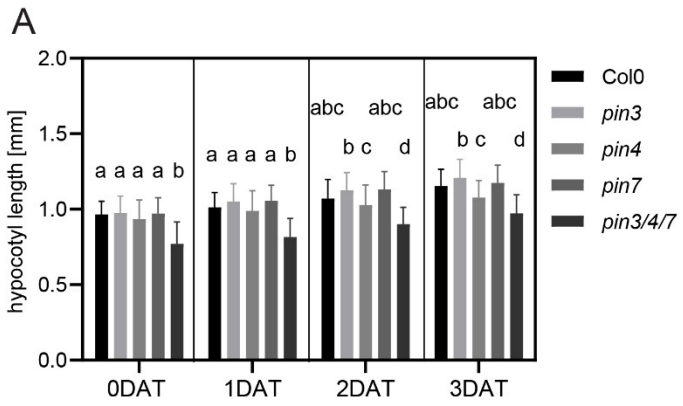
A
hypocotyl length [mm]
2.0
1.5
1.0
0.5
0.0
a a a a b
a a a a b
abc abc
b c d
abc abc
b c d
0DAT
1DAT
2DAT
3DAT
Col0
pin3
pin4
pin7
pin3/4/7

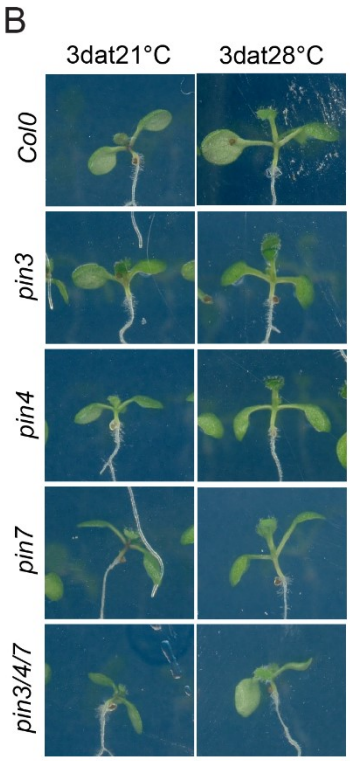
B
3dat21°C
3dat28°C
Col0
pin3
pin4
pin7
pin3/4/7

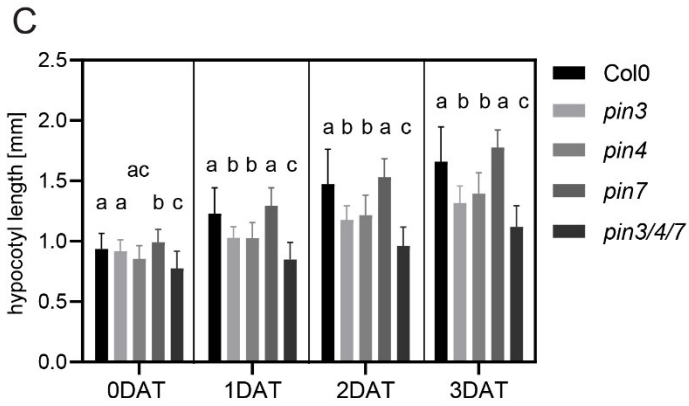
C
hypocotyl length [mm]
2.5
2.0
1.5
1.0
0.5
0.0
ac
a a b c
a b b a c
a b b a c
0DAT
1DAT
2DAT
3DAT
Col0
pin3
pin4
pin7
pin3/4/7

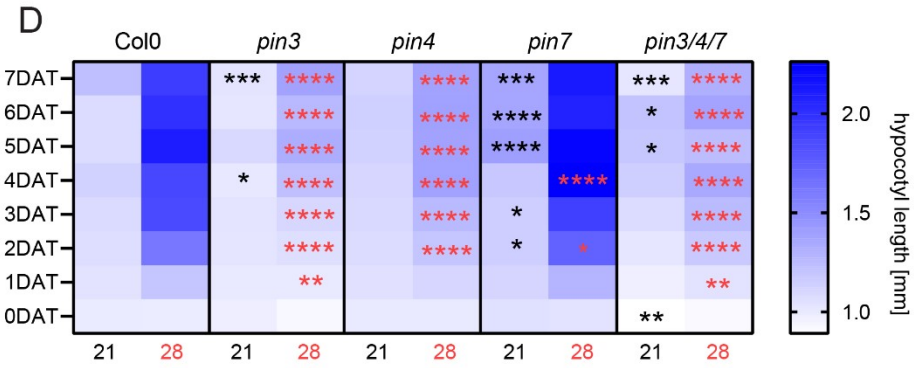
D
Col0
pin3
pin4
pin7
pin3/4/7
7DAT
6DAT
5DAT
4DAT
3DAT
2DAT
1DAT
0DAT
21
28
hypocotyl length [mm]
2.0
1.5
1.0

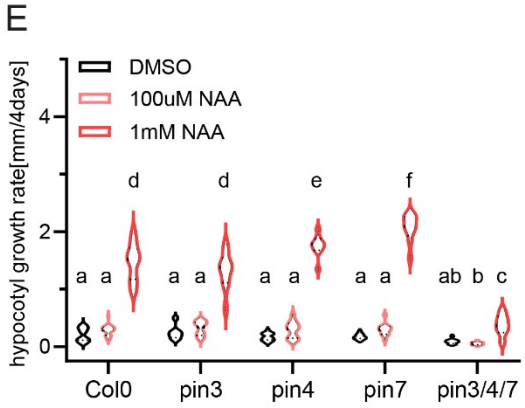
E
hypocotyl growth rate[mm/4days]
DMSO
100uM NAA
1mM NAA
4
2
0
a a d
a a d
a a e
a a f
ab b c
Col0
pin3
pin4
pin7
pin3/4/7

Figure 9: ***pin mutants are defective in hypocotyl growth response to hAT and auxin****. **(A, C)** Hypocotyl length of 5 day old pin3, pin4, pin7 and pin3/4/7 versus Col0 monitored at 21°C (oAT) **(A)** and 28 °C (hAT) **(C)**. Bars represent mean +- s.d., n > 20 hypocotyls with 2-way ANOVA for statistics. **(B)** Representative images of Col0 and pin mutants after 3 days of hAT versus oAT. **(D)** Hypocotyl length during 7 days of hAT versus oAT treatment presented in heat map. Students t-test applied for statistical comparison to Col0 at oAT (black asterisk) or Col0 at hAT (red asterisk), n > 15 hypocotyls, , **** = p < 0.0001 *** = p < 0.001, ** = p < 0.01, * = p < 0.05. **(E)** Hypocotyl growth rate after treatment with 100uM or 1mM NAA-lanolin versus DMSO-lanolin on cotyledons and grown for additional 4 days at oAT. 2-way ANOVA for statistics, n > 15 hypocotyls*

These results demonstrate that hAT induced hypocotyl growth is dependent on PIN-mediated transport of auxin, even though, based on the different *pin* mutant phenotypes observed upon hAT and auxin application, individual PINs seems to play specific functions.

PIN-mediated auxin transport determines epidermal cell elongation pattern in response to hAT

Next, we examined how PINs contribute to the temporal and spatial adjustment of epidermal cell elongation during the first phase of response to hAT. We exposed respective *pin* mutants and wt for 1 day to either hAT or oAT and measured length of epidermal cells along the growth axis. At the level of individual cells, we found significantly shorter hypocotyl epidermal cells in *pin3/4/7* under oAT compared to wt (Figure 10A,C, black asterisks). Notably at hAT, lack of *PIN3, PIN4, PIN7* led to alteration of the elongation pattern when compared to wt (Figure 10A,C). Unlike wt, in which hAT triggered accelerated elongation of cells from middle part of hypocotyls upwards, in the triple *pin* mutant only few cells at the base of hypocotyls underwent moderate elongation (Figure 10A). Similar to triple *pin* mutant, although less severe alterations in the elongation pattern, was observed in single *pin3* and *pin4* mutants (Figure 10B). In contrast, elongation of hypocotyls lacking PIN7 was accelerated by hAT slightly more than in wt (Figure 10B-C). Notably, in *pin7* mutant, we observed a significant induction of epidermal cell elongation in the hypocotyl apex and base with no significant change in the middle part of the hypocotyl compared to wt (Figure 10B-C). These results suggest that coordinated action of PINs determines elongation pattern of hypocotyl epidermal cells in response to hAT.

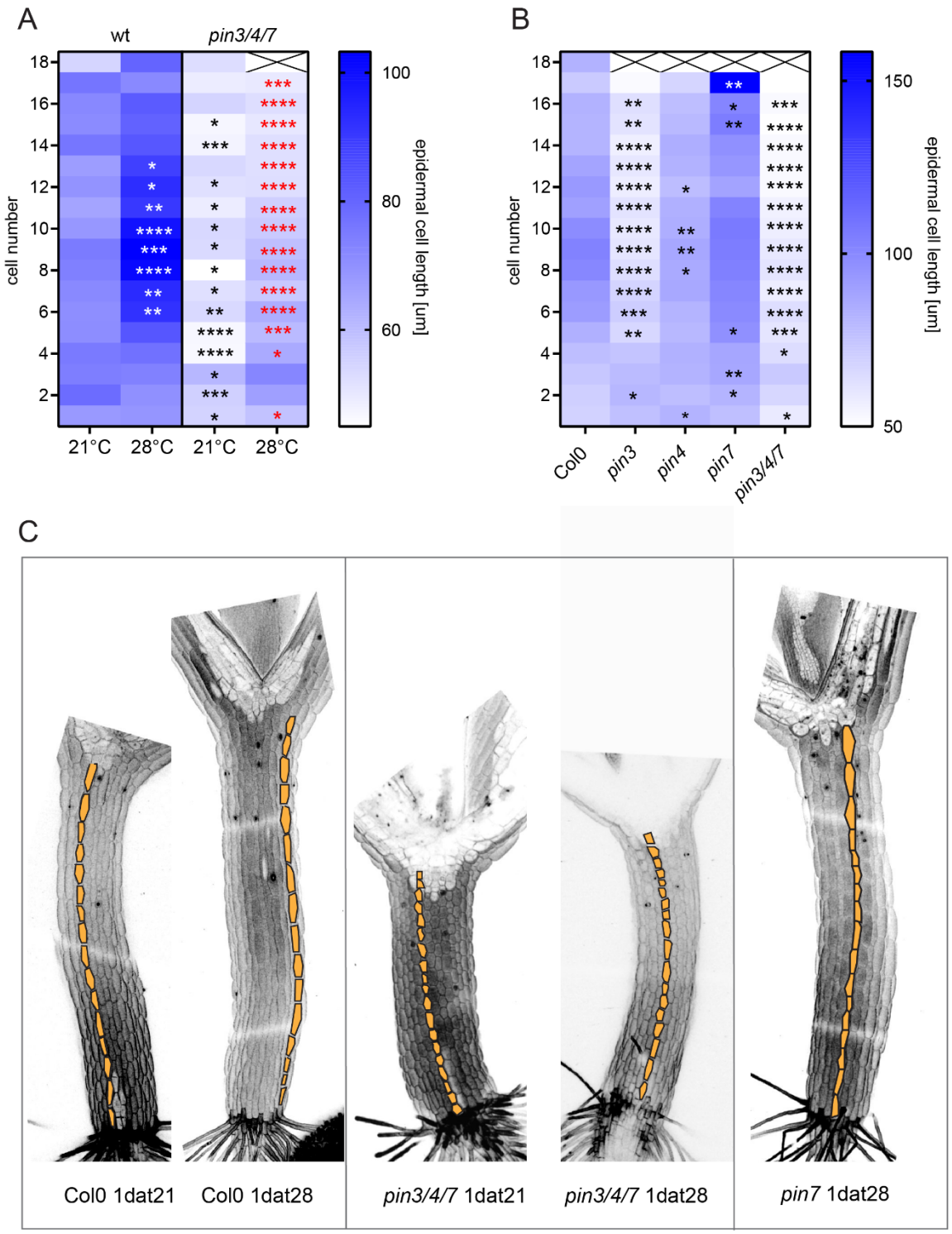
A
wt
pin3/4/7
cell number
epidermal cell length [um]
21°C
28°C
21°C
28°C
B
cell number
epidermal cell length [um]
Col0
pin3
pin4
pin7
pin3/4/7
C
Col0 1dat21
Col0 1dat28
pin3/4/7 1dat21
pin3/4/7 1dat28
pin7 1dat28

Figure 10: ***Pattern of epidermal cell elongation in response to hAT is altered in pin mutants****. **(A)** Length of hypocotyl epidermal cells of 5 day old Col0 and pin3/4/7 seedlings transferred for 1 day to either oAT or hAT. **(B)** Length of epidermal cells of 5 day old pin3, pin4, pin7 and pin3/4/7 and Col0 seedlings transferred for 1 day to hAT. Epidermal cell length was measured and plotted according to the position within the hypocotyl where cell1 is the most bottom cell and cell 18 the most top at the hypocotyl apex. Heat map shows mean hypocotyl length at different time points of treatment **(A,B)**. **(A-B)** Students t-test for statistical comparison to Col at oAT (black asterisk) or Col0 at hAT (red asterisk), n > 7 hypocotyls, **** = p < 0.0001, *** = p < 0.001, ** = p < 0.01, * = p < 0.05. **(C)** Representative images where single cells of representative epidermal cell file were marked in orange. Hypocotyls were stained with propidium iodide for visualization of plasma membranes and analyzed by confocal microscopy **(A-C)**.*

PIN expression in cotyledon is modulated in response to hAT

Our results, demonstrating the important role of PIN proteins in transport of auxin from cotyledons to the hypocotyl, thereby controlling hAT induced hypocotyl growth, motivated us to investigate how hAT affects *PIN* transcript levels and protein abundance in the cotyledons.

To determine *PIN3* expression pattern, we used *PIN3:GUS* transcriptional reporter line. At oAT, *PIN3* expression was found in the vasculature and epidermal cells of cotyledons (Figure 11). After 1 day at hAT, *PIN3:GUS* staining in these tissues could not be detected, however after 2 days at hAT, *PIN3:GUS* started to recover (Figure 11A). In addition, 2 days after transfer to hAT, we noticed a significant enhancement of *PIN3:GUS* staining in the young true leaves. (Figure 11A). RT-qPCR analyses revealed a significant decline in *PIN3* expression after 6h of hAT compared to control conditions while slight but not significant increase was detected after 1 day of hAT versus oAT (Figure 11B). For analysis of PIN3 protein abundance, we monitored *PIN3::PIN3:GFP* translational reporter line. At oAT, we detected PIN3:GFP signal homogenously distributed on the plasma membranes of cotyledon pavement cells (Figure 11C). Therefore, to quantify impact of hAT, we measured the PIN3:GFP signal at membranes of those cells. After 7h, 1 and 2 days at hAT, we observed a significant reduction in PIN3:GFP signal in cotyledon pavement cells compared to oAT (Figure 11D-F), whereas at day 3 no significant difference in PIN3 protein abundance was detected (Figure 11G).

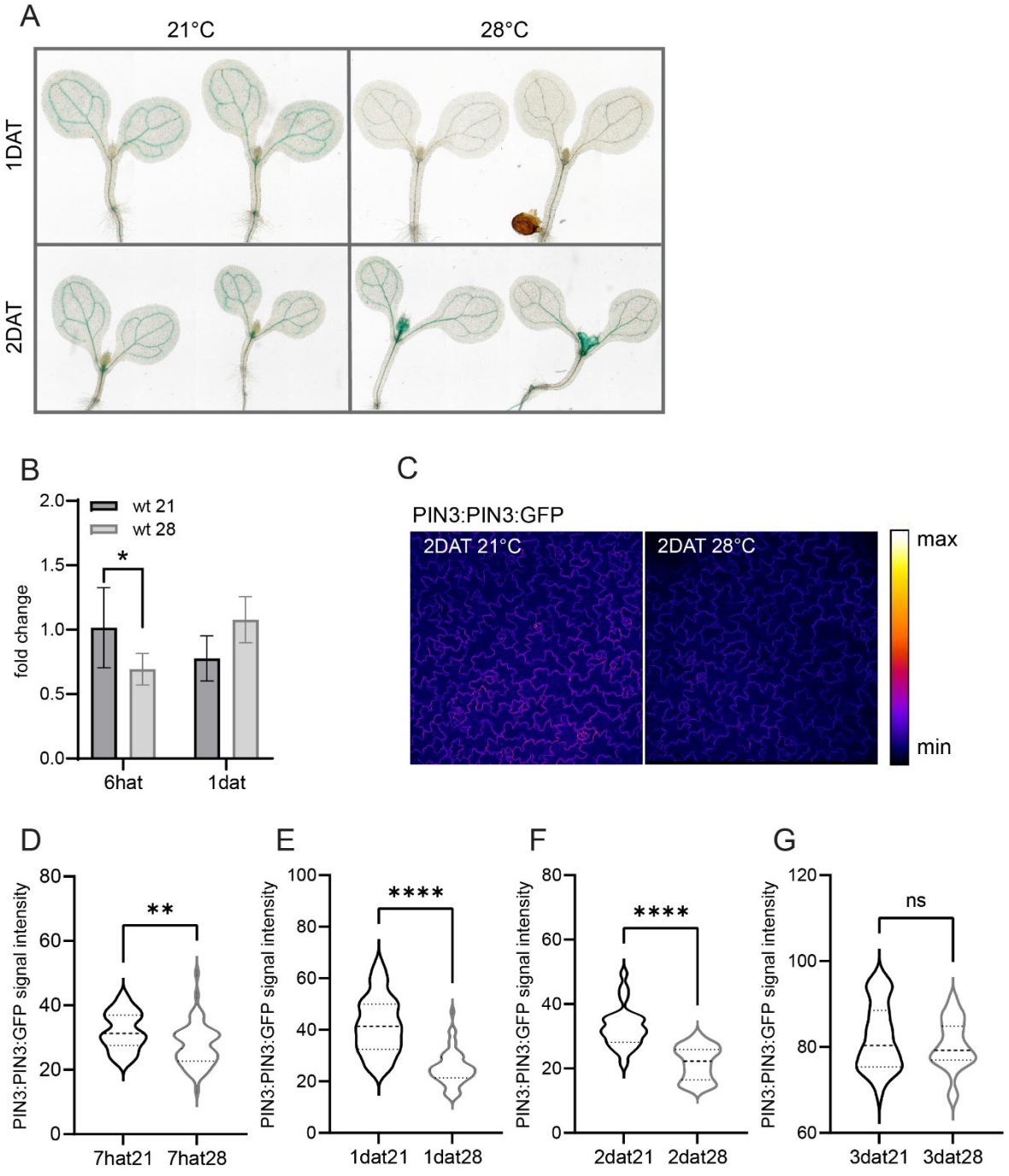

Figure 11: ***Adjustment of PIN3 expression in cotyledons to hAT.*** ***(A)*** *PIN3:GUS expression in 5 day old seedlings transferred for 1 or 2 days to either 21°C (oAT) or 28°C (hAT).* ***(B)*** *RT-qPCR analysis of PIN3 transcription in cotyledons of 5 day old Col0 seedlings exposed for 6h or 1 day to either oAT or hAT. Bars represent mean +- s.d., n = 3 biological replicates* ***(C-G)*** *PIN3:PIN3:GFP expression* ***(C)*** *and quantification* ***(D-G)*** *in cotyledon pavement cells at different time points of exposure to oAT or hAT. PIN3:GFP monitored by confocal microscopy and plasma membrane signal quantified. Violin plot represents median as dashed lines and quartiles as dotted lines, Students t-test was performed for Statistics, n > 10 cotyledons, n > 4cells per cotyledon, **** = p < 0.0001, ** = p < 0.01, hat and dat represent hours and days after transfer, respectively.*

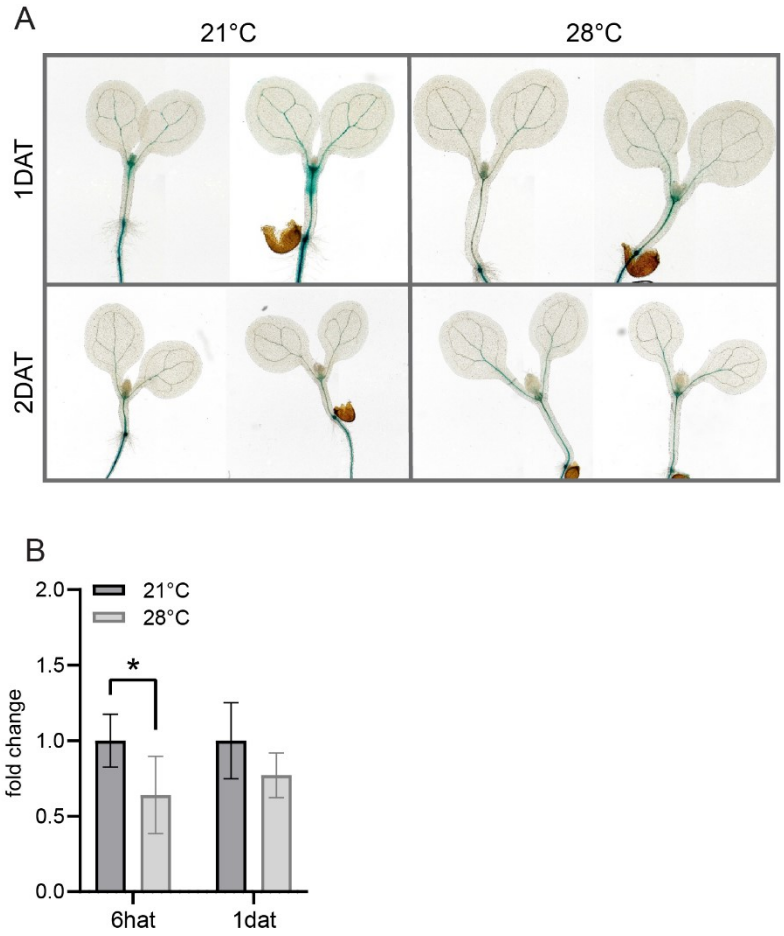

Figure 12: ***Adjustment of PIN4 expression in cotyledon upon hAT.*** *5 day old seedlings were transferred to 21°C (oAT) versus 28°C (hAT)* ***(A)*** *PIN4:GUS seedlings were treated for 1 or 2 days and histochemical stained prior light microscopic analysis.* ***(B)*** *Col0 seedlings were treated for 6h or 1 day before cotyledons were separately harvested and RNA levels were analyzed by qPCR. Bars represent mean +- s.d., Students t-test was performed for Statistics, n = 3 biological replicates, * = p < 0.05*

Monitoring *PIN4:GUS* transcriptional reporter revealed expression in the petiole and cotyledon vasculature as well as in the hypocotyl under oAT (Figure 12A). After 1 day of hAT treatment, we observed a significant reduction in *PIN4:GUS* staining in the petiole and cotyledon vasculature as well as in the hypocotyl (Figure 12A). However, similarly as *PIN3*, after 2 days at hAT, *PIN4:GUS* expression in the vasculature of petioles and cotyledons recovered (Figure 12A). RT-qPCR analysis of cotyledons revealed a slight repression of *PIN4* expression after 6h, and no significant change after 1 day at hAT when compared to oAT (Figure 12B). When we analyzed *PIN4:PIN4:GFP* translational reporter by confocal microscopy, we noticed a general weak and blurry signal (data not shown). Therefore, we could not perform reliable experiments with this line.

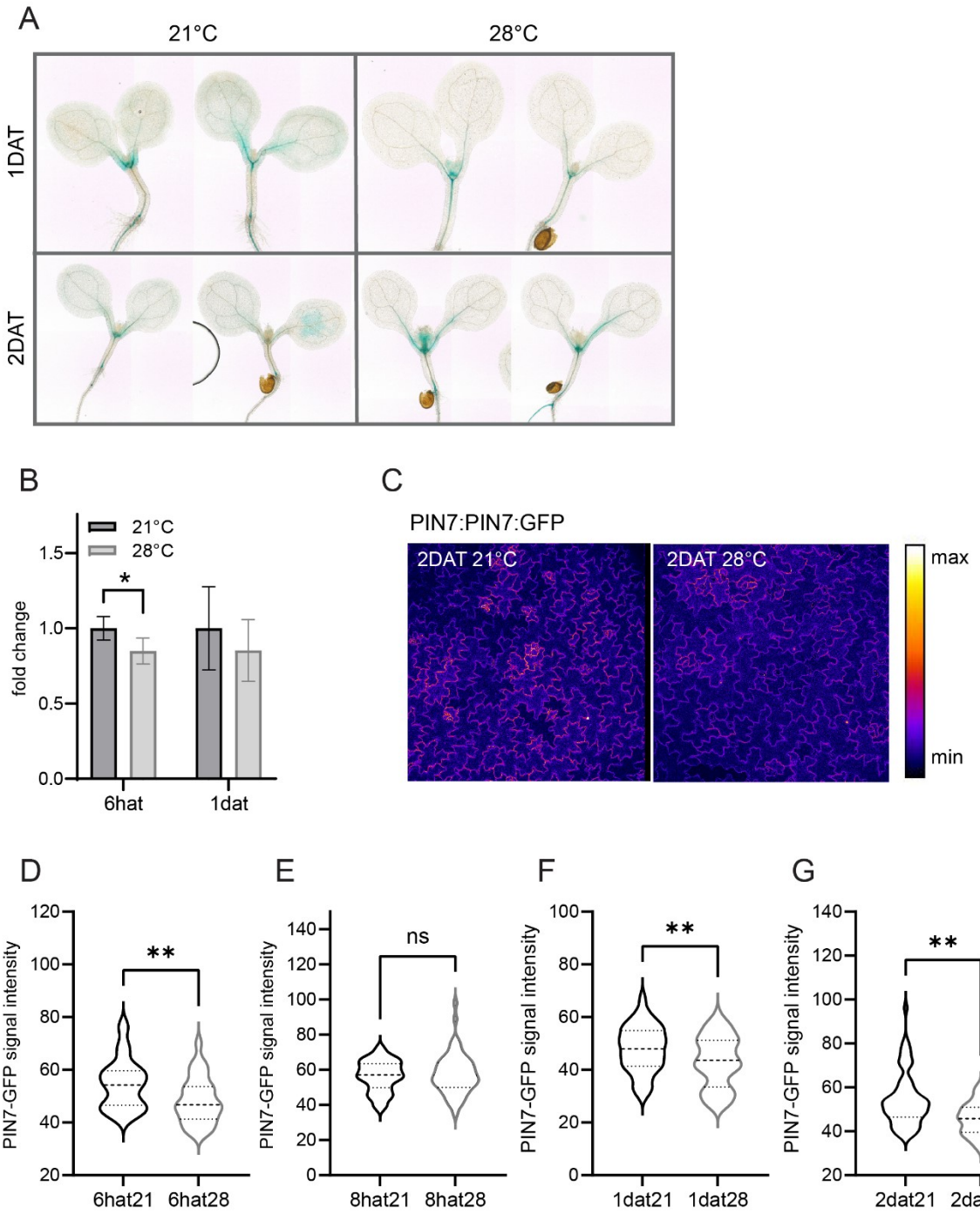

Figure 13: ***Adjustment of PIN7 expression in the cotyledon upon hAT.*** *5 day old seedlings were transferred to 21°C (oAT) versus 28°C (hAT)* ***(A)*** *PIN7:PIN7:GUS seedlings were treated for 1 or 2 days and histochemical stained prior light microscopic analysis.* ***(B)*** *Col0 seedlings were treated for 6h or 1 day before cotyledons were harvested and RNA levels were analyzed by qPCR. Bars represent mean +- s.d., n = 3 biological replicates* ***(C-G)*** *PIN7:PIN7:GFP in cotyledon was analyzed by confocal microscopy after different time points of treatment.* ***(D-G)*** *Violin plot represents median as dashed lines and quartiles as dotted lines, Students t-test was performed for Statistics, n > 10 cotyledons with at least 5 cells each, ** = p < 0.01, ns = p > 0.05*

Unfortunately, expression of *PIN7:GUS* transcriptional reporter was too low to observe reliable staining in the shoot, therefore we used *PIN7:PIN7:GUS* translational fusion to obtain a spatial information about *PIN7* expression in the cotyledon. Under oAT, we detected *PIN7* expression in the cotyledon pavement cells and in the petiole epidermis and vasculature (Figure 13A). After 1 day at hAT, we found decreased PIN7:GUS staining in the cotyledon epidermis and petioles when compared to control conditions (Figure 13A).

After 2 days of hAT, PIN7:GUS staining was visibly enhanced in the petioles and primary leaves when compared to oAT (Figure 13A). Using RT-qPCR, we detected a modest but significant reduction in *PIN7* expression in the cotyledon after 6 hours, while no significant differences were detected after 1 day of hAT versus oAT (Figure 13B). To analyze PIN7 protein abundance we took advantage of the *PIN7:PIN7:GFP* translational reporter line. Similar to PIN3:GFP, we found PIN7:GFP signal homogenously distributed in the cotyledon pavement cell membranes (Figure 13C), thus we measured PIN7:GFP signal in the same way as for *PIN3:GFP*. After 6h, 1day and 2 days of hAT treatment we detected reduced PIN7:GFP protein levels, while no significant reduction was observed after 8h when compared to oAT (Figure 13D-G). Even though PIN7:GFP expression was not significantly decreased after 8h of hAT treatment we could still see the trend of reduction compared to oAT (Figure 13E).

In summary, we observed that at early phase of adaptation to hAT, which correlates with the phase of accelerated hypocotyl elongation growth (Figure 2), transcription of *PIN3*, *PIN4* and *PIN7* in cotyledons is attenuated. Accordingly, reduced abundance of PIN3:GFP and PIN7:GFP at membranes of cotyledon epidermal cells was detected. At the later time points, corresponding to transition of hypocotyl growth into the phase of steady state, *PIN* transcription recovers to the levels comparable or higher than to those detected oAT.

Effect of hAT on *PIN* expression in the hypocotyl

To determine *PIN* expression and protein adjustment in different cell layers of the hypocotyl during response to hAT, we monitored *PIN:GUS* transcriptional and *PIN:PIN:GFP* translational reporter lines in combination with RT-qPCR analyses.

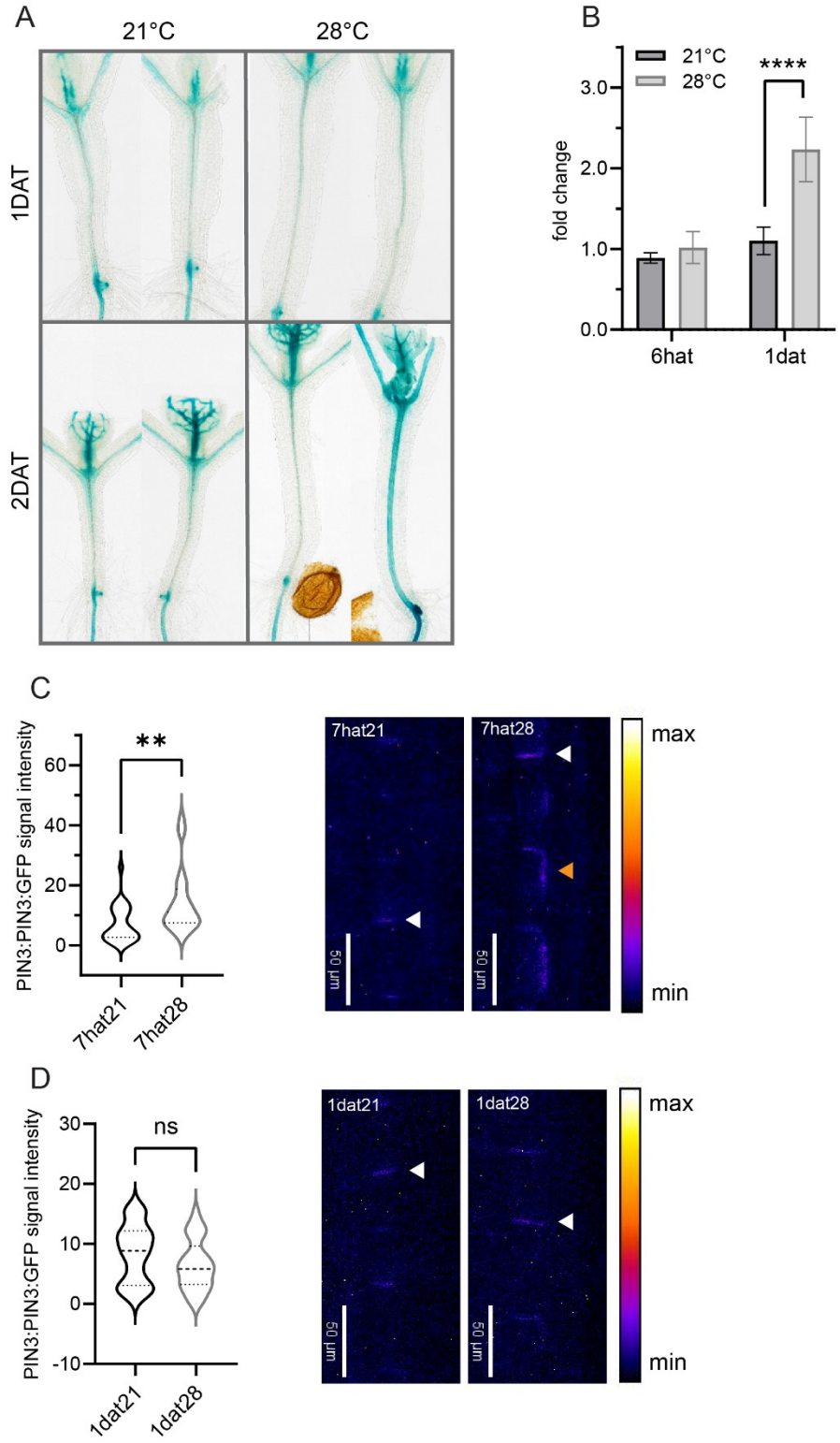

Figure 14: ***Adjustment of PIN3 in the hypocotyl upon hAT,*** *5 day old seedlings were transferred to 21°C (oAT) versus 28°C (hAT)* ***(A)*** *PIN3:GUS seedlings were treated for 1 or 2 days and hypocotyl was histochemical stained prior light microscopic analysis.* ***(B)*** *Col0 seedlings were treated for 6h or 1 day before hypocotyls were harvested and RNA levels were analyzed by qPCR. Bars represent mean +- s.d., n = 3 biological replicates, **** = p < 0.0001* ***(C-D)*** *endodermal PIN3:PIN3:GFP in the hypocotyl was analyzed by multiphoton microscopy after* ***(C)*** *7h or* ***(D)*** *1 day of treatment. Basal membrane signal was measured and represented by violin plot with median as dashed lines and quartiles as dotted lines, n > 4 hypocotyls, ** = p < 0.01, ns = p > 0.05. Pictures on the right side show endodermal PIN3:PIN3:GFP where white arrow mark basal and orange arrow mark lateral signal localization.*

Histochemical staining of *PIN3:GUS* reporter line revealed a weak expression in the hypocotyl vasculature under oAT (Figure 14). While no significant change in expression pattern of *PIN3:GUS* after 1 day of hAT was observed, we detected a visible induction after 2 days at hAT compared to oAT (Figure 14A). RT-qPCR revealed no change in *PIN3* expression within first 6 hours, but 2 fold increase after 1 day of hAT compared to oAT (Figure 14B). To determine effect of hAT on PIN3 protein abundance, we used *PIN3:PIN3:GFP* reporter. Using multiphoton microscopy we were able to detect a weak PIN3:GFP signal on the basal membrane of endodermal cells in the hypocotyl at oAT (Figure 14C-D). In hypocotyls exposed for 7h to hAT, PIN3:GFP signal accumulated on the lateral and significantly increased on basal membranes of endodermal cells compared to oAT (Figure 14C). After 1 day of hAT treatment, PIN3:GFP signal on lateral membranes of endodermal cells was under detection limit and no significant difference in PIN3-GFP accumulation on basal membranes of endodermal cells when compared to oAT could be detected (Figure 14D). Hence, in the endodermal cells at hAT PIN3 protein transiently increases on the basal membranes and lateralizes towards the cortex. Thereby, it presumably re-direct flow of auxin towards outer tissues to promote hypocotyl growth.

In addition to the endodermis, we detected PIN3:GFP signal in the hypocotyl epidermis, where it localized to the basal and radial cell membranes (Figure 15F). At oAT, PIN3:GFP signal distribution followed a gradient like pattern with the maximum on the hypocotyl apex (cell Nr20, Figure 15) gradually decreasing towards base (cell Nr1, Notably, at 2 day after transfer to hAT auxin response in all epidermal cells reached equal levels, unlike hypocotyls exposed to oAT where graded auxin distribution gradually increasing from apex towards base was detected (Figure 6F).

15). When we compared the level of PIN3:GFP signal at the basal and the radial membrane in individual epidermal cells, we did not detect any significant difference (data not shown). We assume that the radial localization of PIN3 is important for radial distribution of auxin, but not for longitudinal transport of auxin along the hypocotyl growth axis, which might be more critical for establishment of epidermal cell elongation pattern (Figure 3). Therefore, we decided to focus on the PIN3:GFP signal at the basal side in hypocotyl epidermal cells. After 8 hours at hAT, we observed a significant reduction in PIN3:GFP signal in the epidermal cells close to the hypocotyl apex compared to oAT (Figure 15A).

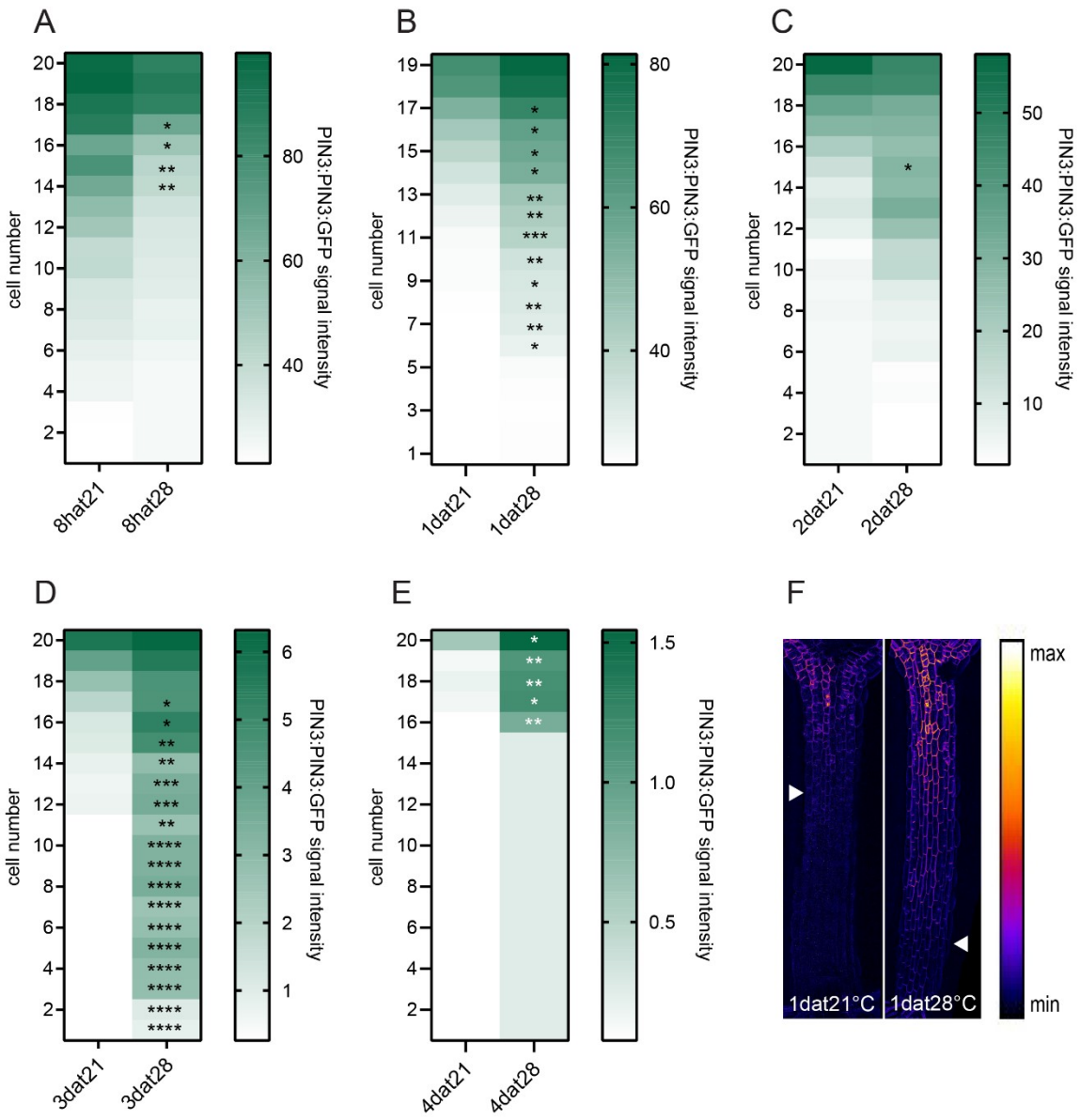

Figure 15: ***Adjustment of PIN3:PIN3:GFP expression in the hypocotyl epidermis upon hAT.*** *5 days old PIN3:PIN3:GFP reporter seedlings were transferred to either 21°C (oAT) versus or 28°C (hAT) for different time points as indicated (hat and dat - hours and days after transfer, respectively) prior analysis by multiphoton microscopy.* ***(A-E)*** *PIN3-GFP signal at basal membranes in the hypocotyl epidermal cells was measured and mean values were plotted in heat map according to its position along the hypocotyl growth axis, where cell1 and cell 20 are the most bottom and top cells respectively. Students t-test was performed for statistics, n > 4 hypocotyls, **** = p < 0.0001 *** = p < 0.001, ** = p < 0.01, * = p < 0.05.* ***(F)*** *Representative images of hypocotyl after 1 day of treatment at oAT and hAT. White arrows mark end of PIN3:GFP signal expression zone.*

After 1day at hAT, PIN3-GFP signal at plasma membrane of epidermal cells consistently increased when compared to oAT, and the zone of PIN3-GFP expression expanded towards hypocotyl base

(Figure 15B). PIN3:GFP signal remained increased also at later time points including 4 days of hAT incubation compared to oAT (Figure 15D-E).

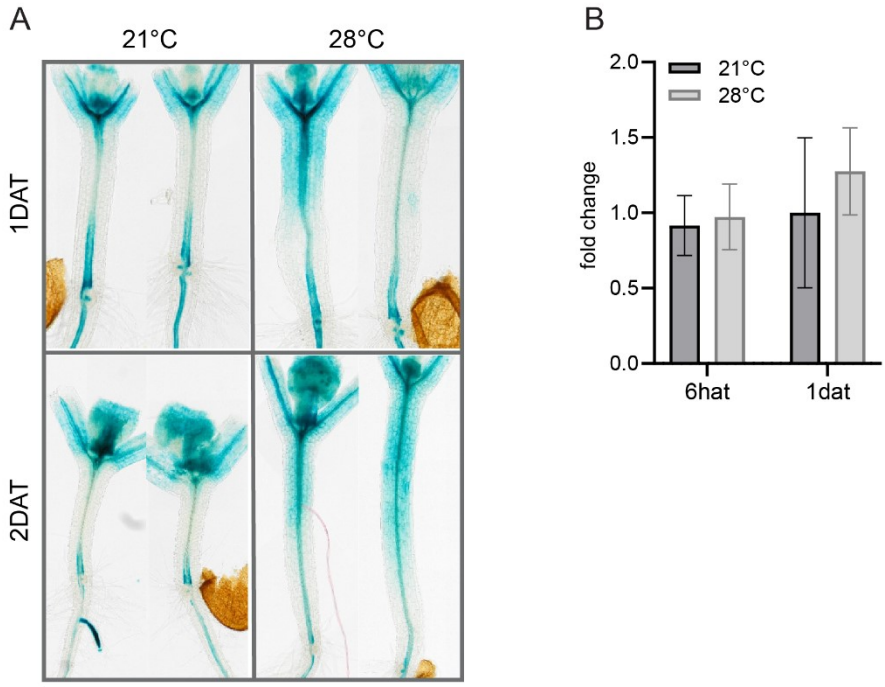

Figure 16: ***Adjustment of PIN7:PIN7:GUS expression in the hypocotyl upon hAT.*** *5 day old seedlings were transferred to 21°C (oAT) versus 28°C (hAT)* ***(A)*** *PIN7:PIN7:GUS seedlings were treated for 1 or 2 days at hAT versus oAT and hypocotyl were histochemical stained prior light microscopic analysis.* ***(B)*** *Col0 seedlings were treated for 6h or 1 day before hypocotyls were harvested and RNA levels were analyzed by qPCR, bars represent mean +- s.d. Students t-test was performed for Statistics, n = 3 biological replicates*

Histochemical analysis of *PIN7:PIN7:GUS* reporter revealed enhanced staining in the outer cell layers and vasculature in the middle and upper zones of hypocotyls exposed for 1 and 2 to hAT compared to oAT (Figure 16A). However, we could not observe any significant changes in *PIN7* expression in the hypocotyl by RT-qPCR analysis after 6h or 1 day of hAT versus oAT incubation (Figure 16B). To determine the effect of hAT on PIN7 protein abundance, we monitored *PIN7:PIN7:GFP* reporter at hAT versus oAT by multiphoton microscopy.

Under oAT, similarly to PIN3:GFP, we found PIN7:GFP expression in hypocotyl epidermis with the maximum signal at the hypocotyl apex gradually decreasing towards the hypocotyl base (Figure 16E). Likewise, we detected PIN7:GFP on the basal and lateral membranes of epidermal cells, and quantified PIN7-GFP on the basal membranes. 6h after transfer to hAT, PIN7:GFP signal intensity increased in all parts of hypocotyls when compared to oAT (Figure 16B).

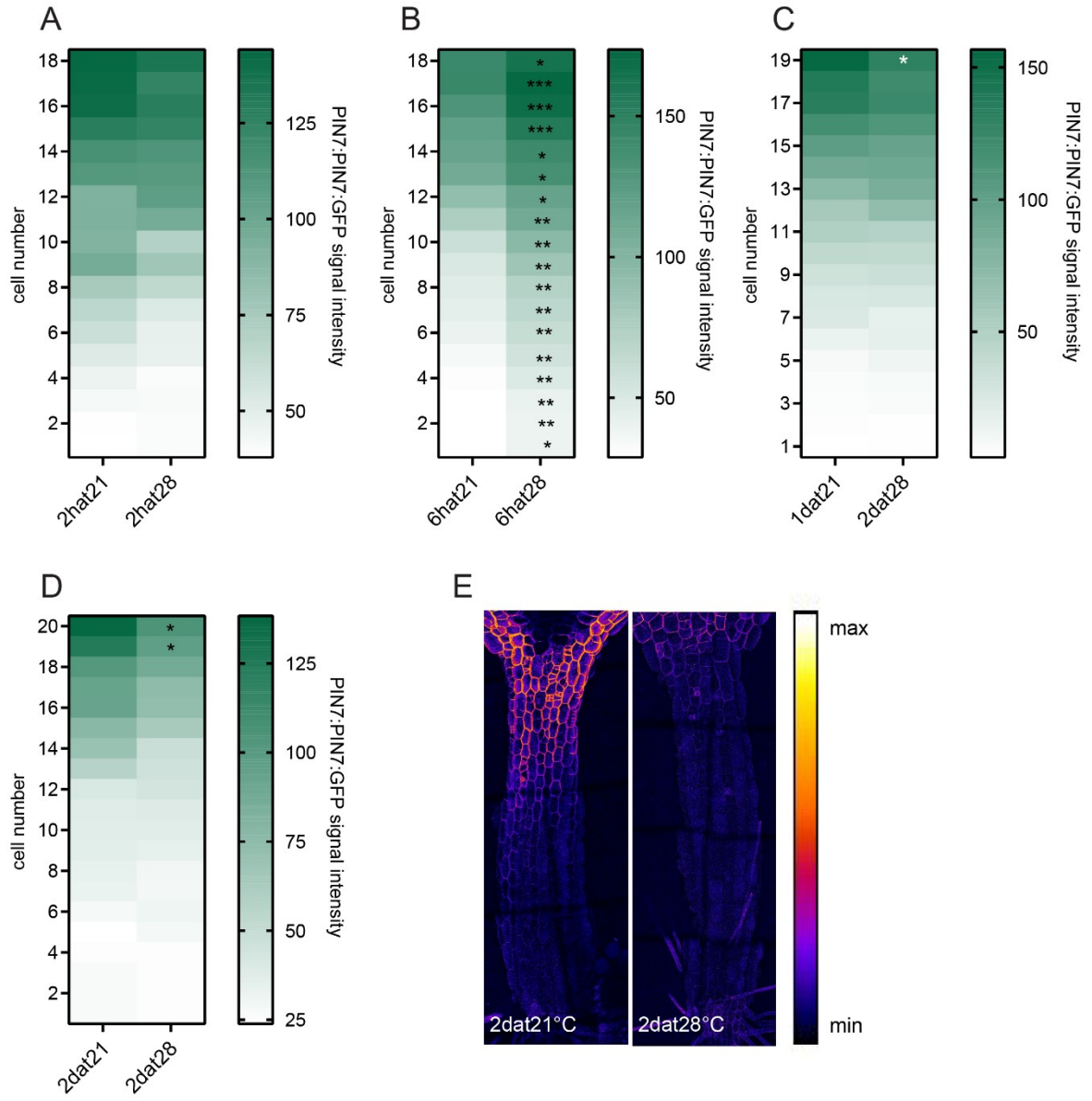

Figure 17: ***Adjustment of PIN7:PIN7:GFP expression in the hypocotyl epidermis upon hAT.*** *5 day old PIN7:PIN7:GFP reporter seedlings were transferred to 21°C (oAT) versus 28°C (hAT) for different time frames prior analysis by multiphoton microscopy.* ***(A-D)*** *basal membrane signal in the hypocotyl epidermis was measured and mean values were plotted in heat map according to its position within the hypocotyl where cell1 is the most bottom cell and cell 20 the most top at the hypocotyl apex. Students t-test for statistics, n > 4 hypocotyls, *** = p < 0.001, ** = p < 0.01, * = p < 0.05* ***(E)*** *representative picture of hypocotyl after 1 day treatment. White arrows mark end of PIN7:GFP signal expression zone.*

However, at later time points, exposure to hAT led to gradual decay of PIN7:GFP protein and after 2 days at hAT, PIN7:GFP signal at upper part of hypocotyls was significantly decreased when compared to oAT (Figure 16C-D). While analyses of *PIN7:PIN7:GUS* and *PIN7:PIN7:GFP* reporters

consistently support enhancement of PIN7 expression after transfer to hAT, discrepancy detected at later time points might reflect different dynamics of PIN7:GUS and PIN7:GFP turnover. This needs to be dissected by additional analyses.

In summary, upon hAT PIN3-GFP signal at lateral and basal cells of endodermis as well as in epidermal cells increases when compared to oAT. In contrast, PIN7:GFP expression in epidermis, after transient increase (at 6h), tends to decline after 1 day of transfer to hAT. Altogether, these data show that in response to hAT auxin transport in hypocotyls might be fined-tuned through modulation of expression patterns of individual PINs.

Discussion

When plants experience a mild increase in temperature up to 29°C, they adjust their development by enhancement of petiole growth, hyponastic leaf movement, narrowing of leaf width and induction of hypocotyl growth (Casal & Balasubramanian, 2019). These so called thermo-morphogenic responses are improving plant cooling capacity (Crawford et al., 2012).

Arabidopsis hypocotyl growth response to hAT

Increased hypocotyl growth in Arabidopsis wt seedlings upon hAT compared to optimal temperature has been firstly reported many years ago (Gray et al., 1998). Interestingly, hAT response in the hypocotyl was mostly monitored during 4 days, later time points were never closely investigated. To explore hypocotyl growth response upon sudden hAT treatment over a longer time frame, we grew seedlings for 5 days at oAT and subsequently transferred them at Zeitgeber 2 to hAT versus oAT with daily monitoring. After 1, 2 and 3 days we observed a significant increase in hypocotyl length at hAT versus oAT (Figure 2A). Accordingly, hypocotyl growth rate was significantly elevated at the first and second day of hAT treatment. (Figure 2B). From day 3 on, hypocotyl elongation ceased and no difference in growth rate could be observed when compared to hypocotyls at oAT (Figure 2C).

These results suggest that hypocotyl growth response to hAT might encompass two phases. In the first phase starting from the time of transfer to hAT, hypocotyl growth is strongly enhanced. In the second phase starting between 3-4 days after transfer to hAT, no hypocotyl growth can be detected compared to earlier time points of hAT treatment, suggesting feedback mechanisms that might prevent exaggerated elongation growth.

Induction of hypocotyl growth at hAT is mainly driven by induction of cell elongation rather than additional cell divisions (Bellstaedt et al., 2019; Gray et al., 1998). After 4 days of transfer from 20°C to 29°C, increased cortex cell length was found in the middle and top part of the hypocotyl compared to 20°C (Bellstaedt et al., 2019). Based on our observation, hAT treated seedlings reached its maximum hypocotyl length after 3-4 days (Figure 2A), which overlaps with the time

point of observations by Bellstaedt and co-workers. To assess spatio-temporal pattern of cell elongation during the first phase of hypocotyl growth response at hAT (0-2dat), we quantified epidermal cell length. We found that initially, during the first day of hAT treatment, epidermal cells in the middle part of hypocotyl elongated most (Figure 3A-B), followed by elongation of cells at hypocotyl apex at day 2 (Figure 3C-D). Thus, acceleration of hypocotyl growth in response to hAT appears to be driven by gradual expansion of epidermal cells from middle towards hypocotyl apex.

While hypocotyl growth during hAT response is solely driven by cell elongation (Figure3, within the first 2 days), seedlings grown in the darkness promote cell expansion in the middle and hypocotyl base, but carefully balance cell growth and division around the apex to enable hook formation (Deepika, Ankit, Sagar, & Singh, 2020; Žádníková et al., 2010). Under shade conditions, when seedlings are exposed to photosynthetically active wavelength-depleted light, hypocotyl growth is mainly facilitated by epidermal cell elongation similar to hAT (L. Ma & Li, 2019). Even though hAT and shade are both sensed by the same mechanism and partially share similar downstream signaling components (Franklin et al., 2014), hypocotyl growth response to shade is much faster and adjustment of cell growth pattern during SAR presumably following different pattern compared to hAT (Das, St Onge, Voesenek, Pierik, & Sasidharan, 2016). Thus, it would be interesting to carefully investigate the spatio-temporal modulation of epidermal cell growth under both stress conditions to see, whether they follow similar dynamic.

Auxin and auxin transport during hAT response

With increasing temperature, plants activate auxin synthesis genes *YUC8* and *YUC9* in cotyledons via PIF4, thereby increasing local accumulation of auxin (Bellstaedt et al., 2019; Stavang et al., 2009). We confirmed published data by gene expression analysis and monitoring of different auxin signaling reporter lines. Within one day, auxin synthesis gene *YUC8* was significantly induced (Figure 4G). Already within the first 4-6 hours and 1 day after hAT, we observed a significant upregulation of DR5:nlsGFP signal intensity in the cotyledons (Figure 4A-C). During this time frame hypocotyl growth rate is strongly induced upon hAT compared to oAT (Figure 2B).

Measurements of endogenous auxin levels in seedlings grown at hAT revealed elevated auxin levels in the hypocotyl at 29°C compared to 20°C (Gray et al., 1998). We investigated local adjustment of endogenous auxin metabolism after transfer to hAT by analysis of auxin metabolites in cotyledons and hypocotyl separately after 1 day at hAT versus oAT (Figure 5B). Enhancement of endogenous auxin level and decline of auxin precursor IPyA (Figure 5B) points towards YUC dependent pathway as main auxin synthesis route during hAT response.

During SAR, adjustment of local auxin signaling in the hypocotyl epidermis was shown within 60 minutes (Kohnen et al., 2016). Zheng at co-workers detected visibly induced auxin response a few days after transfer from 22°C to 29°C by analysis of *DR5:GUS* reporter line (Zheng et al., 2016). In addition, a general increase in auxin signaling response (IAA29) was reported in the hypocotyl upon hAT by qPCR (Bellstaedt et al., 2019; Stavang et al., 2009; Zheng et al., 2016). Our attempts to quantify auxin metabolites in hypocotyls did not reveal any significant alterations after 1 day of hAT versus oAT (Figure 6B). Because of low IAA levels detected in the hypocotyl compared to cotyledon at oAT, we suggest usage of more hypocotyls to obtain reliable results. To determine spatio-temporal pattern of auxin response in the hypocotyl after hAT treatment, we monitored *DR5:nlsGFP* reporter line after different incubation times of hAT versus oAT. Previous studies showed that blocking of auxin signaling in the hypocotyl epidermis inhibits shade and hAT triggered hypocotyl growth (S. Kim et al., 2020; Procko et al., 2016). In addition, many auxin early response genes including *SAURs* were specifically induced by shade in *Brassica* hypocotyl epidermis (Procko et al., 2016). Thus, we decided to focus our auxin signaling analysis on the hypocotyl epidermis, where hAT induced cell elongation was observed (Figure 3). Under oAT, we found significantly higher *DR5:nlsGFP* level in cells close to the hypocotyl base (1till2) compared to others (Figure 6A). This auxin signaling pattern is in accordance with the longer epidermal cells at the hypocotyl base at oAT (Figure 3). After 5h of hAT treatment, auxin signaling was gradually enhanced close to the hypocotyl apex compared to oAT (Figure 6B,G). Exposure to hAT for 2 days significantly increased auxin signaling in such a way, that all epidermal cells finally reached similar response levels (Figure 6D,F-G).

In accordance with the gradual adjustment of auxin signaling in the hypocotyl epidermal cell layer (Figure 6), the observed changes in cell elongation pattern (Figure 3) suggest modulation of auxin

distribution coordinating spatio-temporal cell growth during the first phase of hypocotyl response to hAT.

Auxin can induce hypocotyl growth when applied exogenously (Chapman et al., 2012; Du et al., 2018) or through constitutive overexpression of auxin synthesis gene such as *YUC4* that results in increase of endogenous levels of auxin (Munguía-Rodríguez et al., 2020). However, when auxin transport is blocked by application of NPA in *YUC4* overexpressing seedling, hypocotyl growth is repressed, hinting at important role of auxin transport in this process (Munguía-Rodríguez et al., 2020). In general, auxin is mainly synthesized in young leaves and further transported across all plant organs (Ljung, Bhalerao, & Sandberg, 2001). However, in recent reports application of auxin on cotyledons and leaves failed to trigger hypocotyl growth (Bellstaedt et al., 2019), but positively affected hyponastic leaf movement (Michaud et al., 2017). We demonstrated that local application of 1mM and 10mM NAA on cotyledon induces hypocotyl growth at oAT (Figure 7). We assume, that usage of more stable and easier up taken NAA instead of IAA together with lanolin results in stronger hypocotyl growth response compared to DMSO (Hošek et al., 2012). Together with previous data, these results point towards the important role of auxin transport from the cotyledon towards the hypocotyl thus enabling hypocotyl growth response.

At hAT, repression of PIN-mediated auxin transport by NPA inhibit hypocotyl growth compared to oAT (Zheng et al., 2016) and local inhibition of auxin transport in the petioles at 29°C block hypocotyl elongation (Bellstaedt et al., 2019). Additionally, when cotyledons are dissected, hAT fails to induce hypocotyl growth, suggesting the importance of cotyledon derived auxin for modulation of hypocotyl growth response (Bellstaedt et al., 2019). All these findings collectively show that auxin transport from the cotyledon towards the hypocotyl is of utmost importance for hAT induced hypocotyl growth response. We decided to dissect the role of auxin transport in cotyledons versus hypocotyl at hAT triggered hypocotyl growth response to understand their local importance in this process. Specific application of NPA on cotyledon right before transfer to hAT resulted in significant reduction in hypocotyl growth already after 1 day compared to DMSO

(Figure 8A). After local inhibition of auxin transport via NPA treatment on the hypocotyl we observed significant reduction of hypocotyl growth after 3 days of hAT (Figure 8B).

Based on these results we hypothesize that adjustment of auxin transport in the cotyledon is highly important in the early hAT triggered hypocotyl growth response. Due to the delayed inhibitory effect of NPA in the hypocotyl on hAT triggered hypocotyl growth response we assume, that auxin transport within the hypocotyl is important, but less limiting as in the cotyledon.

Cotyledon vasculature is a well-known long distance transport route for different molecules and hormones in plants (De Schepper, De Swaef, Bauweraerts, & Steppe, 2013). To enable auxin loading onto the phloem for further transport to other organs, short distance transport mechanisms are essential to modulate auxin flow towards vasculature in cotyledon tissue. If those transport mechanisms are blocked in the cotyledon by NPA treatment, auxin remains spread all over the cotyledon (Munguía-Rodríguez et al., 2020). Thus we assume, that local blockage of short distance auxin transport in the cotyledon by NPA application (Notably, at 2 day after transfer to hAT auxin response in all epidermal cells reached equal levels, unlike hypocotyls exposed to oAT where graded auxin distribution gradually increasing from apex towards base was detected (Figure 6F).

8A) will inhibit the initial auxin redirection towards and loading onto the vasculature for further long distance transport towards the hypocotyl leading to severe attenuation of hypocotyl growth at hAT.

PIN proteins are auxin efflux carriers, facilitating polar short distance auxin transport in different plant organs (Křeček et al., 2009). Within this family, PIN1, PIN3, PIN4 and PIN7 are expressed in the cotyledon and hypocotyl, suggesting their involvement in auxin movement in these tissues (Adamowski & Friml, 2015). Some of them are implicated in SAR (Keuskamp et al., 2010) and hAT growth response in leaf petioles (Park et al., 2019). During SAR, *pin3* displays lower induction of hypocotyl growth compared to wt and *pin3/4/7* exhibits reduced hyponastic leaf movement (Keuskamp et al., 2010; Michaud et al., 2017). Interestingly, PIN1 does not seem to be a central player in those processes, as *pin1* did not show attenuated hyponastic leaf movement after shade

treatment (Michaud et al., 2017). In hAT response, only PIN3 has been implicated so far, as *pin3* exhibits repressed hyponastic leaf movement upon 28°C versus 23°C (Park et al., 2019).

To dissect the role of PIN proteins in hAT triggered hypocotyl growth response, we analyzed different *pin* mutant lines at hAT versus oAT. In contrast to *pin single* mutants, *pin3/4/7* displayed shorter hypocotyl already under oAT compared to wt (Figure 9A). Upon hAT we observed significantly reduced hypocotyl growth in *pin3*, *pin4* and *pin3/4/7* compared to wt (Figure 9B), whereas hypocotyls of *pin7* showed opposite response. Notably, *pin3*, *pin4* and *pin* triple mutant never reached the hypocotyl length of Wt, while *pin7* partially showed even longer hypocotyl as Wt when exposed to hAT over longer period (Figure 9D). Local treatment of *pin* mutant cotyledons with NAA revealed severely attenuated hypocotyl growth response in *pin3/4/7*, no alteration in *pin3*, slight enhancement in *pin4* and even stronger induction in *pin7* single mutant compared to wt (Figure 9E).

To confirm the involvement of PIN-dependent auxin distribution in hAT triggered hypocotyl growth on the cellular level, we investigated their epidermal cell elongation pattern after 1 day of hAT versus oAT. In accordance with the shorter hypocotyl length under oAT in *pin3/4/7* (Figure 9A), shorter hypocotyl epidermal cells were observed when compared to wt at oAT (Figure 10A,C). With increasing temperature, epidermal cell growth remained mostly unaffected in *pin3/4/7* compared to wt (Figure 10A,C). Upon hAT treatment, *pin3* and *pin4* mutants displayed significantly reduced epidermal cell growth in the middle hypocotyl compared to wt (Figure 10B). Interestingly *pin7* did not show any difference in hypocotyl length in the middle hypocotyl, but increased epidermal growth in the hypocotyl apex and base upon hAT treatment compared to wt (Figure 10B,C). While wt exhibited its typical increased hypocotyl epidermal cell growth in the middle of the hypocotyl upon 1 day of hAT, *pin7* displayed distinct cellular elongation response (Figure 10B,C).

In conclusion, we demonstrated the importance of PIN dependent auxin transport in hAT induced hypocotyl growth by chemical PIN inhibition via NPA and analysis of respective *pin* single and *pin* triple mutants. Additionally, we revealed the involvement of PIN3, PIN4 and PIN7 in establishment of epidermal cell elongation pattern, implicating their role in modulation of auxin

distribution within this process. While PIN3 role in hAT triggered hyponastic movement was reported (Park et al., 2019), relevance of PIN7 was never demonstrated in SAR or hAT response so far. In dark grown seedlings, *pin7* showed similar attenuated hook formation as *pin4,* but less severe when compared to *pin3* (Žádníková et al., 2010). Due to opposite cell elongation pattern and hypocotyl growth response in *pin7* mutant compared to *pin3* and *pin4* upon hAT treatment, we hypothesize about a specific function for PIN7 in coordinating auxin distribution. Altogether, these findings hint towards distinct roles for PIN3, PIN4 and PIN7 during hypocotyl growth adaptation to hAT.

Expression pattern of PIN proteins and their biological function during hAT response

PIN protein importance has been studied during SAR, where endodermal PIN3 in the hypocotyl was found to be lateralized, thus enhancing auxin transport towards the epidermis to induce epidermal cell growth (Keuskamp et al., 2010). Few years later, Park and co-workers demonstrated a role of PIN3 during hAT thermonastic leaf movement, where hAT triggered lateralization of endodermal PIN3. This change in PIN3 polarity promoted auxin flow towards the abaxial petiole epidermis, thus inducing local cell elongation and upward leaf movement (Park et al., 2019). However, detailed information about temporal adjustment of different PINs during hAT response in the hypocotyl has not been reported.

To determine spatio-temporal adjustment of PIN expression, we investigated their transcript and protein abundance after different time points at hAT versus oAT. Under oAT, *PIN3* expression was found in the cotyledon vasculature and less profound in hypocotyl vasculature (Figure 11A). After 1 day at hAT we observed a significant reduction of *PIN3* expression in the cotyledon vasculature while no obvious difference was observed after 2 days compared to oAT (Figure 11A). Analysis of *PIN3* expression in the cotyledon by qPCR revealed slight, but not significant induction after 1 day of hAT versus oAT (Figure 11B). PIN3:GFP protein was homogenously localized to the cotyledon pavement cell membrane under standard and hAT conditions (Figure 11C). Upon hAT treatment, we detected significant reduction of overall PIN3 protein abundance in the pavement cell membrane of cotyledon after 7h, 1day and 2 days compared to oAT (Figure 11D-F). Interestingly, we could not detect any significant difference in PIN3 protein abundance in the

second phase of hAT response, when hAT induced hypocotyl length reached its maximum (Figure 2A). Analysis of *PIN4:GUS* transcriptional reporter line revealed expression in the cotyledon, petiole and hypocotyl vasculature under oAT (Figure 12A). With increasing temperature, *PIN4* expression was visibly reduced after 1 day, but enhanced in the petiole and neighboring cotyledon vasculature within 2 days of hAT compared to oAT (Figure 12A). However, we could not observe an overall significant change in *PIN4* transcript level in the cotyledon or hypocotyl after 6h or 1 day of hAT versus oAT (Figure 12B-C). *PIN7* expression was observed in cotyledon epidermis as well as in vasculature and outer cell layers of the petiole at oAT (Figure 13A). 1 day after transfer to hAT, *PIN7* expression was reduced in the cotyledon epidermis and petiole, but induced in the petiole vasculature and the neighboring cotyledon vasculature after 2 days of hAT compared to oAT (Figure 13A). Similar to *PIN4,* we could not detect any general adjustment of *PIN7* transcript level in the cotyledon within 6h or 1 day of hAT compared to oAT by qPCR (Figure 13B). PIN7:GFP protein was found to be localized in the cotyledon pavement cell membrane homogenously distributed comparable to PIN3:GFP (Figure 13C). Analysis of PIN7 protein abundance revealed significant reduction after 6h, 1day and 2 days of hAT compared to oAT (Figure 13D, F-G).

In conclusion, *PIN3* and *PIN4* in the vasculature as well as *PIN3* and *PIN7* expression in the cotyledon epidermis was firstly attenuated, but subsequently enhanced in petiole and neighboring cotyledon vasculature during the first phase of hAT response. Due to homogenous localization pattern of PIN3:GFP and PIN7:GFP in cotyledon pavement cells, we assume their involvement in auxin distribution across the whole epidermis to ensure optimal hormone levels in all cells. During the first phase of hAT response, auxin flow needs to be redirected towards the vasculature, thus expression of epidermal PINs decline. In parallel, PIN3, PIN4 and PIN7 expression is enhanced upon hAT in cotyledon and petiole vasculature to presumably facilitate root-wards auxin transport. During second phase of hAT response, when hypocotyl reaches its maximum length (Figure 2A) we observed partial recovery of PIN3:GFP and PIN7:GFP in cotyledon pavement cells compared to oAT to reestablish homogenous epidermal auxin distribution.

According to the currently proposed model, auxin is transported along the cotyledon and petiole vasculature towards the hypocotyl during SAR and hAT response (Bellstaedt et al., 2019; Procko, Crenshaw, Ljung, Noel, & Chory, 2014). Once arrived to hypocotyl cylinder, auxin redirection towards the epidermis is facilitated by PIN proteins. During SAR, PIN3 was reported to refocus from the basal endodermal cells towards the lateral membrane facing the cortex layer, however the molecular mechanism behind remains unclear (Keuskamp et al., 2010). High ambient temperature was shown to induce *PIN3* transcription and protein abundance in the lateral membrane of endodermis on the abaxial (lower) side of leaf petioles, thus enabling local auxin accumulation in the abaxial petiole epidermis (Park et al., 2019). Interestingly a role for PIN proteins in auxin transportation specifically during hAT induced hypocotyl growth was not reported yet.

Histochemical analysis of *PIN3:GUS* reporter displayed staining in the hypocotyl vasculature and endodermis at oAT, which was not visibly affected after 1 day, but slightly enhanced around the hypocotyl cylinder after 2 days of hAT treatment compared to oAT (Figure 14A). Hypocotyl analysis by qPCR revealed significant 2,2 fold induction of *PIN3* expression after 1 day of hAT versus oAT (Figure 14B). On the protein level, we observed *PIN3:GFP* localized to the basal membrane of endodermal cells in the hypocotyl at oAT (Figure 14C-D). Exposure to hAT triggered PIN3:GFP protein lateralization towards the cortex cell layer after 6h treatment, which declined after 1 day of hAT compared to oAT (Figure 14C-D). Besides, we measured increased PIN3 protein abundance on the basal endodermal membrane upon 6h, which decreased after 1 day of hAT versus oAT (Figure 14C-D). In accordance with enhanced *PIN3* transcription in hAT treated hypocotyl versus oAT, we assume, that general enhancement of PIN3 on the basal endodermal membrane is due to transcriptional regulation upon hAT.

In parallel to the endodermal localization, *PIN3:PIN3:GFP* was detected on the hypocotyl epidermis, distributed in a gradient like pattern with the maximum on the hypocotyl apex (cell Nr20, Fig) gradually decreasing towards hypocotyl-root junction (Figure 15F). In the epidermal cells, PIN3 protein was localized to the basal and radial membrane, suggesting their role in radial and longitudinal auxin distribution along the hypocotyl growth axes respectively (Figure 15F). We focused our analysis on basal PIN3:GFP signal, which might be more critical for establishment of

epidermal cell elongation pattern in the hypocotyl. Within the first 8h of hAT treatment PIN3:GFP signal intensity was slightly reduced, but gradually enhanced after 1 day of hAT compared to oAT (Figure 15A-B). Notably we observed consistently increased PIN3:GFP protein abundance until 4 days of hAT (Figure 15B-E).

Histochemical analysis of *PIN7:PIN7:GUS* reporter revealed *PIN7* expression in the vasculature with the maximum on the hypocotyl apex and base at oAT (Figure 16A). After 1 day of hAT, we detected enhanced staining in the vasculature and outer cell layers of the hypocotyl apex, which was more profound after 2 days of hAT versus oAT (Figure 16A). On the protein level, PIN7:GFP showed similar epidermal membrane localization and gradual distribution as PIN3:GFP (Figure 17E). Similar to PIN3:GFP, we focused on analysis of PIN7:GFP basal signal. We detected gradual PIN7:GFP signal enhancement after 6h of hAT, which started to decline after 1 day of hAT versus oAT. (Figure 17A-B).

In conclusion, hAT treatment triggers elevated PIN3:GFP abundance on the basal and lateral membrane of endodermal cells in the hypocotyl. In the hypocotyl epidermis, PIN3 is significantly enhanced, while PIN7 is shortly elevated, but later on declines during the first phase of hAT response. We propose a model, where lateralized endodermal PIN3 pumps auxin from the inner cell layers towards the hypocotyl epidermis and PIN3 together with PIN7 coordinate auxin distribution along the epidermis to modulate local cell elongation. It was reported, that during hAT response, endodermal PIN3 is lateralized in petioles due to local activation of PID expression triggering PIN3 phosphorylation (Park et al., 2019). We hypothesize that hAT affect endodermal PIN3 lateralization in the hypocotyl endodermis via posttranslational mechanisms. Recent report demonstrated that hAT activate different kinases, which could potentially directly phosphorylate and consequently adjust PIN polarization during hAT response (Vu et al., 2021). The opposite adjustment of epidermal PIN3 and PIN7 abundance in the hypocotyl epidermis (Figure 15, Figure 17) together with the contrary hypocotyl phenotypes (Figure 9) and epidermal cell elongation patterns (Figure 10) of *pin3* and *pin7* point towards a particular and partially contrasting function for both proteins at hAT. Based on our results, we assume that the first enhancement of epidermal PIN7 facilitate auxin accumulation towards the middle part of the hypocotyl triggering local cell expansion (Figure 3) while PIN3 remains mostly unaffected upon hAT.

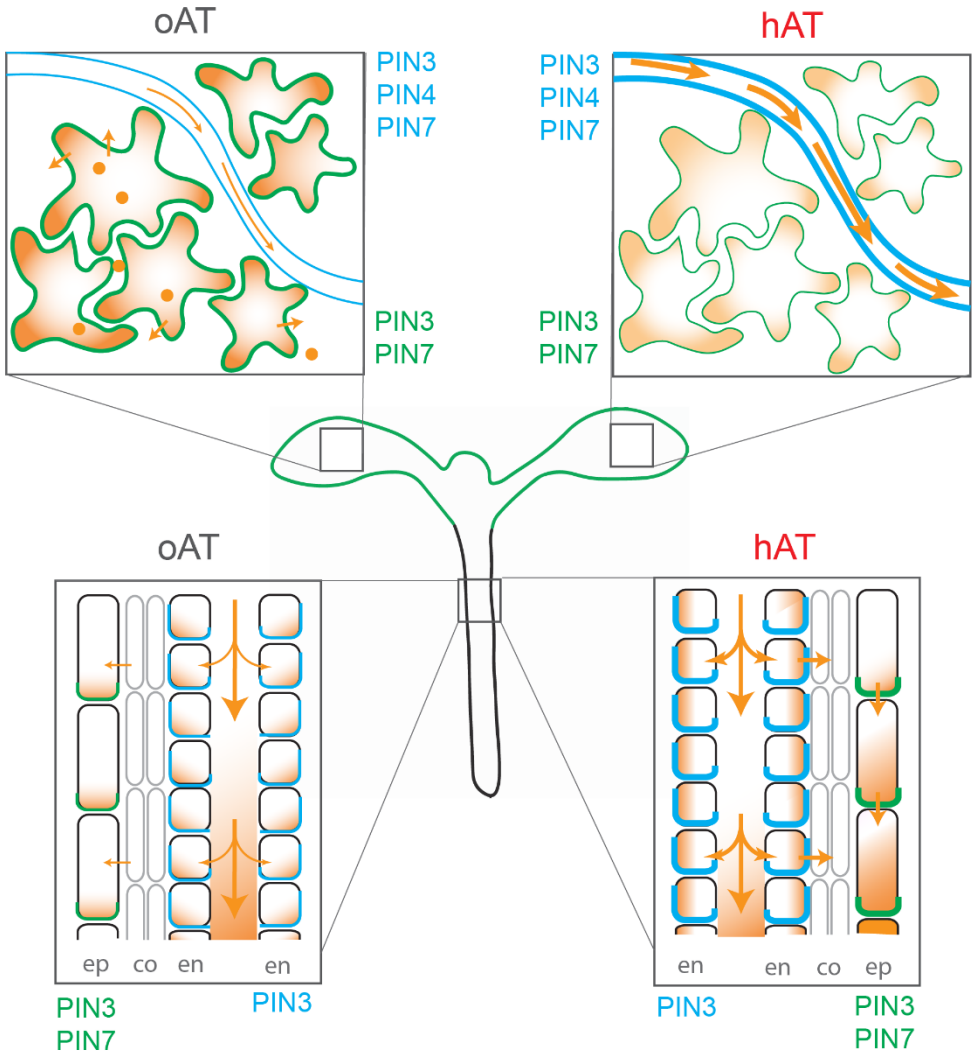

Figure 18: Figure 9: ***Schematic representation of PIN expression adjustment and auxin distribution during hAT response in Arabidopsis.*** *At oAT PIN3 and PIN7 within the cotyledon pavement cells ensure overall auxin distribution across the whole cotyledon. In the hypocotyl PIN3 in the endodermis mainly localized to the basal membrane partially restricts auxin transport towards the hypocotyl epidermis. Epidermal PIN3 and PIN7 transport auxin towards the hypocotyl base. Upon hAT, PIN3 and PIN7 in the cotyledon pavement cells are reduced, but their expression is increased in the cotyledon vasculature potentially facilitating auxin transport along the vasculature towards the hypocotyl. In the hypocotyl lateral PIN3 in the endodermis enhance auxin transport towards the epidermis where PIN3 and PIN7 readjust auxin distribution. Orange color represent auxin gradient, green color in the cotyledon mark PIN3 and PIN7 protein localization and expression pattern in the cotyledon pavement cell membrane and vasculature respectively, blue shows PIN3 localization in the hypocotyl endodermis.*

At the moment when PIN3 is increased, PIN7 starts to decline, thus enabling auxin accumulation towards the hypocotyl apex and equalizing auxin response level (Figure 6) and cell length pattern (Figure 3) in the whole hypocotyl epidermis during hAT response.

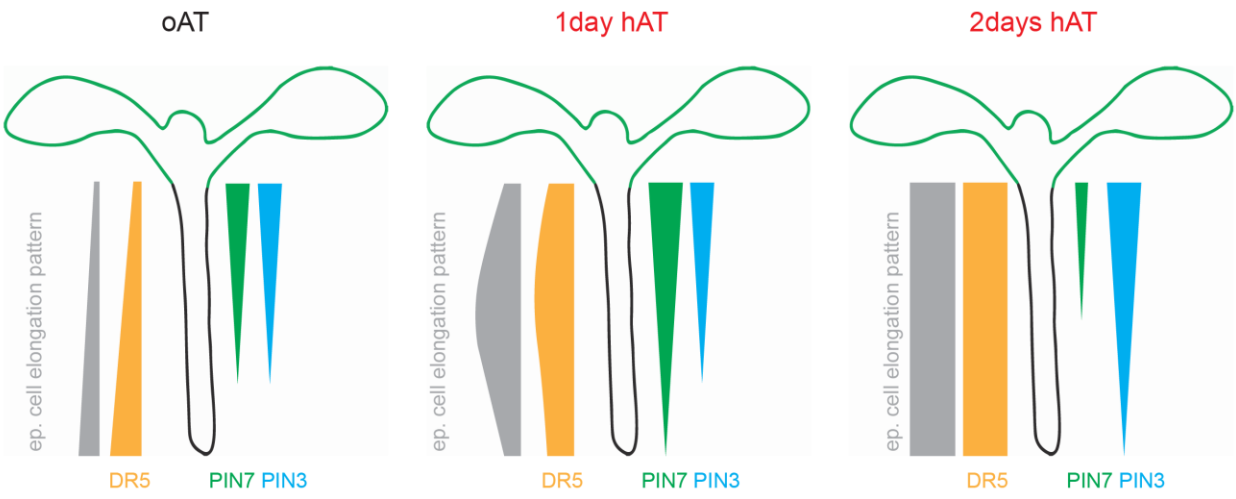

Figure 19: ***Schematic representation of spatio-temporal adjustment of PINs, Auxin response and cell elongation during hAT response*** *While auxin response and cell length maximum is at the hypocotyl base, PIN3 and PIN7 maximum expression level is on the hypocotyl apex at oAT. After 1 day of hAT epidermal cell growth and auxin response is mostly enhanced around the middle part of the hypocotyl, while PIN7 expression is gradually increased. After 2 days of hAT all epidermal cells reach similar length and auxin response, while PIN7 and PIN3 expression decline and increase respectively. PIN3 and PIN7 gradient in blue and green respectively, Auxin response (DR5) in orange and epidermal cell length in grey.*

Consequently, we propose epidermal *PIN7* and *PIN3* as important player for spatio-temporal modulation of auxin distribution and cell elongation pattern in the hypocotyl epidermis during hAT response.

Conclusion

In conclusion, we show that acceleration of hypocotyl growth by hAT is a spatio-temporally regulated process. We found that after exposure to hAT, seedlings enter phase of enhanced elongation characterized by gradual expansion of epidermal cells from middle part of hypocotyls towards apex. About three days after transfer to hAT, all epidermal cells reach the same length and hypocotyl growth ceases. This spatio-temporally controlled adjustment of hypocotyl growth to hAT is dependent on PIN-mediated transport. Notably, comprehensive analyses of PIN reporters revealed that expression pattern of PINs including PIN3, PIN4 and PIN7 is dynamically modulated during seedlings adaptation to hAT. However, what are the upstream factors that might fine-tune expression of *PINs* in response to hAT is largely unknown.

In the second part of my thesis, we address this question by performing in depth functional analysis of zinc-finger (ZF) factors, transcriptional regulators, which were identified in Y1H screen as direct regulators of *PIN* transcription (Šimášková et al., 2015).

ZFs and their role in hAT response

Introduction

Zinc-finger proteins (ZFPs) represent one of the largest transcription factor families in plants. As their name suggest they contain zinc-finger domains, which are composed of an α-helix and an antiparallel β-structure including a certain amount of cysteines and histidines holding a zinc atom enabling interacting with DNA (Takatsuji, 1999). According to the number and combination of cysteines and histidines per zinc-finger domain they are separated into different groups (Xie, Sun, Gong, & Kong, 2019). The C2H2 (2 cysteines and 2 histidines)- type ZFP subfamily is one of the largest ZFP families in plants which is split into three sets called A,B,C where set A and C are further split into A1-A4 and C1-C3 (Ciftci-Yilmaz & Mittler, 2008; Englbrecht, Schoof, & Böhm, 2004). Within the C subset C1 represents one of the evolutionary youngest and best studied families implicated in different developmental and stress related processes in plants (Xie et al., 2019). The C1-2i subclass contain only ZFPs with 2 zinc finger domains and represent one of the largest sub-classes involved in plant abiotic stress responses (Englbrecht et al., 2004). Most of the ZFPs within this sub-group contain a short repressive EAR domain. *ZF1*, *ZF2* and *ZAT10* together with *ZAT6*, *ZF3* and *ZAT13* are located in one clade in the ZFP phylogenetic tree (Xie et al., 2019). They were suggested to regulate expression of proteins by recognizing similar nucleotide motif (A(G/C)T-X3-4-A(G/C)T) in certain promoters (Ohta, Matsui, Hiratsu, Shinshi, & Ohme-Takagi, 2001).

In planta, ZF1 and *ZF2* expression was demonstrated in root and shoot (Sakamoto et al., 2004; Sakamoto, Araki, Meshi, & Iwabuchi, 2000). They are transcriptionally upregulated under various stress conditions and play an important role during water stress response (Sakamoto et al., 2004, 2000). In accordance with presence of the Abscisic acid (ABA)-responsive element (ABRE) in *ZF2* promoter, adjustment of *ZF2* expression and involvement in ABA dependent stress responses and seed germination was shown (Drechsel, Raab, & Hoth, 2010; Kodaira et al., 2011; Sakamoto et al., 2004).

Similar to *ZF2*, *ZAT10* is strongly expressed in various plant organs including root and shoot and is significantly enhanced upon different stress treatments including salt stress, osmotic stress,

drought, cold, reactive oxygen-species, as well as ABA (Mittler et al., 2006; Rossel et al., 2007; Sakamoto et al., 2004, 2000). Constitutive *ZAT10* overexpression plants exhibit growth retardation and enhanced tolerance to drought and photo-oxidative stress (Rossel et al., 2007; Sakamoto et al., 2004). Interestingly *zat10* single mutant show similar resistance to drought as *ZAT10* overexpressing seedlings (Mittler et al., 2006). In parallel, *ZAT10* is involved in cold stress response via C-REPEAT BINDING FACTORs (CBFs), the key regulatory transcription factors modulating cold responsive gene expression (Zhou, Shen, Wu, Tang, & Lin, 2011). Additionally *ZAT10* has been found as direct substrate for MITOGEN ACTIVATED KINASE (MPK) 3 and MPK6 during osmotic stress response (Nguyen et al., 2012). Elimination of the MPK3 and MPK6 phosphorylation sites in the ZAT10 protein results in similar osmotic stress sensitive phenotype as observed for *zat10* single mutant (Nguyen et al., 2016). Even though the biological relevance of EAR domain has been proposed (Sakamoto et al., 2004), elimination of the domain in ZAT10 protein does not affect osmotic stress tolerance *in planta* (Nguyen et al., 2012, 2016). Thus, the biological role of EAR motif for ZAT10 transcriptional function during various stress responses still remains to be elucidated.

Results

ZFs and their role in PIN regulation

We showed that PIN-mediated transport of auxin is required for proper hypocotyl growth response to hAT and that expression patterns of *PIN3*, *PIN4* and *PIN7* are adjusted to hAT (Figure 9, Figure 11-17) Interestingly, in Y1H screen for direct upstream regulators of *PIN* gene transcription, three members from the Zinc finger gene family, namely *ZAT10*, *ZF1* and *ZF2* were found to interact with *PCRE1* and *PCRE7* elements in promoters of *PIN1* and *PIN7* genes (Šimášková et al., 2015, unpublished results). All three genes belong to C1-2i subclass of ZF transcriptional regulators, which has been associated with plant adaptive responses to abiotic stresses (Xie et al., 2019). Thus, we considered them as a promising potential regulators of *PIN* expression in response to hAT. To corroborate that ZFs physically interact with *PIN* promoters, we performed chromatin Immunoprecipitation (ChIP) analyses followed by quantitative RT-PCR (ChIP-qPCR). Using this assay, we confirmed direct binding of ZF1 and ZAT10 to the *PCRE1* and *PCRE7* elements (Figure 20C, Krisztina Ötvös). To explore whether these transcriptional regulators might target also other homologues of *PIN* family, we extended analyses for *PIN3* and *PIN4*. Using specific primer combinations, we inspected enrichment for the short fragments spanning *PIN3* and *PIN4* promotors (Figure 20F). Increased enrichment detected for fragments R11-12, R14 in *PIN3* and R7, R9 in *PIN4* promoter suggest that ZFs might through direct transcriptional regulation of *PINs* contribute to fine tuning of polar auxin transport (Figure 20D-E).

To gain insight into the role of ZFs in regulation of *PIN* transcription, we performed a transient expression assay in *Arabidopsis* protoplasts. Co-expression of ZF1, ZF2 or ZAT10 with *PINs::LUCIFERASE* reporters in protoplasts resulted in dramatic decrease of luciferase activity compared to control *35S:LUC* (Figure 20B), suggesting that ZFs act as negative regulators of *PIN1*, *PIN4* and *PIN7* expression.

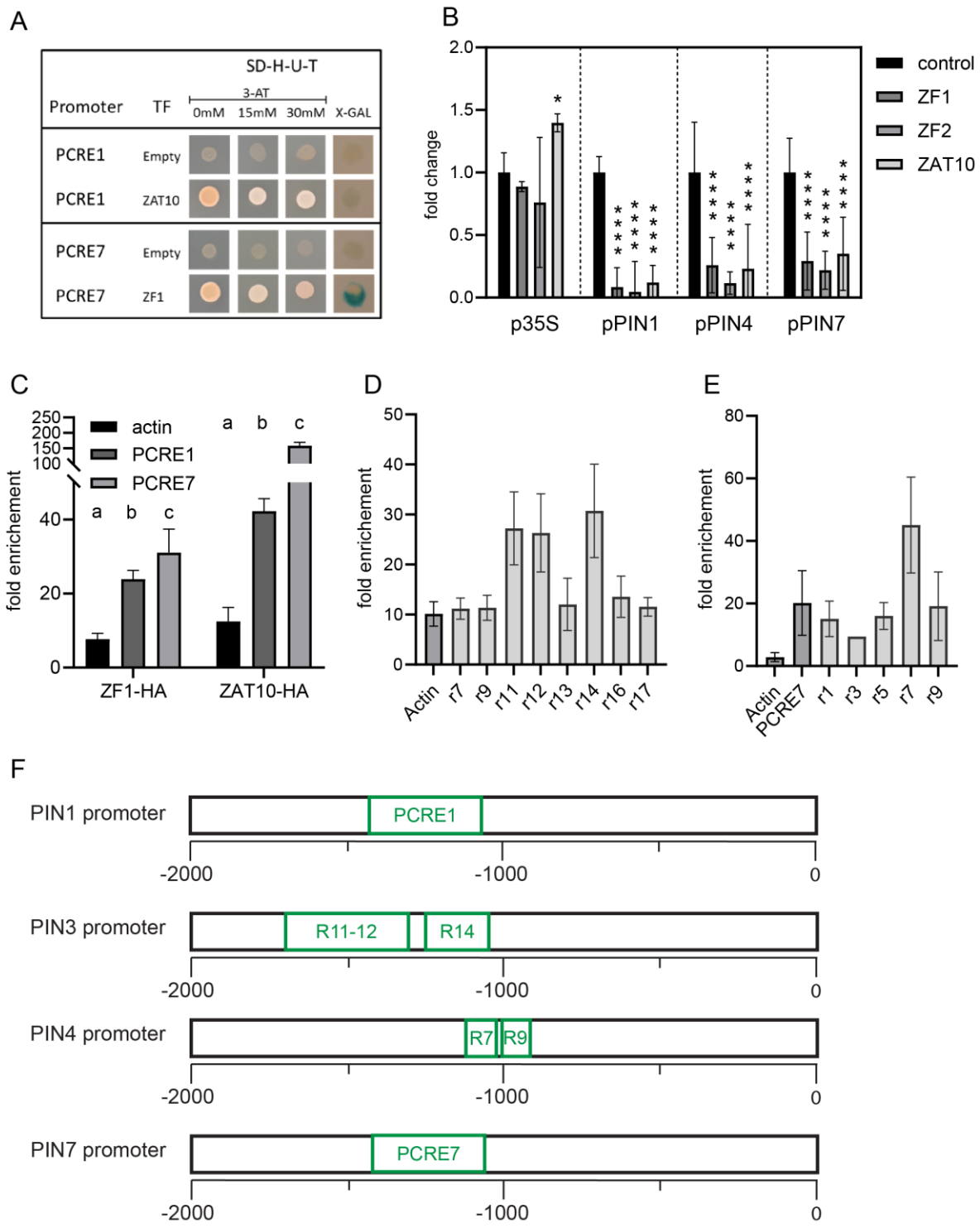

Figure 20: ***ZF proteins directly bind PIN promoter and repress PIN expression (A)*** *ZF1 and ZAT10 interaction with PIN promoter in an Y1H assay. Yeast cells were grown on SD-H-U-T minimal media without histidine (H), uracil (U) and tryptophan (T), supplemented with 3-amino-1,2,4-triazole (3AT).* ***(B)*** *ZFs transcription factors suppress PIN expression in transient protoplasts assay* ***(C-E)*** *Analysis of ZAT10 binding to* ***(C)*** *PIN1 and PIN7* ***(D)*** *PIN3 and* ***(E)*** *PIN4 promoter by Chromatin Immunoprecipitation (ChIP) analysis* ***(F)*** *representation of PIN promoters with binding regions marked in green (R1-9, PCRE1, PCRE7)*

To explore the role of ZFs in regulation of *PIN* expression *in planta,* we generated ZF-estradiol inducible overexpression lines (ZFoe). We decided for an inducible system due to previously reported problems with the selection of constitutive *ZAT10* overexpression lines (Sakamoto et al., 2004). After induction of *ZAT10* expression with 1uM estradiol, we found a significant repression of *PIN3*, *PIN4* and *PIN7* transcripts in shoots already after 3h with even stronger reduction after 6h when compared to DMSO treatment (Figure 21B,D). Interestingly, we did not detect any reproducible changes in *PIN1* transcription upon estradiol treatment compared to DMSO presumably due to low expression in the cotyledon tissue (Figure 21B,D). In addition, we observed a strong repression of *ZF1* expression in both estradiol treatments compared to DMSO. (Figure 21A,C). Similarly, like in shoots, induction of *ZAT10* in roots resulted in significant repression of *PIN3*, *PIN4* and *PIN7* transcription after 6h treatment with 1uM estradiol when compared to DMSO (Figure 21F). In addition, ZAT10 in roots attenuated transcription of *PIN2* and partially also of *PIN1* (Figure 21F). As shown for the shoot, we found that *ZF1* as well as *ZF2* expression was negatively affected by ZAT10 overexpression (Figure 21E), suggesting regulatory cross-talk among ZFs. However, we need to keep in mind, that in the estradiol inducible system we induce expression of the gene of interest ubiquitously in all organs and cells where the protein under normal conditions might not be present.

Altogether, based on this data, we conclude that ZFs act as negative transcriptional regulators of different *PINs* in shoot and root.

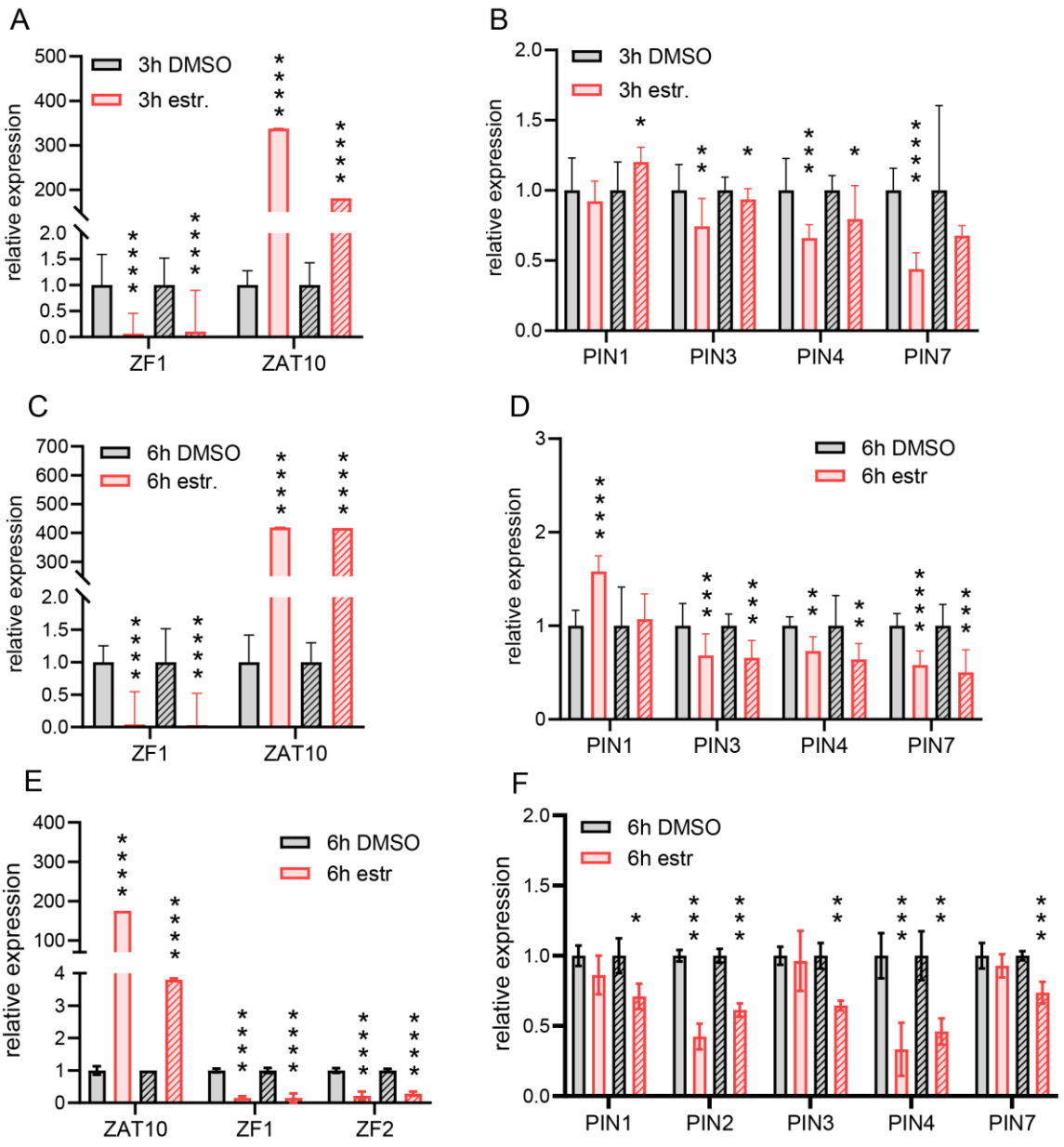

Figure 21: ***ZAT10 overexpression repress PIN expression in planta*** *5 day old estradiol inducible ZAT10 overexpression seedlings were treated with 1uM estradiol versus DMSO for different time frame prior separate harvesting of shoot and root and analysis by qPCR.* ***(A-B)*** *Incubation for 3h, analysis of shoot samples* ***(C-F)*** *Incubation for 6h, analysis of* ***(C-D)*** *shoot and* ***(E-F)*** *root. Bars represent mean +- s.d. with students t-test for statistical comparison to DMSO, n=3 biological replicates, **** = p < 0.0001 *** = p < 0.001, ** = p < 0.01, * = p < 0.05*

Regulatory function of ZFs EAR repression motif on PIN expression

The EAR motif represents one of the best known transcriptional repression motifs in plants (Kagale & Rozwadowski, 2011). Z1, ZF2 and ZAT10 belong to the C2H2 Zinc finger gene family carrying the EAR domain, thus they are proposed to act as repressors (Ohta et al., 2001). Sakamoto and co-workers showed that the repressive function of ZAT10 on *DREB1A* was compromised after removal of the DLN (EAR motif) amino acid sequence (Sakamoto et al., 2004). However, it remains unclear if the simple removal of the DLN amino acids might have a general effect on the overall protein function, thus resulting in declined repression of *DREB1A*. To test the involvement of the EAR motif in ZF negative regulatory activity on *PIN* expression, we converted the EAR corresponding DLN/L amino acid motif to AAA/A by site directed mutagenesis. Using protoplast assay, we tested repressing activity of mutated ZFs on *PIN::LUCIFERASE* reporters when compared to non-mutated variants. Mutated ZF proteins showed similar significant repressive effect on *PIN1* and *PIN7* promoter compared to wild-type ZF proteins (Figure 22A), thus EAR motif plays presumably less significant role in the negative regulatory function of ZFs on *PIN* expression.

ZF proteins were recovered in the Y1H screen using 200bp cis-regulatory elements *PCRE1* and *PCRE7* as a bait. These elements were found to determine cytokinin responsive transcription of *PIN1* and *PIN7* and their deletion in *ΔpPIN1:LUC* and in *ΔpPIN7:LUC* interferes with Cytokinin Reponse Factor2 (CRF2) and CRF6-mediated regulation of *PIN1* and *PIN7* expression (Šimášková et al., 2015). Unlike CRFs, ZF proteins were able to reduce Luciferase readout in the *pPIN1:LUC* and *pPIN7:LUC* as well as *ΔpPIN1:LUC* and *ΔpPIN7:LUC* constructs (Figure 22B,C), suggesting the presence of additional ZF binding sites in both *PIN1* and *PIN7* promoters. Consequently, we generated additional constructs with LUCIFERASE driven by promoter of *PIN1* and *PIN7* shortened to 795bp and 608bp upstream of ATG, respectively, to create *Δ1pPIN1:LUC* and *Δ1pPIN7:LUC* (Figure 22F). While *Δ1pPIN7:LUC* was not repressed by ZF1 compared to *pPIN7:LUC* (Figure 22D), we found a significant reduction of the reporter signal of *Δ1pPIN1:LUC* with all three ZF proteins compared to *pPIN1:LUC* (Figure 22E).

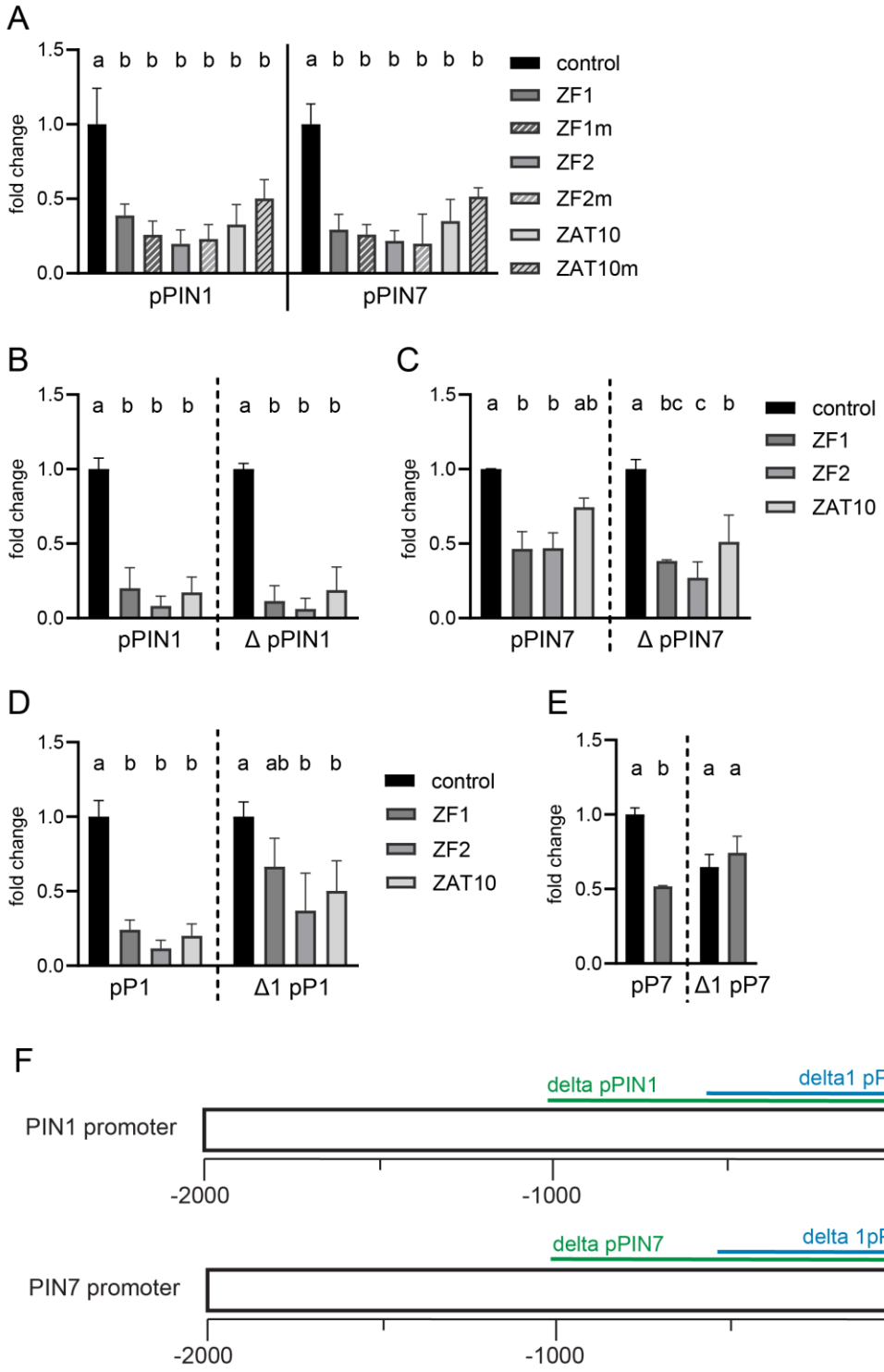

Figure 22: ***Functional role of EAR motif in PIN promoter binding and gene expression (A)*** *Analysis of EAR motif by testing the repressive function of 35S:ZF EARm (ZFm) versus 35S:ZF EARwt (ZF) on PIN:LUC expression by protoplast assay.* ***(B-E)*** *Analysis of PIN promoters for additional ZF binding sites by testing different PIN1 and PIN7 promoter deletion constructs in protoplast assay* ***(F)*** *Visual representation of tested PIN1 and PIN7 promoter deletion constructs, 2-way ANOVA for statistical comparison to control, n>2*

In conclusion, ZF1 binding motifs in the *PIN7* promoter might be concentrated at region 1420 to 608bp upstream of ATG. For *Δ1pPIN1:LUC*, we still observed repressed Luciferase activity with ZF proteins suggesting additional ZF binding sites located in 795bp promoter region upstream of ATG.

ZFs are temperature responsive transcription factors

Identification of ZFPs as direct transcriptional regulators of *PIN* motivated us to explore their regulatory role *in planta*, initially by monitoring their expression pattern in different plant organs. In 5 day old seedlings grown at oAT, we detected strong *ZF1:GUS* staining in the cotyledon vasculature (Figure 23A). In addition to the primary root cap and columella cells (data not shown), *ZAT10:GUS* expression was found in the hypocotyl-root junction and in the cotyledon epidermal cells displaying patchy pattern (Figure 23B,C). Thus, *ZAT10* expression overlaps with *PIN3*, *PIN4* and *PIN7* expression in the primary root columella cells (Michniewicz, Brewer, & Friml, 2007) and partially with *PIN3* and *PIN7* in the cotyledon epidermis (Figure 11, Figure 13) (Michniewicz et al., 2007). Expression of *ZF1* overlaps with *PIN3*, and *PIN4* in the cotyledon vasculature (Figure 11, Figure 12).

Since *ZFs* were found to be transcriptionally upregulated by various stresses in seedlings and older plants (Sakamoto et al., 2004, 2000), we asked whether ZFs might be factors that fine-tune *PIN* expression in response to increase in ambient temperature. Exposure to hAT for 1 day strongly induced *ZF1::GUS* expression in the cotyledon vasculature, while no change was observed in the hypocotyl compared to oAT (Figure 23A). In accordance, using RT-qPCR, we found *ZF1* expression approximately 1.8 fold upregulated after 1 day at hAT (Figure 23E), while in earlier time points we did not detect any significant differences in *ZF1* transcription when compared to oAT (Figure 23D). In the hypocotyl, no significant changes in *ZF1* transcript level at hAT compared to oAT were detected by RT-qPCR (Figure 23F-G). In fact, *ZF1* transcript levels in the hypocotyl were significantly lower compared to ZAT10 at oAT and hAT (comparison not shown). At increased temperature, *ZAT10:GUS* displayed enhanced patchy staining in the cotyledons when compared to oAT at 8 hours and 1 day after transfer (Figure 23C).

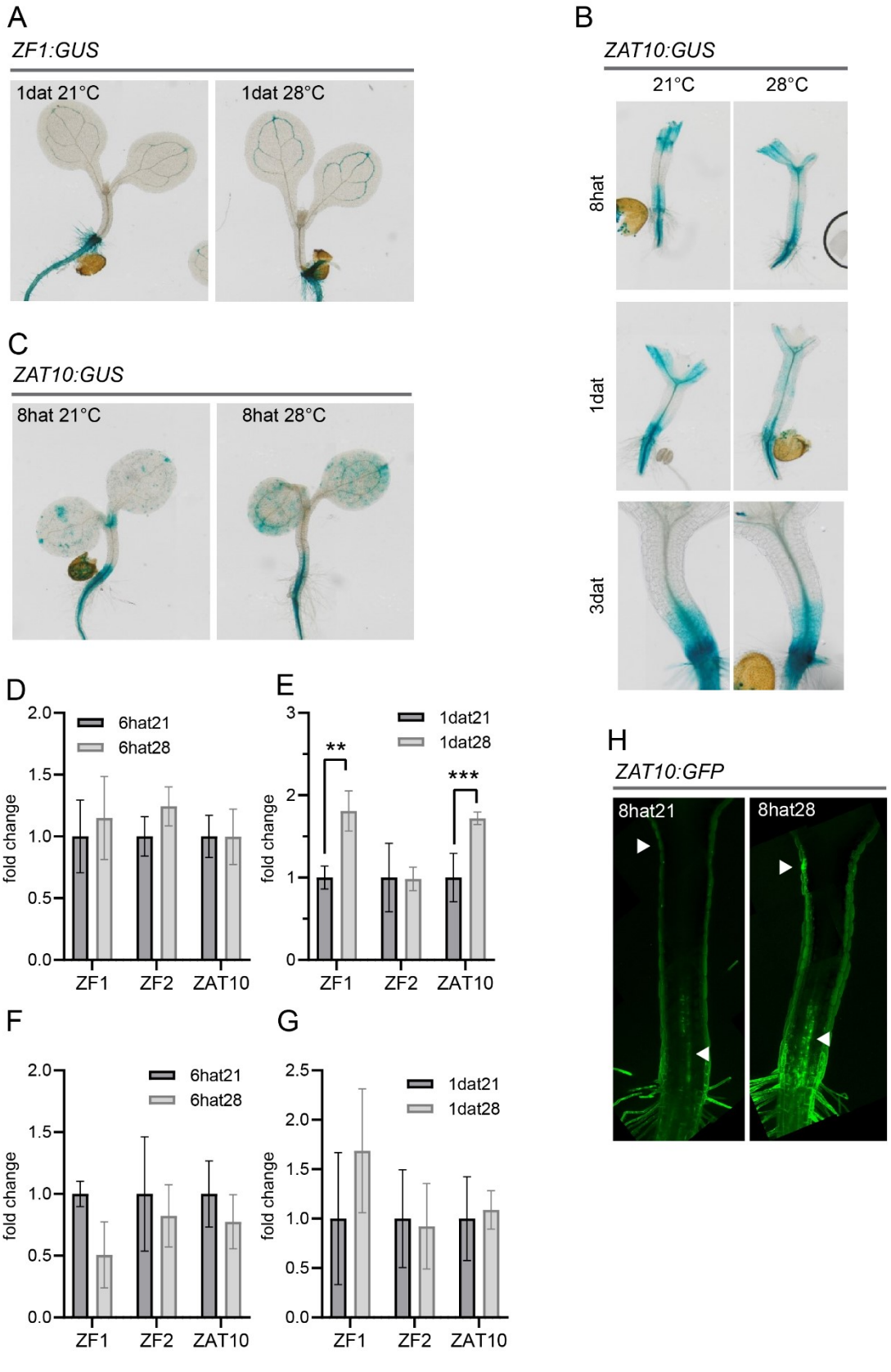
A
ZF1:GUS
1dat 21°C
1dat 28°C
B
ZAT10:GUS
21°C
28°C
8hat
1dat
3dat
C
ZAT10:GUS
8hat 21°C
8hat 28°C
D
6hat21
6hat28
fold change
ZF1
ZF2
ZAT10
E
1dat21
1dat28
**
***
F
G
H
ZAT10:GFP
8hat21
8hat28

Figure 23: ***ZF expression pattern is affected during hAT response*** *5 day old seedlings were transferred to 28°C (hAT) versus 21°C (oAT) for different time frames* ***(A)*** *ZF1:GUS was treated for 1 day, stained and analyzed by light microscopy* ***(B-C)*** *ZAT10:GUS was treated for* ***(B)*** *8h, 1day and 2 days and for* ***(C)*** *8h, stained and analyzed by light microscopy* ***(D-G)*** *seedlings were treated for* ***(D,F)*** *6h or* ***(E,G)*** *1 day and subsequently* ***(D-E)*** *cotyledon and* ***(F-G)*** *hypocotyl were harvest and analyzed by qPCR separately. Bars represent mean fold change +- s.d. students t-test for statistics* ***(H)*** *ZAT10:GFP treated for 8h with subsequent analysis by multiphoton microscopy. Students t test for statistics, *** = p < 0.001, ** = p < 0.01, n=3 biological replicates* ***(D-G)***

In parallel, RT-qPCR analysis revealed approximately 1.6 fold increase of *ZAT10* expression in the cotyledon within in the first day of hAT treatment compared to oAT (Figure 23E).

In hypocotyl exposed to hAT, *ZAT10:GUS* expression pattern altered compared to those at oAT (Figure 23). While *ZAT10* expression was mainly restricted to the hypocotyl base under oAT, after 8h and 1d of hAT, we observed expansion of *ZAT10* expression domain towards middle/upper part of hypocotyl localized to the vasculature and outer cell layers (Figure 23B). Simultaneously, *ZAT10:GUS* staining at the hypocotyl base weakened. However, after 3 days at hAT, *ZAT10* expression pattern was restricted to the hypocotyl base similar to oAT (Figure 23B). In addition, we investigated *ZAT10:GFP* transcriptional reporter line by multiphoton microscopy. Under oAT, we found *ZAT10:GFP* signal localized in the vasculature as well as in the epidermis close to the hypocotyl base (Figure 23H). Upon 8h of hAT we detected enhanced *ZAT10:GFP* signal in the hypocotyl vasculature tissue compared to oAT (Figure 23H). Furthermore, GFP signal was enhanced in epidermal cells at the apical part of hypocotyl compared to oAT (Figure 23H). No significant changes in *ZAT10* transcription in hypocotyl incubated at hAT versus oAT were detected by RT-qPCR analysis (Figure 23F-G). *ZAT10:ZAT10:GFP* translational reporter showed almost no signal in the cotyledon or hypocotyl and only weak signal was detectable in the root (data not shown). Hence, we assume, that abundance of ZAT10 protein is very low in general or undergoes quick turnover.

In summary, we observed ZF expression being affected by hAT treatments in shoot tissues. Upon hAT, *ZF1* transcript level is enhanced in the cotyledon vasculature, but not affected in the hypocotyl compared to oAT. *ZAT10* shows enhanced patchy expression in the cotyledon compared to control conditions. In hypocotyls expose to hAT, expression pattern of ZAT10 expands from base toward upper zones, while simultaneously strength of ZAT10 expression at the hypocotyl base decreases.

Enhanced hypocotyl growth of *zf* triple mutant at hAT

As expression pattern of *ZFs* is affected by hAT and they were found to repress *PIN* transcription, we asked about their biological role during temperature stress responses *in planta,* in processes where auxin transport is essential. Enhanced hypocotyl growth represents one of the hallmarks of plant thermomorphogenesis, where PIN-mediated auxin transport has been implicated (Michaud et al., 2017; Park et al., 2019)

In our experimental setup, we grew seedlings for 5 days at oAT followed by transfer to hAT versus oAT for few days with daily monitoring. wt showed increased hypocotyl growth after 1 day of hAT compared to oAT (Figure 24A). Interestingly, we observed significantly enhanced hypocotyl growth of *zf* triple mutant within the first days of hAT treatment compared to wt at hAT (Figure 24A). Also at the later time points. When hypocotyl elongation at hAT ceased, hypocotyls length of *zf* triple mutant was significantly longer than wt (Figure 24A). Notably, no obvious phenotype was detected for *zf* triple under oAT at any time point compared to wt (Figure 24A).

We further tested, how hypocotyl growth is affected by local *ZF* overexpression at hAT. For this purpose, we applied estradiol vs DMSO either on the cotyledon (Figure 24B,D) or hypocotyl (Figure 24C,E) of 5 day old estradiol inducible *ZAT10oe* and *ZF1oe* lines and immediately transferred them to hAT. The local application of estradiol induced expression of respective ZFs in the treated plant organs, thus enabled investigation of the phenotypic response upon sudden local enhancement of transcriptional regulator at hAT. Local induction of *ZAT10* by estradiol application on the cotyledon did not change hypocotyl growth at hAT compared to DMSO (Figure 24B). Specific estradiol treatment on the cotyledon of *ZF1oe* seedlings showed a slightly, but still significant reduction of hypocotyl growth at hAT after 3 days compared to DMSO treatment (Figure 24D). In contrast, when *ZAT10oe* and *ZF1oe* lines were treated with estradiol directly on the hypocotyl, we observed a significant repression of hAT induced hypocotyl growth compared to DMSO (Figure 24C,E). We need to keep in mind that due to immediate transfer of estradiol or DMSO treated seedlings to hAT, effect of hAT might precede induction and accumulation of ZF sufficient to trigger changes in transcription of target genes.

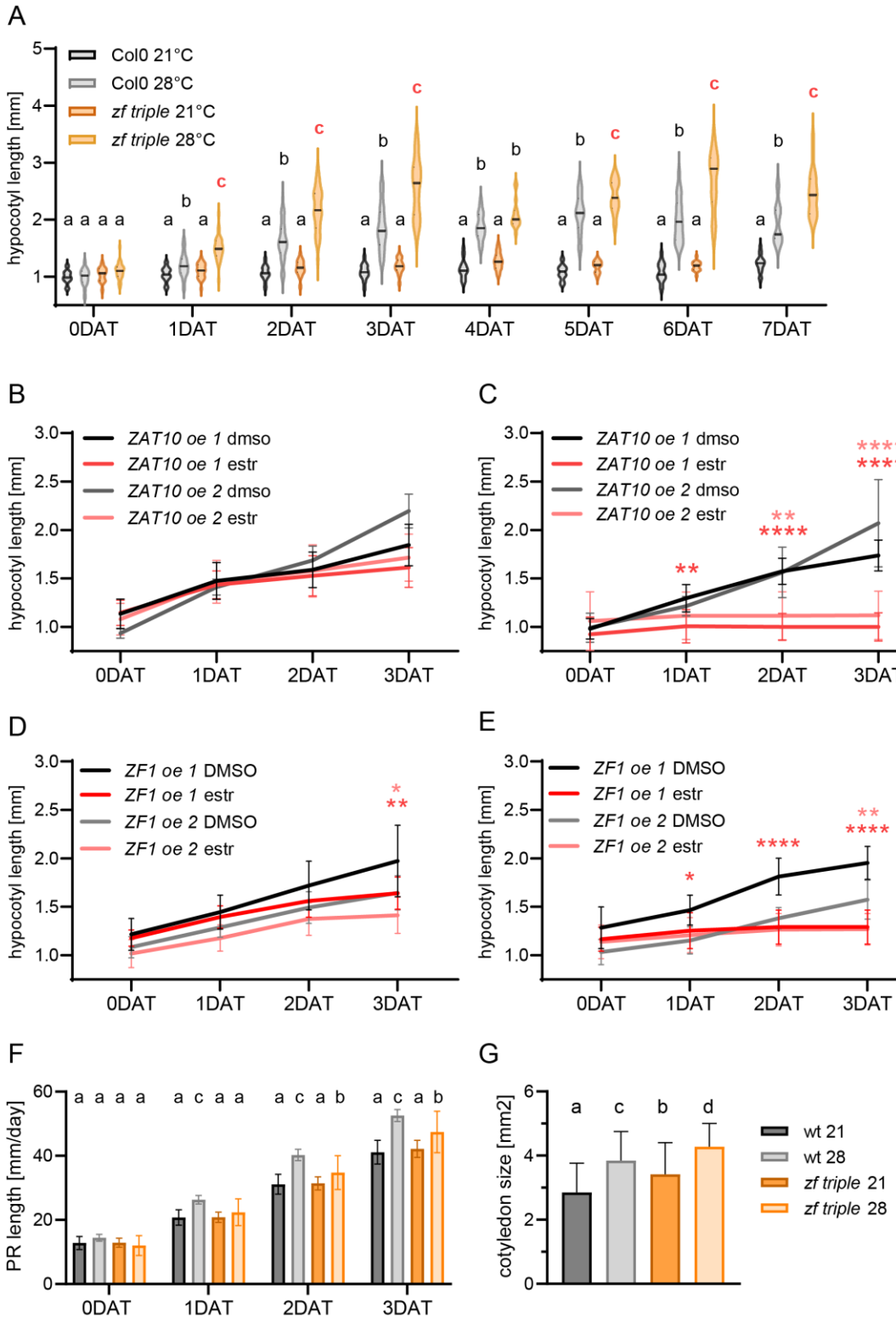
A
Col0 21°C
Col0 28°C
zf triple 21°C
zf triple 28°C
hypocotyl length [mm]
0DAT
1DAT
2DAT
3DAT
4DAT
5DAT
6DAT
7DAT
B
ZAT10 oe 1 dmso
ZAT10 oe 1 estr
ZAT10 oe 2 dmso
ZAT10 oe 2 estr
C
D
ZF1 oe 1 DMSO
ZF1 oe 1 estr
ZF1 oe 2 DMSO
ZF1 oe 2 estr
E
F
PR length [mm/day]
G
cotyledon size [mm2]
wt 21
wt 28
zf triple 21
zf triple 28

Figure 24: ***Enhanced hypocotyl growth in zf triple mutant upon hAT (A)*** *5 day old seedlings were transferred to 28°C versus 21°C and hypocotyl length was measured over time and visualized in violin plot with median as dashed lines and quartiles as dotted lines, n>15 hypocotyls* ***(B-C)*** *5 day old estradiol inducible ZAT10 overexpressing seedlings and* ***(D-E)*** *estradiol inducible ZF1 overexpressing seedlings were treated with 100uM estradiol-lanolin versus DMSO-lanolin on* ***(B,D)*** *cotyledon or* ***(C,E)*** *hypocotyl and transferred to 28°C for daily monitoring. Lines represent mean hypocotyl length +- s.d.* ***(F)*** *Primary growth growth analysis of zf triple versus Col0 at oAT versus hAT, bars represent mean +- s.d., n>15 roots.* ***(G)*** *cotyledon size after 2 days of hAT versus oAT treatment, bars represent mean +- s.d., n>20 cotyledons. Students t-test for statistical comparison to DMSO, n>13 hypocotyls **** = p < 0.0001, ** = p < 0.01, * = p < 0.05* ***(B-E).*** *2-way ANOVA for statistics* ***(A,F,G)***

Presumably, therefore, we did not observe the effect of enhanced *ZF1* and *ZAT10* expression in cotyledons on the hypocotyl growth response to hAT. For this purpose, we are planning to pretreat the seedlings with estradiol versus DMSO for few hours prior transfer to hAT. In addition, we observed significantly increased *zf* triple mutant cotyledon size at oAT compared to wt, which was further enhanced upon exposure to hAT (Figure 24G). Analysis of the root revealed no significant differences in growth between *zf* triple versus wt at oAT. Upon hAT, we observed enhanced primary root in wt compared to oAT (Figure 24F). However, in *zf* triple mutant primary root growth was significantly less enhanced upon hAT when compared to hAT treated wt (Figure 24F).

Based on our observations *zf*-triple mutant showed strongly enhanced hypocotyl growth at hAT compared to wt. Specific induction of *ZF1* or *ZAT10* expression in the cotyledon did not affect hAT triggered hypocotyl growth much. However local enhancement of *ZF1* and *ZAT10* transcript in the hypocotyl significantly repressed hypocotyl growth during hAT. Consequently, *zf* triple mutant and ZF overexpression lines show opposite hypocotyl growth phenotype at hAT. In addition, we observed reduced primary root growth upon hAT in *zf* triple mutant compared to wt and enhanced cotyledon size in oAT and hAT treated *zf* triple cotyledons. We conclude that ZF proteins are involved in hAT modulated cotyledon, hypocotyl and root growth. Interestingly, while ZFs seem to act as negative regulators of hypocotyl growth at hAT, they might be required for promoting root growth in response to hAT.

Altered epidermal cell elongation pattern in *zf* triple at hAT

Since *zf* triple mutant exhibited increased hypocotyl growth at hAT compared to wt (Figure 2), we asked how cell growth and divisions are affected in the hypocotyl lacking activity of ZFs.

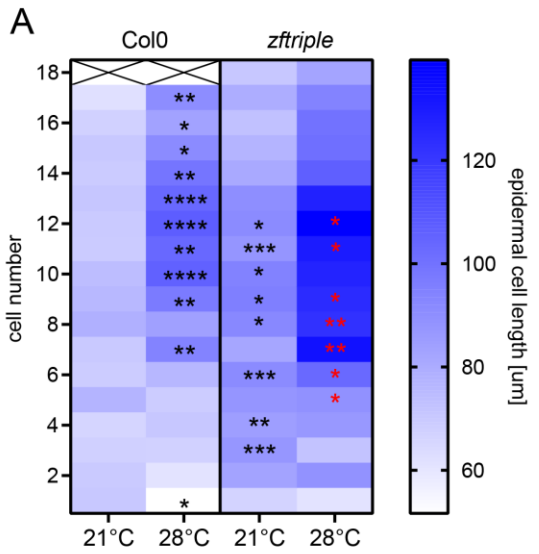
A
Col0
zftriple
cell number
epidermal cell length [um]
21°C
28°C
21°C
28°C

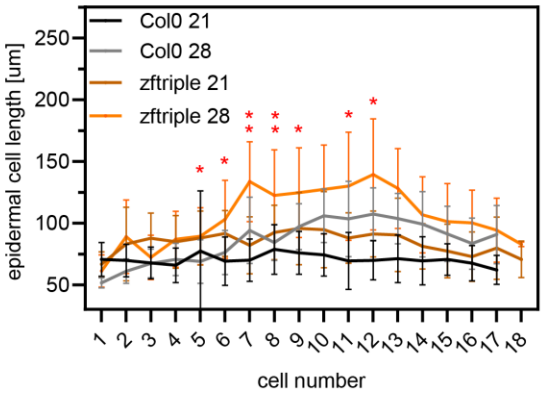
B
Col0 21
Col0 28
zftriple 21
zftriple 28
epidermal cell length [um]
cell number

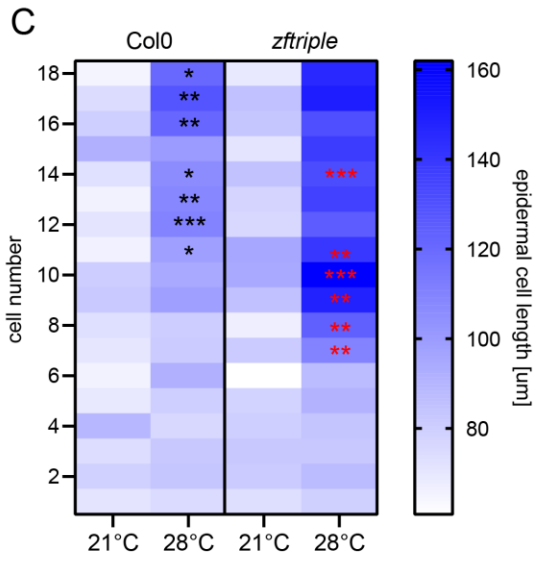
C
Col0
zftriple
cell number
epidermal cell length [um]
21°C
28°C
21°C
28°C

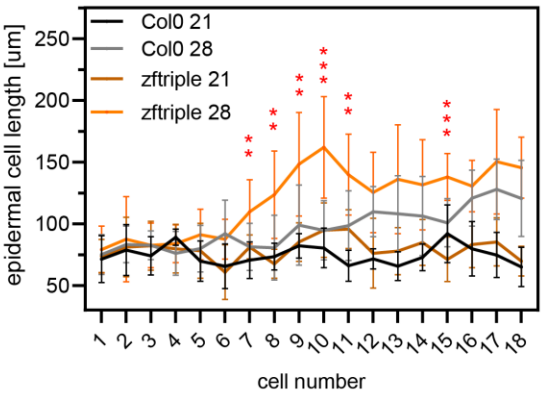
D
Col0 21
Col0 28
zftriple 21
zftriple 28
epidermal cell length [um]
cell number

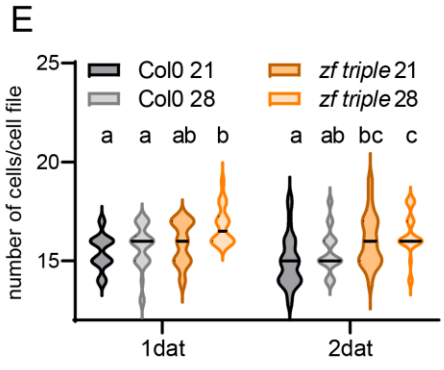
E
Col0 21
Col0 28
zf triple 21
zf triple 28
a a ab b
a ab bc c
number of cells/cell file
1dat
2dat

Figure 25: ***Altered adjustment of hypocotyl epidermal cell length pattern in zf triple during hAT response (A-D)*** *5 day old zf triple versus Col0 seedlings were transferred to 28°C (hAT) versus 21°C (oAT) and subsequently stained with Propidium iodid and analyzed by confocal microscopy. Hypocotyl epidermal cells length was measured and plotted against their position in the hypocotyl starting from the hypocotyl base with cell number 1 until hypocotyl apex with cell number 18. Black asterisk correspond to Students t-test with Col0 21°C , red asterisk correspond to Students t-test with Col 28°C, n>8 hypocotyls, **** = p < 0.0001, *** = p < 0.001, ** = p < 0.01, * = p < 0.05.* ***(A-B)*** *treatment for 1 day,* ***(C-D)*** *treatment for 2 days.* ***(A,C)*** *heat map of hypocotyl epidermal cell length pattern* ***(B,D)*** *line graph of hypocotyl epidermal cell length pattern where line represents mean cell length +- s.d.* ***(E)*** *Number of epidermal cells per cell file after 1 or 2 days of treatment displayed in Violin plot with median as dashed lines and quartiles as dotted lines. 2-way ANOVA for statistics, n>8 hypocotyls with 2 cell files each*

Consequently, we analyzed their epidermal cell length pattern in the hypocotyl at hAT versus oAT. Under oAT, we found slightly increased epidermal cell length in 5-day old *zf* triple mutant seedlings versus wt (Figure 25A, black asterisk), but no significant difference could be detected 2 days after transfer to oAT (Figure 25C, black asterisk). Upon 1 day of hAT, we observed significantly enhanced cell elongation in the middle zone of hypocotyl in *zf* triple mutant when compared to wt (Figure 25A-B, red asterisk). While after 2 days of hAT treatment, induction of epidermal cell growth in wt is mainly restricted to the apex (Figure 25C-D, black asterisk), *zf* triple mutant exhibited significantly enhanced elongation in the middle part of the hypocotyl compare to wt (Figure 25C-D, red asterisk). Analysis of the number of epidermal cells revealed no significant difference in the *zf* triple mutant versus wt at day 1 after transfer to oAT. (Figure 25E). However, 1 day after transfer to hAT, number of epidermal cells in the hypocotyls of *zf* triple mutant increased when compared to those at oAT. 2 days after transfer, number of epidermal cells in *zf* triple was significantly increased when compared to wt at both oAT and hAT (Figure 25 E).

In conclusion *zf* triple mutant exhibited strongly elevated epidermal cell growth in the middle part of the hypocotyl after 1 day of hAT versus oAT. Interestingly after 2 days at hAT, when epidermal cell growth in wt is mainly restricted to the apex compared to oAT (black asterisk), we noticed strongly enhanced cell growth in the middle hypocotyl in hAT treated *zf* triple mutant compared to wt hAT (red asterisk). Consequently *zf* triple mutant epidermal cell growth follows a different pattern upon hAT compared to wt. In addition to altered cell elongation pattern, we noticed slightly higher amount of epidermal cells in hAT treated *zf* triple mutant hypocotyl, while no significant change was observed at oAT when compared to wt.

Hyponastic leaf movement of *zf* triple mutant

In parallel to enhanced hypocotyl growth, hAT triggers additional physiological and growth responses including hyponastic leaf movement (Casal & Balasubramanian, 2019). It was shown that leaf movement at hAT is enabled by adjustment of auxin gradient in the petiole via PIN proteins (Park et al., 2019).

Initially, when plants were grown on soil at 22°C, we noticed unusual leaf positioning in *zf* triple mutant compared to wt (Figure 26C). To evaluate our observation, we monitored 14-day old *zf* triple mutant and wt seedlings grown on soil for 24h with our webcam setup at 22°C. The resulting video was analyzed by measurement of the angle between either two petioles or leaf blade tips from the first two outgrown true leaves. For visualization, we subtracted those values from 360°C and plotted the resulting data points against the time (Figure 26A-B). In wt, we detected gradual decrease in leaf tip and petiole angle from 7am till 9am, which later on increased to maximum of 218° and 245°, respectively, at 5pm (A-B). In accordance with our finding, rhythmic leaf movement was already reported in many plant species including *Arabidopsis* (C Robertson McClung, 2006) Interestingly, upwards movement of leaves in *zf* triple mutant was significantly enhanced reaching maximum leaf tip angle of 240° at 4pm and petiole angle of 260° at 7pm (Figure 26A-B).

The monitoring experiment on soil revealed an increased leaf up-movement in *zf* triple mutant at oAT control conditions compared to wt. The petiole angle of *zf* triple started to significantly increase from 10am on, while the difference in leaf tip angle was detected around 6pm compared to wt. This discrepancy could be explained due to the positioning of the leaf blade. As reported, the leaf tip angle is usually smaller than the petiole angle (Dornbusch, Michaud, Xenarios, & Fankhauser, 2014). However, both methods finally give comparable results, hence, enhanced upward movement of leaves in *zf* triple mutant approximately at 5pm compared to wt. In addition, we found *zf* triple leaf petioles strongly elongated compared to wt.

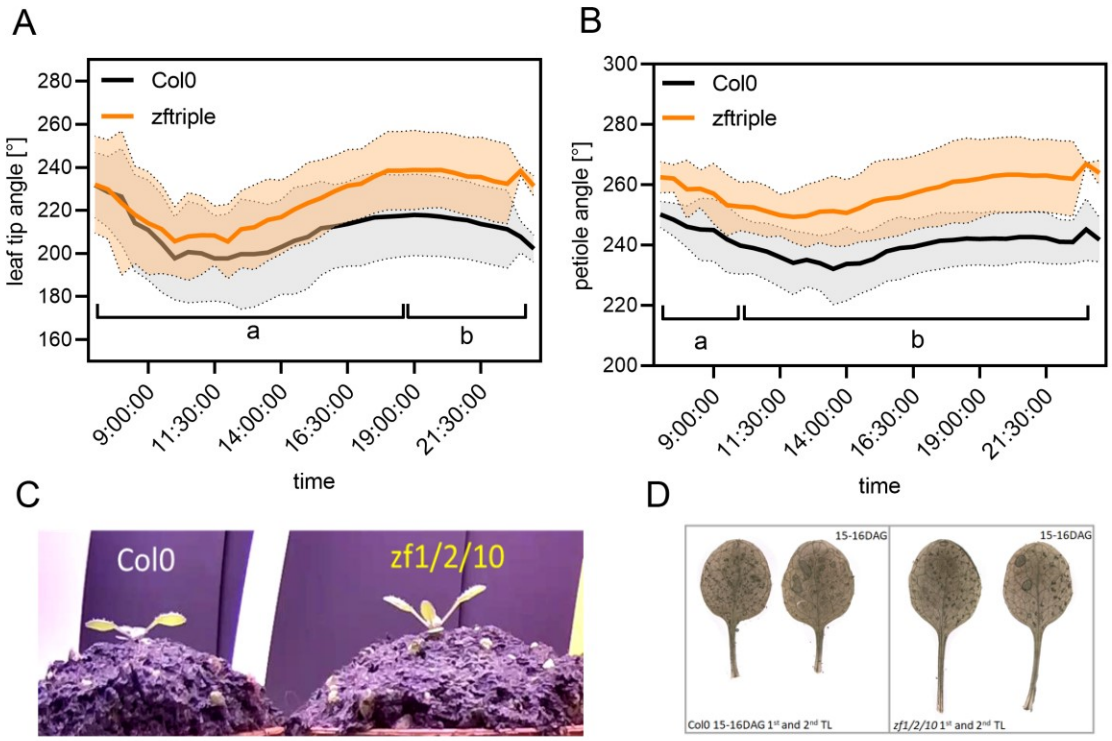

Figure 26: ***Zf triple mutant exhibit altered leaf hyponasty*** *14 days old Col0 and zf triple mutant seedlings germinated and grown on soil were vertically monitored by webcam set up for analysis of first true leaf movement during light period at 22°C* ***(A)*** *true leaf tip angle and (B) petiole angle was calculated and plotted over time. Line represents mean angle +- s.d. 2-way ANOVA for statistics, n=2.* ***(C)*** *Representative picture of Col0 and zf triple at 3pm,* ***(D)*** *First true leaf of Col0 versus zf triple mutant after 20 days.*

Plant hyponastic leaf movement and hypocotyl growth represent physiological responses, which are sensitive to light and temperature changes (Park et al., 2021; Yang & Li, 2017). Both processes depend on accurate modulation of PIN-dependent auxin transport. Our experiments show that ZF-mediated regulation of PIN-mediated transport is involved in fine-tuning of leaf movements during day and prevents exaggerated response.

Enhanced hypocotyl growth of *zf* triple mutant at hAT depends on polar auxin transport

Based on our previous experiments, hypocotyl growth of wt at hAT is strongly repressed by NPA (Figure 8). NPA can directly inhibit PIN proteins, thereby blocking polar auxin transport (Abas et al., 2021).

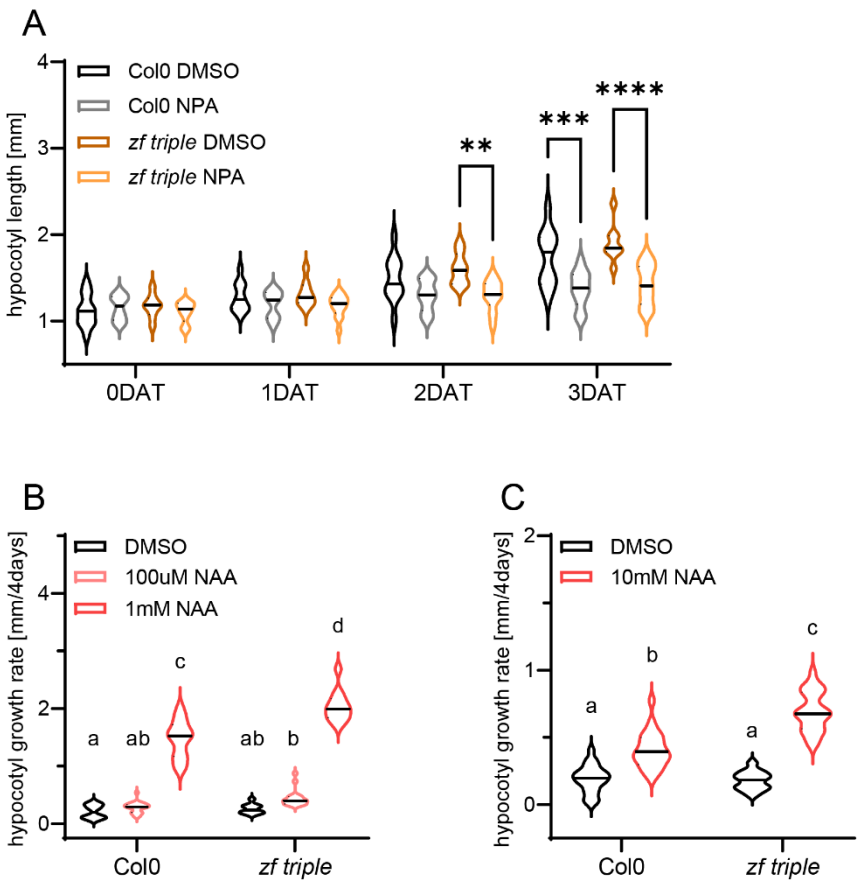

Figure 27: ***Auxin transport is essential for enhanced zf triple hypocotyl growth upon hAT*** *5 day old zf triple versus Col0 seedlings were treated and hypocotyl length was monitored over time* ***(A)*** *treatment with 100uM NPA-lanolin versus DMSO-lanolin on hypocotyl prior transfer to 28°C (hAT). Hypocotyl length over time. Students t-test for statistics, n>16 hypcotyls, **** = p < 0.0001, *** = p < 0.001, ** = p < 0.01.* ***(B-C)*** *treatment with 100uM or 1mM NAA-lanolin versus DMSO-lanolin and transfer to 21°C (oAT). Hypocotyl growth rate is shown in Violin plot with median as dashed lines and quartiles as dotted lines as. 2-way ANOVA for statistics*

Since we found that ZFs can repress transcription of *PINs* (Figure 20, Figure 21) and loss of ZFs function results in increased hypocotyl growth at hAT compared to wt (Figure 24), we asked whether this acceleration of hypocotyl growth in *zf* triple mutant is caused by enhanced PIN mediated auxin transport. Thus, we chemically blocked PIN activity by NPA and observed effect on hypocotyl growth in *zf* triple mutant at hAT. For this purpose, we treated *zf* triple and wt seedlings with NPA versus DMSO locally on the hypocotyl and monitored their hypocotyl growth after transfer to hAT. DMSO treated *zf* triple exposed to hAT displayed increased hypocotyl growth compared to wt, which is in accordance with our previous experiments (Figure 27A). However, local application of NPA on hypocotyl resulted in significant reduction of hypocotyl

growth in both *zf* triple and Wt compared to DMSO (Figure 27A). Thus, we suggest that *zf* triple mutant hypocotyl phenotype at hAT is a result of altered PIN-mediated transport of auxin.

Auxin is able to trigger hypocotyl growth (Chapman et al., 2012) (Figure 7). However, if auxin transport is blocked, high auxin levels alone are not sufficient to induce hypocotyl growth (Munguía-Rodríguez et al., 2020). To test whether loss of ZFs- mediated negative regulation of *PIN* expression affects sensitivity of hypocotyls to auxin, we conducted local auxin application experiments. 100uM NAA applied on cotyledons did not have any effect on hypocotyl growth in either Wt or *zf* triple mutant (Figure 27B). Notably, 1mM and 10mM NAA applied on cotyledons enhanced hypocotyl growth significantly more in *zf* triple mutant when compared to wt (Figure 27B-C).

In summary, chemical blocking of PIN proteins abolished hAT induced hypocotyl elongation in *zf triple* and Wt compared to DMSO, while auxin treatment on the cotyledon enhanced hypocotyl growth significantly more in *zf* triple compared to wt. Altogether, these results support a model, in which ZFs through fine-tuning *PIN* transcription control PAT-mediated hypocotyl growth in response to hAT.

Impact of ZFs on adjustment of *PIN* expression to hAT

To determine the biological relevance of ZF-dependent adjustment of *PIN* expression during hAT response in the cotyledon, we monitored expression of *PIN:PIN:GFP* reporters in *zf triple* mutants versus wt at hAT versus oAT. For RT-qPCR analysis we transferred 5 day old seedlings to hAT versus oAT and subsequently harvested cotyledons in the late afternoon (6h after transfer) or next day morning (1day after transfer). RT-qPCR analyses in cotyledons revealed that at oAT there is significant reduction of *PIN3* transcript in *zf* triple mutant when compared to wt 6 hours after transfer, while 1 day after transfer expression of *PIN3* in mutant background was significantly higher than in wt (Figure 28A-B).While on one side these results support role of ZFs in the regulation of *PIN3* transcription, the opposite trends at 6 versus 24 hours after transfer at oAT (Figure 28A-B) might hint on cross-talk with mechanisms controlling circadian rhythmicity. This is particularly, when we take the different daytimes for material harvesting into consideration.

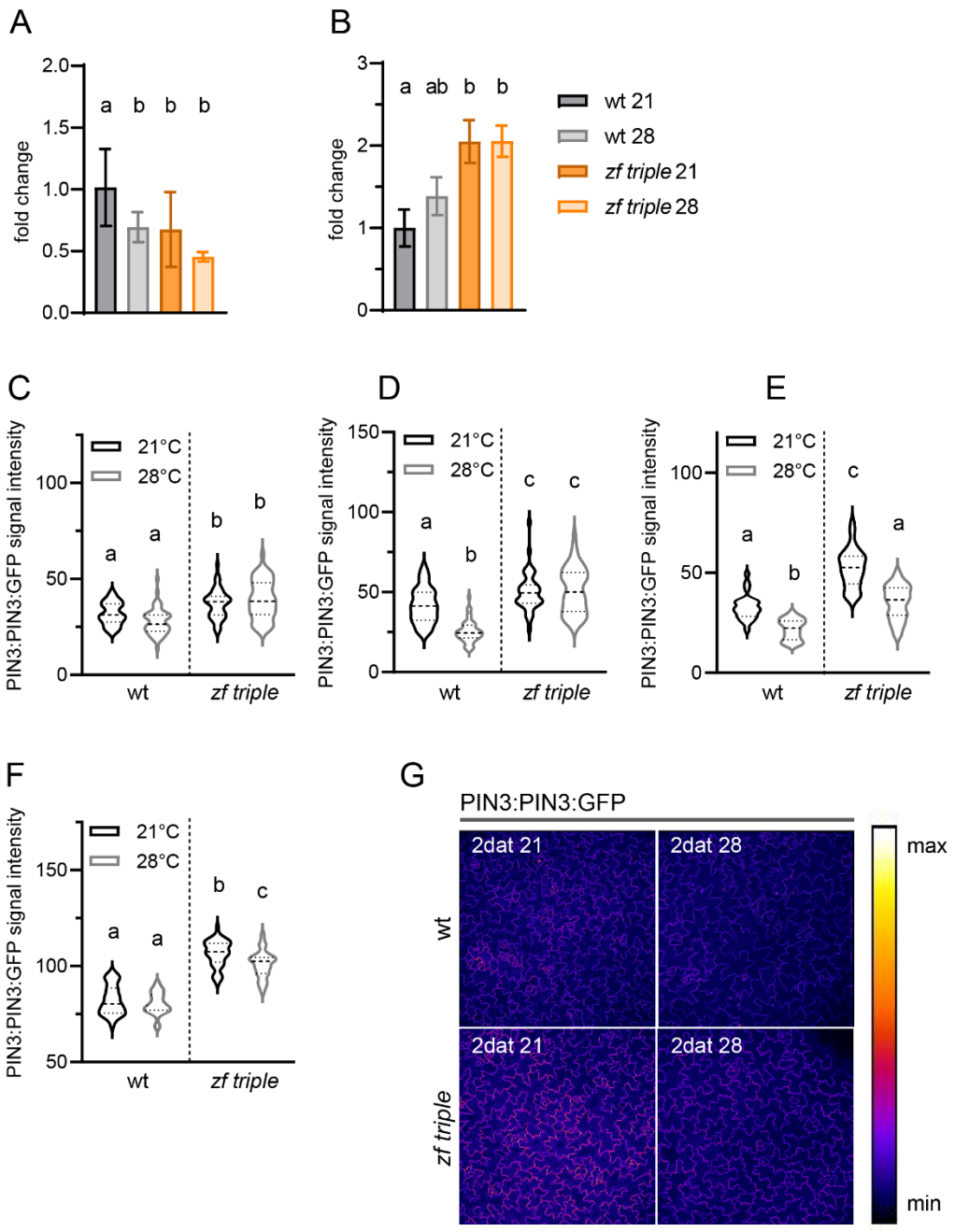

Figure 28: ***Adjustment of PIN3 expression in zf triple cotyledon at oAT and hAT*** *5 day old seedlings were transferred to 28°C (hAT) versus 21°C (oAT) for different time frame prior analysis* ***(A-B)*** *zf triple and Col0 cotyledon was harvested and PIN3 transcript level was analyzed by qPCR after* ***(A)*** *6h and* ***(B)*** *1 day of treatment. Bars represent mean fold change +- s.d, n= 3 biological replicates* ***(C-F)*** *PIN3:PIN3:GFP analysis by multiphoton microscopy where pavement cell membrane PIN3-GFP signal was measured and visualized by violin plot with median as dashed lines and quartiles as dotted lines. 2-way ANOVA for statistics, n>10 cotyledons with 5 cells each* ***(G)*** *representative picture of PIN3:PIN3:GFP in zf triple versus wt background after 2 days of treatment*

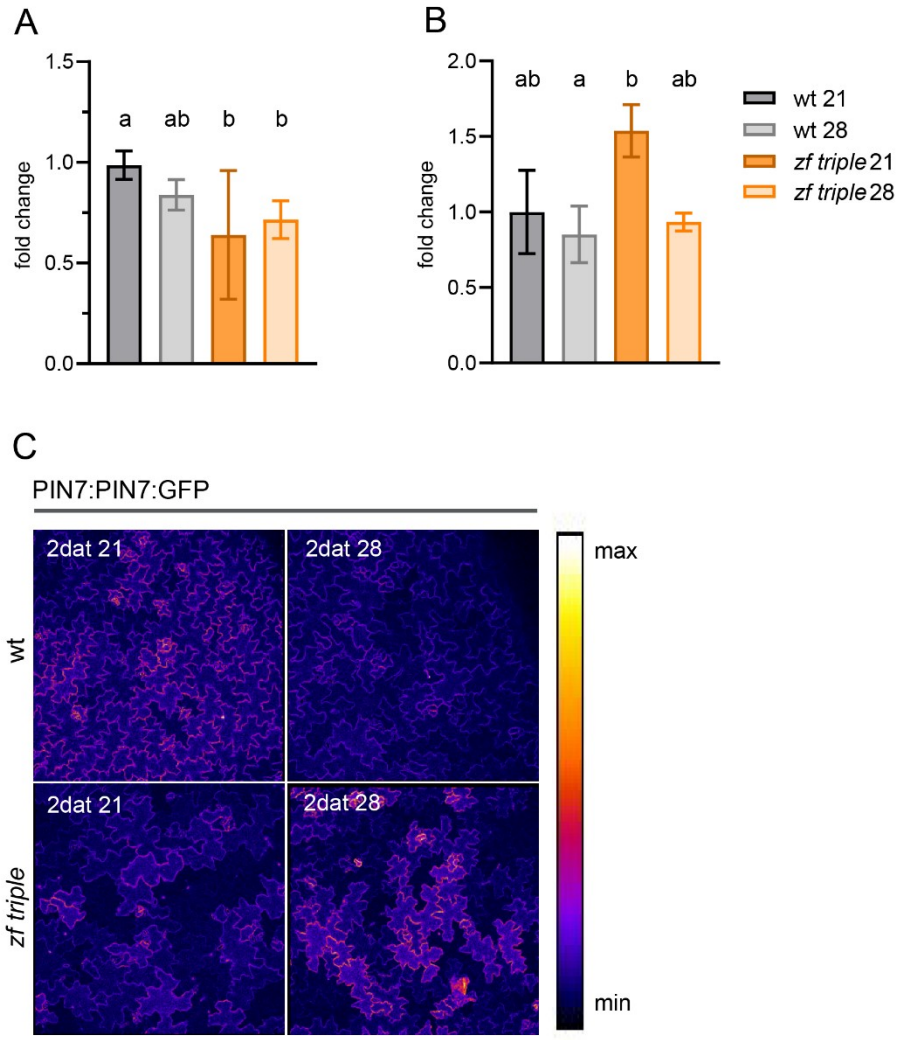

Figure 29: ***Adjustment of PIN7 expression in zf triple cotyledon at oAT and hAT*** *5 day old seedlings were transferred to 28°C (hAT) versus 21°C (oAT) for different time frame prior analysis* ***(A-B)*** *zf triple and Col0 cotyledon was harvested and analyzed by qPCR after* ***(A)*** *6h and* ***(B)*** *1 day of treatment. Bars represent mean fold change +- s.d. 2-way ANOVA for statistics, n= 3 biological replicates* ***(C)*** *representative picture of PIN7:PIN7:GFP in zf triple versus wt background analysis by multiphoton microscopy after 2 days of treatment*

Notably, in wt transfer to hAT triggers alterations in *PIN3* transcription when compared to oAT, whereas in *zf* triple mutant, transcription of *PIN3* remains unaffected by hAT (Figure 28A-B). These results support role of ZFs in fine-tuning *PIN3* expression in response to hAT.

Investigation of *PIN3:PIN3:GFP* reporter in *zf* triple mutant versus wt at oAT revealed homogenous distribution of the signal on the plasma membranes of the cotyledon pavement cells (Figure 28G). Exposure to hAT did not affect the localization of *PIN3:GFP* in either of those backgrounds (Figure 28G).

To compare the PIN3:GFP signal intensity at different temperatures we measured cotyledon pavement cell membrane signal. Under oAT, PIN3:GFP signal intensity in *zf triple* mutant was significantly higher compared to Wt (Figure 28C-F). At hAT, unlike wt, where reduction of PIN3-GFP was detected when compared to oAT, in *zf* triple mutant, we did not observe any difference in PIN3:GFP levels within the first day of hAT response and oAT (Figure 28C-D). In later time points of hAT (2-3dat to hAT) we observed similar trend of PIN3:GFP decline in both wt and *zf* triple mutant compared to oAT(Figure 28E-G).

Similarly to *PIN3*, RT-qPCR analysis revealed deregulation of *PIN7* transcription in *zf* triple mutant when compared to wt at oAT (Figure 29B). In response to hAT, moderate decrease of *PIN7* transcript was observed in wt as well as in *zf* triple mutant 6 hours after transfer. Interestingly, exposure to hAT for 1 day resulted in significantly reduced expression of *PIN7* in *zf triple* mutant when compared to oAT, while no change was detected in wt (Figure 29B). Thus, as for *PIN3*, loss of ZFs function compromised transcriptional regulation of *PIN7* in response to hAT, although cross-talk with circadian rhythmicity pathway might be involved.

Analysis of *PIN7:PIN7:GFP* translational reporter revealed different pattern of protein abundance in pavement cells in cotyledons of *zf* triple versus wt (Figure 29G). While in wt, PIN7:GFP was homogenously expressed at the plasma membranes of all pavement cells, in *zf* triple mutants we detected patchy pattern with islands of pavement cells lacking PIN7:GFP signal (Figure 29C). Upon 2 days of hAT, PIN7:GFP signal in wt declined when compared to oAT (Figure 29C), whereas in *zf* triple mutant we observed enhanced signal in cells expressing PIN7:GFP, although numerous pavement cells with suppressed expression of PIN7 were still detected (Figure 29C).

In summary, we observed that the daytime of harvest might impact *PIN3*, and *PIN7* expression at oAT, suggesting a potential effect of the day-night rhythm on ZF dependent *PIN* regulation. However, regardless of daytime, loss of ZFs affected adjustment of *PIN3* and *PIN7* expression to hAT. Interestingly, patchy pattern *of PIN7:PIN7:GFP* expression observed in *zf* mutant hints on additional factor(s) controlled by ZFs that interferes with *PIN7* expression. However, its identification requires further research.

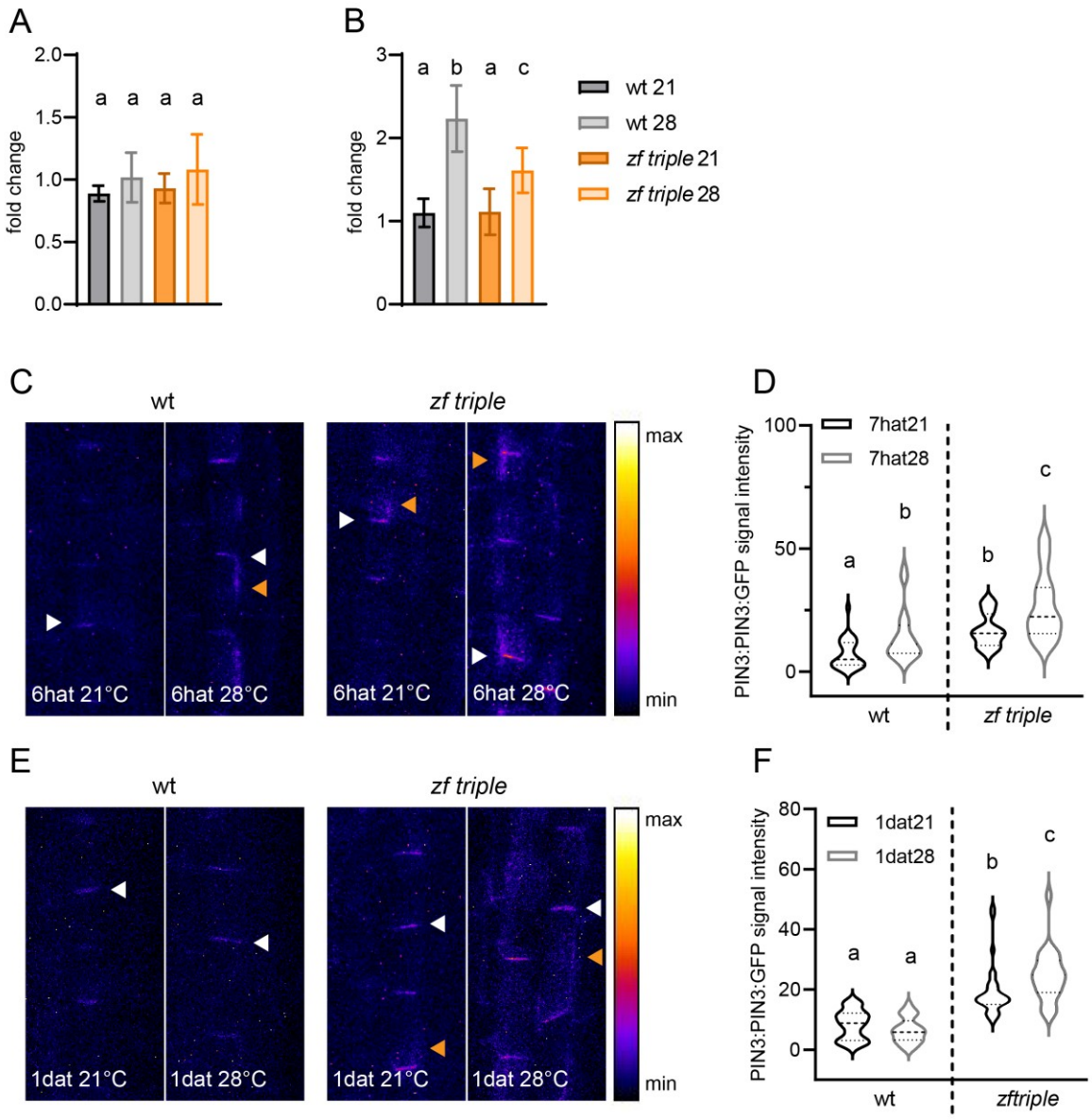

Figure 30: ***Adjustment of PIN3 expression in zf triple hypocotyl upon hAT*** *5 day old seedlings were transferred to 21°C (oAT) versus 28°C (hAT) for different time frame prior analysis* ***(A-B)*** *zf triple and Col0 hypocotyl PIN3 transcript level analysis after* ***(A)*** *6h and* ***(B)*** *1 day of treatment by qPCR. Bars represent mean +- s.d., n= 3 biological replicates* ***(C-F)*** *PIN3:PIN3:GFP analysis in zf triple versus wt in the hypocotyl endodermis by multiphoton microscopy* ***(C,E)*** *representative pictures of PIN3-GFP endodermal signal, white arrow mark basal signal, orange arrow mark lateral signal* ***(D,F)*** *Analysis of basal PIN3-GFP signal visualized by violin plot with median as dashed lines and quartiles as dotted lines. 2-way ANOVA for statistics, n>4 hypocotyls with 5 cells each*

Next we explored, whether and how ZFs regulate *PIN* expression in hypocotyls. After 6h of hAT, *PIN3* transcription did not significantly change in either wt or *zf* triple mutant when compared to oAT (Figure 30A). After 1 day at hAT, *PIN3* expression was 2 fold higher in wt and 1,5 fold higher in *zf* triple mutant when compared to oAT (Figure 30B).

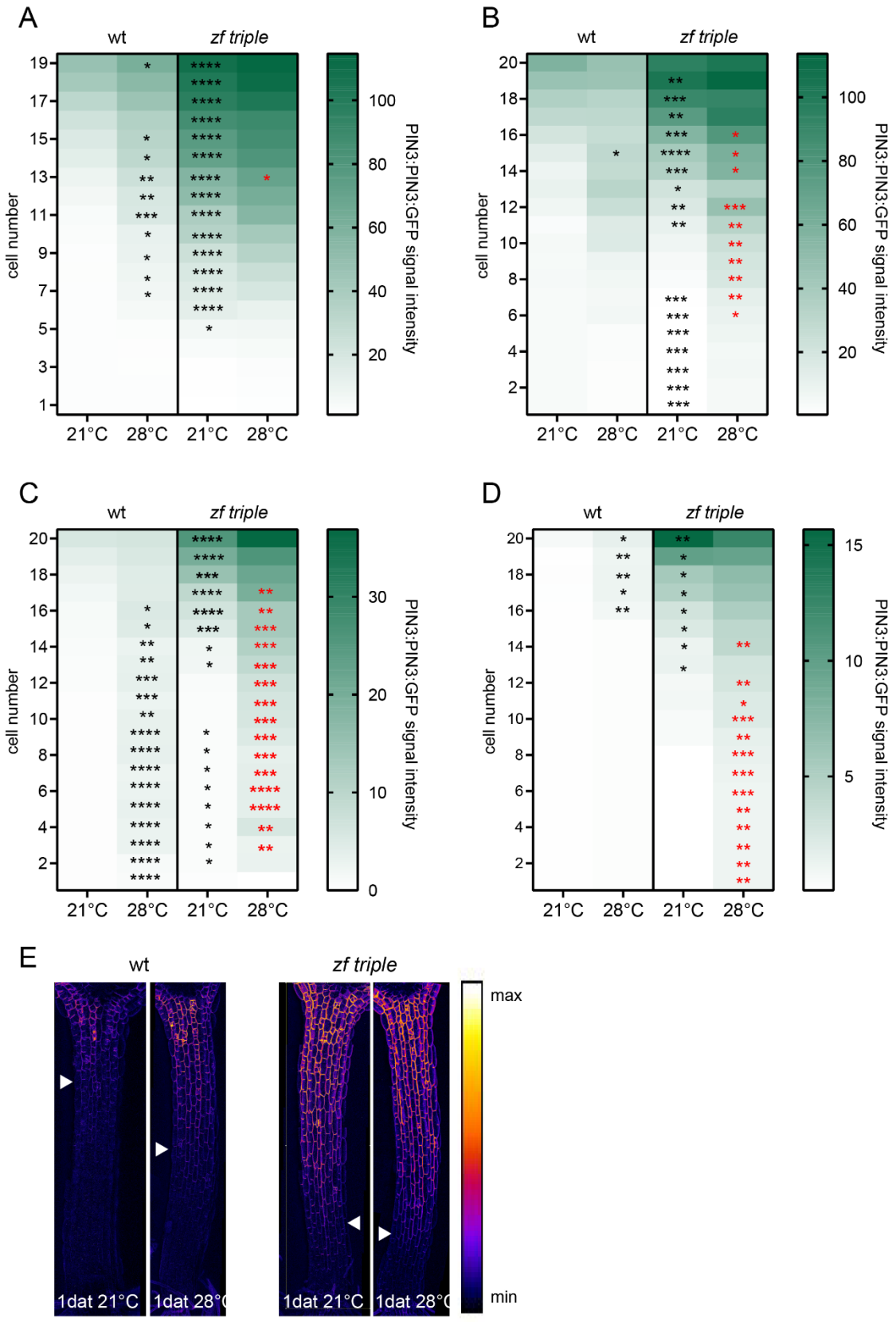
A
wt
zf triple
cell number
21°C
28°C
21°C
28°C
PIN3:PIN3:GFP signal intensity
B
C
D
E
max
min
1dat 21°C
1dat 28°C

Figure 31: ***Adjustment of PIN3 in epidermis of zf triple mutant upon hAT*** *5 day old PIN3:PIN3:GFP reporter seedlings in wt versus zf triple mutant background were transferred to 21°C (oAT) versus 28°C (hAT) for different time frame prior analysis of hypocotyl epidermis by multiphoton microscopy.* ***(A-D)*** *Basal epidermal PIN3-GFP signal was analyzed, visualized and plotted via heat map against their position in the hypocotyl starting from the hypocotyl base with cell number 1 until hypocotyl apex with cell number 20, Students t-test for statistical comparison to Col0 21 (black asterisk) and zf triple 21 (red asterisk), **** = p < 0.0001, *** = p < 0.001, ** = p < 0.01, * = p < 0.05, n>8 hypcotyls with 2 cell files each* ***(E)*** *representative images of PIN3-GFP epidermal signal, white arrow mark PIN3-GFP expression area.*

To examine the adjustment of PIN3 protein abundance to hAT, we monitored *PIN3:PIN3:GFP* reporter in *zf triple* mutant versus wt background by multiphoton microscopy. Similarly like in wt, at oAT in the *zf* triple mutant PIN3:GFP was detected at the basal membranes of endodermal cells, however intensity of signal in *zf* triple mutant was significantly higher than in wt (Figure 30C-D). Exposure to hAT significantly elevated PIN3:GFP basal signal in *zf* triple mutant compared to oAT (Figure 30C-F). After 6 hours at hAT, PIN3:GFP accumulated in addition also at the lateral membranes towards cortex in both wt and *zf* triple mutant (Figure 30C-D). After 1 day at hAT, PIN3:GFP decayed from lateral membranes in wt, but it remained clearly detectable in *zf* triple mutant (Figure 30E-F).

In epidermal cells of *zf* triple mutant, PIN3:GFP signal was detected at basal and radial membranes in a gradient like pattern transiently decreasing towards hypocotyl base, as previously shown for wt (Figure 16). However, expression zone of PIN3:GFP in *zf* triple mutant expanded more towards hypocotyl base when compared to wt at oAT (Figure 31). Measurements of PIN3:GFP signal at the basal membranes of epidermal cells along the hypocotyl growth axis revealed significantly higher accumulation of PIN3:GFP in *zf* triple mutant when compared to Col at oAT (Figure 31A-D). Over time, PIN3 protein abundance in wt decreased and was at the limit of detection at 3rd and 4th day of observation (Figure 31C-D). Similar trend was detected in *zf* triple mutant, although the PIN3:GFP signal remained proportionally stronger when compared to wt (Figure 31C-D).

Analysis of *PIN7* expression in hypocotyls by RT-qPCR did not reveal any significant change in *PIN7* transcript level in *zf* triple mutant versus wt after 6h of exposure to hAT versus oAT (Figure 32A). After 1 day of hAT, we detected a 0.2 fold decrease of *PIN7* expression in *zf* triple at hAT and oAT compared to wt (Figure 32B). During microscopic analysis of *PIN7:PIN7:GFP* reporter expression, we observed a reduced and patchy pattern of PIN7:GFP signal in the epidermis of *zf* triple mutant compared to wt under oAT (Figure 32C).

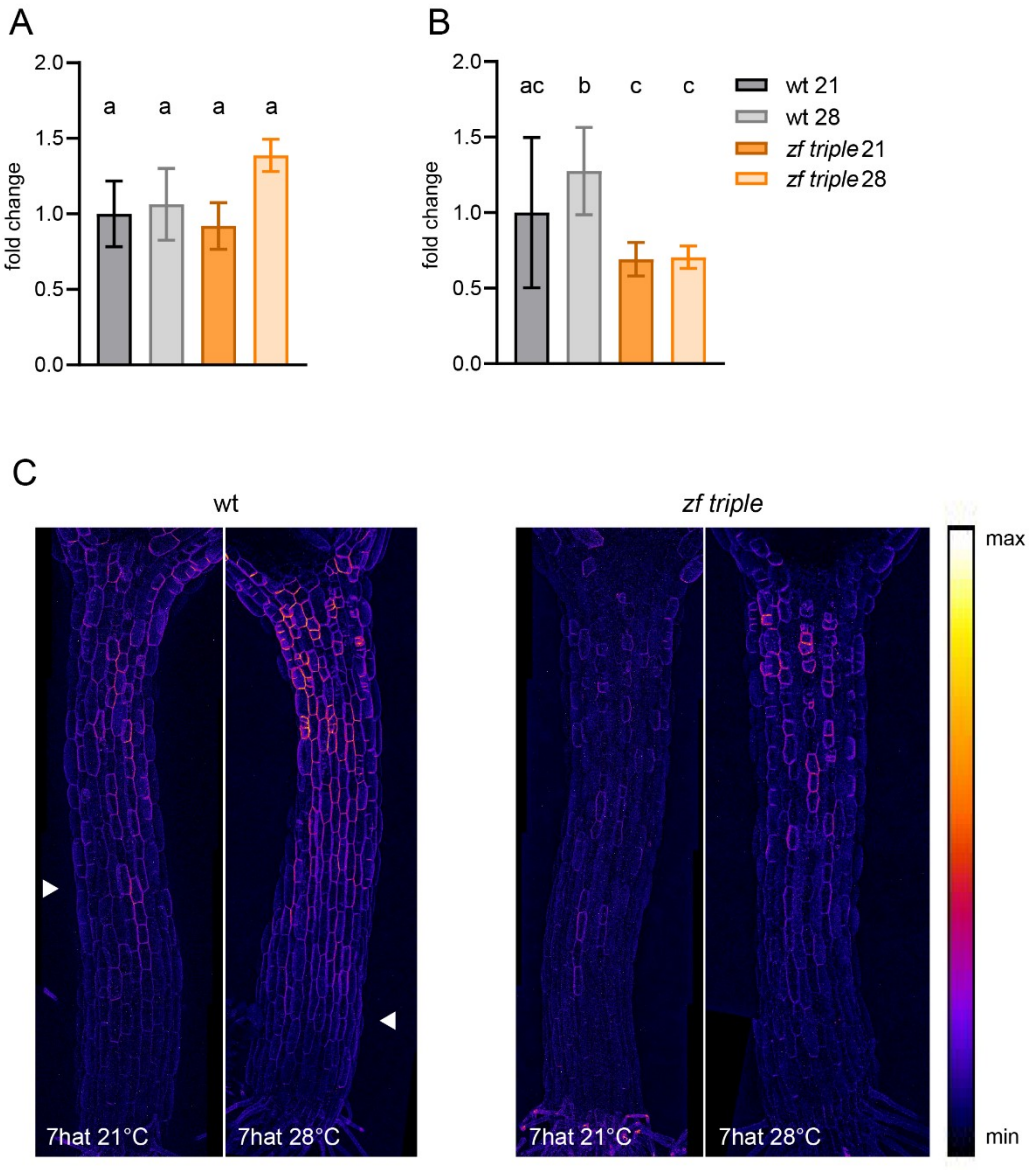

Figure 32: ***Adjustment of PIN7 expression in zf triple hypocotyl upon hAT*** *5 day old seedlings were transferred to 21°C (oAT) versus 28°C (hAT) for different time frame prior analysis* ***(A-B)*** *zf triple and Col0 hypocotyl analysis after* ***(A)*** *6h and* ***(B)*** *1 day of treatment by qPCR. Bars represent mean +- s.d. 2-way ANOVA for statistics, n= 3 biological replicates* ***(C)*** *representative pictures of PIN7:PIN7:GFP analysis in zf triple versus wt in the hypocotyl epidermis by multiphoton microscopy. White arrow mark zone of PIN7 expression*

After 7h of exposure to hAT, overall PIN7:GFP signal was stronger when compared to oAT in wt, whereas in *zf* triple mutant we noticed more scattered PIN7-GFP signal, increased in individual epidermal cells (Figure 32C).

In summary, our result support the role of ZFs in regulation of *PIN3* and *PIN7* expression in hypocotyls and show that loss of their function might interfere with proper adjustment of PIN-mediated transport to hAT.

Auxin signaling response of *zf* triple upon hAT

To determine impact of ZF regulated *PIN* expression on auxin distribution in cotyledons and hypocotyls in response to hAT, we monitored auxin signaling response using *DR5::nlsGFP* reporter in *zf* triple mutant versus wt at hAT versus oAT.

Measurements of *DR5::nlsGFP* signal in pavement cells of cotyledons revealed slightly enhanced auxin signaling response in *zf* triple mutant compared to wt at oAT (Figure 33A,C). At hAT, auxin signaling in wt was significantly enhanced when compared to oAT at all time points (Figure 33A-C). Unlike wt, in *zf* triple mutant no or modest decrease in *DR5::nlsGFP* expression was detected at 6 hours and 1 day after transfer to hAT (Figure 33A-B), and enhancement of nlsGFP signal was detected only 3 days after transfer to hAT (Figure 33C). Hence, loss of ZFs interfere with auxin response in cotyledons and its adjustment to increase in hAT.

Next, we asked how ZF mediated regulation of *PIN* expression contributes to distribution of auxin in hypocotyls during adaptation to hAT. Hence, we monitored expression of *DR5:nlsGFP* reporter in hypocotyl epidermis of Col and *zf* triple mutant at hAT versus oAT. We measured the nuclear GFP signal intensity in individual epidermal cells and grouped the results according to cell position along the hypocotyl growth axis. Similar to wt, we observed maximum signal intensity in the most bottom cells of the *zf* triple hypocotyl (1till2) under oAT (Figure 34A). Surprisingly, we noticed that *DR5:nlsGFP* signal level was lower in *zf* triple mutant compared to wt at oAT, particularly in apical zone of hypocotyl. In response to hAT, we detected overall increase of *DR5::nlsGFP* signal in *zf* triple when compared to oAT within first 8 hours, whereas no significant difference could be detected 1 and 2 days after transfer (Figure 34A-C, Figure 35). At day 3 after transfer to hAT, *DR5::nlsGFP* signal in *zf* triple mutant raised again when compared to oAT (Figure 34D, Figure 35). Overall, in the *zf* triple mutant, when compared to wt, we detected earlier increase in auxin signaling in response to hAT (Figure 35, 6 to 8 hat in *zf* triple and 1dat in wt).

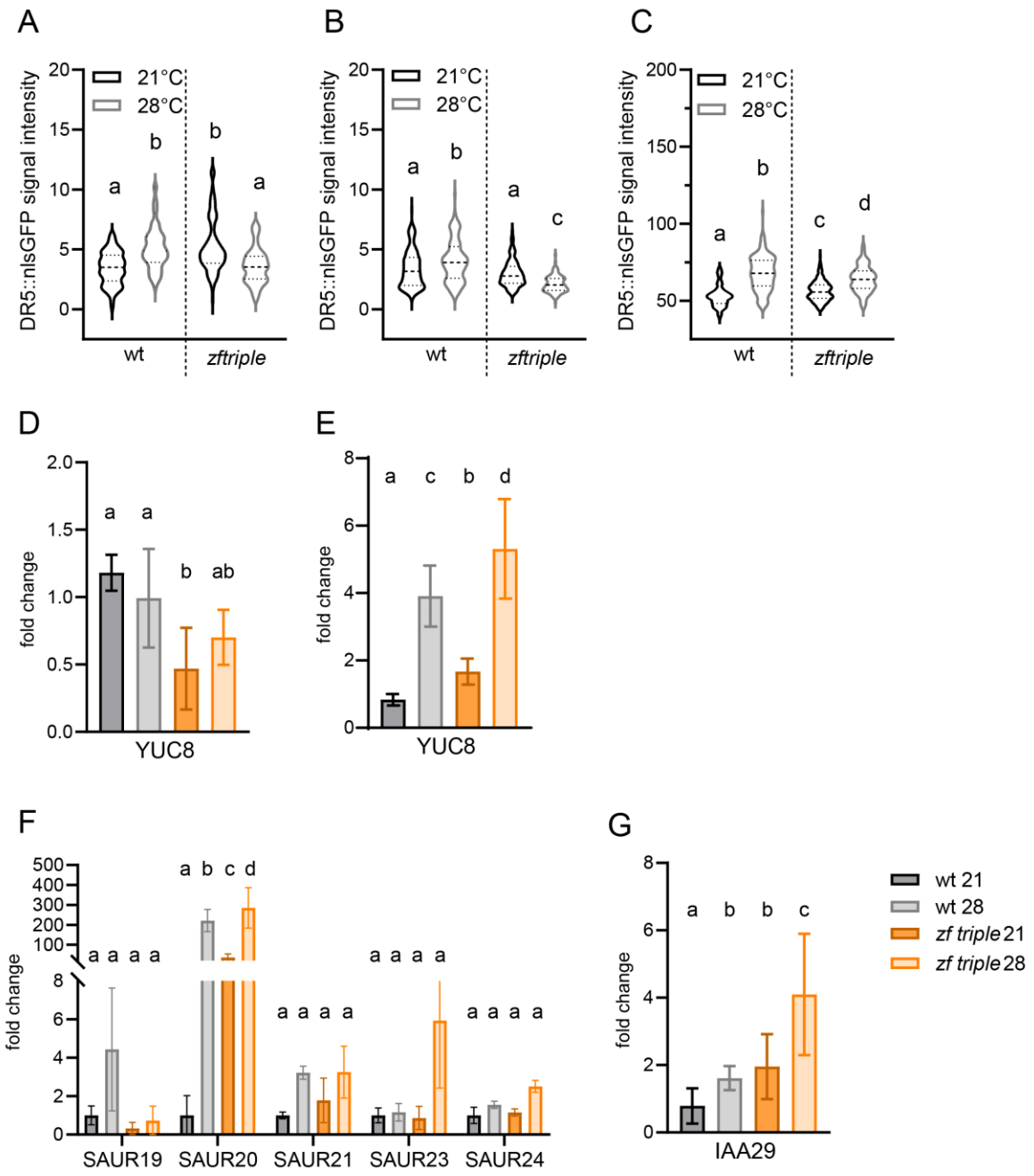

Figure 33: ***Adjustment of Auxin signaling response in zf triple cotyledon during hAT response*** *5 day old seedlings were transferred to 21°C (oAT) versus 28°C (hAT) for different time frame prior analysis* ***(A-C)*** *cotyledon DR5:nlsGFP in zf triple versus wt background were analyzed by confocal microscopy after* ***(A)*** *6h* ***(B)*** *1day and* ***(C)*** *3 days of treatment. Nuclear GFP signal was analyzed and visualized by violin plot with median as dashed lines and quartiles as dotted lines, n>9 cotyledons with 4 cells each* ***(D-E)*** *zf triple and Col0 cotyledon analysis of YUCCA8 expression after* ***(D)*** *6h and* ***(E)*** *1 day of treatment by qPCR. Bars represent mean +- s.d., n=3 biological replicates* ***(F-G)*** *zf triple and Col0 hypocotyl analysis of SAUR genes (F) and IAA29 (G) expression after 6h treatment by qPCR. Bars represent mean +- s.d. 2-way ANOVA for statistics, n>2 biological replicates*

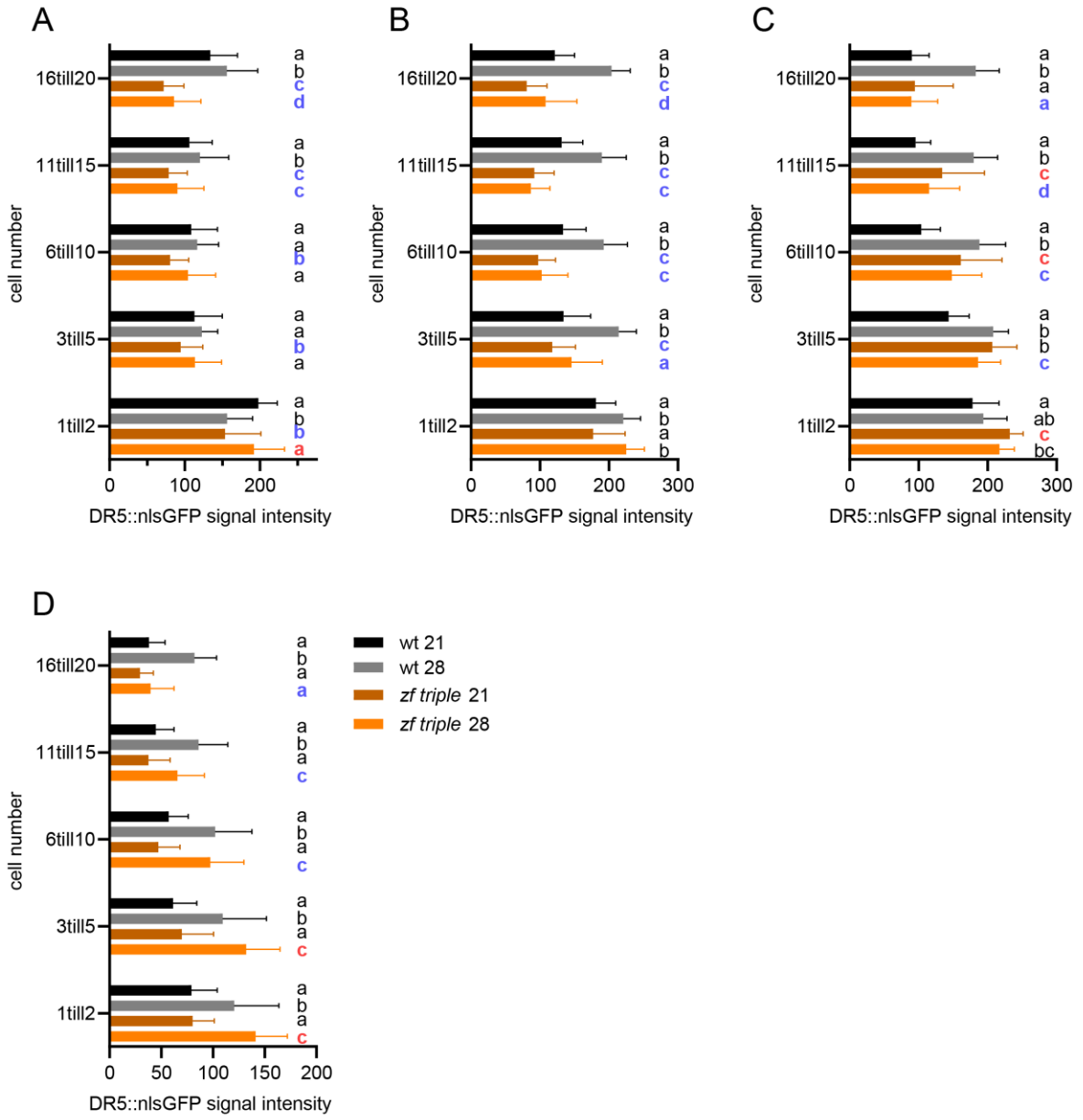

Figure 34: ***Adjustment of auxin signaling in epidermis of zf triple mutant at hAT*** *5 day old DR5:nlsGFP seedlings in zf triple versus wt background were transferred to 21°C (oAT) versus 28°C (hAT) for* ***(A)*** *5h* ***(B)*** *1 day* ***(C)*** *2 days****(D)*** *3 days prior multiphoton microscopic analysis. Nuclear GFP signal was measured and grouped according to their position within the hypocotyl where 1 till2 represent the first 2 cells on the hypocotyl base while 16till20 mark the 5 most top cells in the hypocotyl apex. 2-way ANOVA for statistics where red and blue mark significant up and down regulation respectively, n>4 hypocotyls with at least 5 cells per group.*

Surprisingly, we did not observe any dramatic increase in DR5 signaling in *zf* triple mutant when compared to Col in response to hAT at any time point of observations (Figure 35).

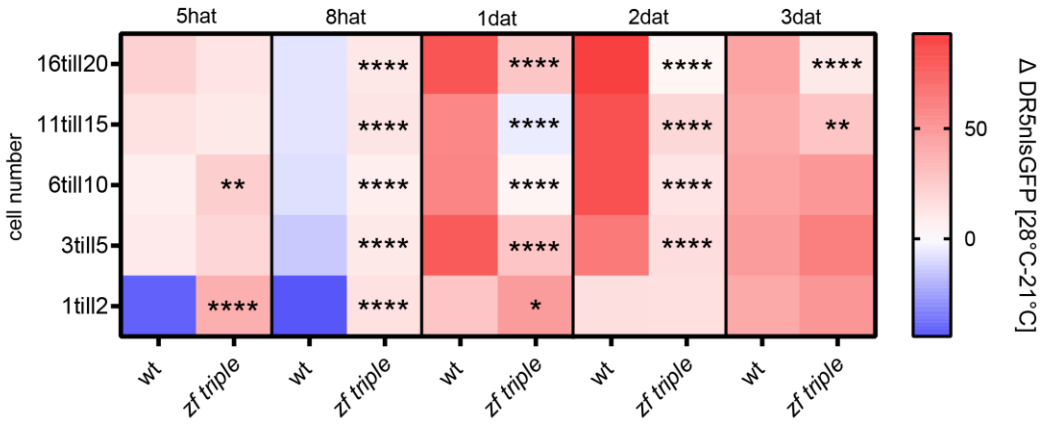

Figure 35: ***Auxin signaling response in zf triple hypocotyl epidermis during hAT response*** *5 day old DR5:nlsGFPseedlings in zf triple mutant versus wt background were transferred to 21°C (oAT) versus 28°C (hAT) for different time frames prior multiphoton analysis of the nuclear signal. Analysis of average difference of DR5:nlsGFP signal intensity between 21°C and 28°C resulting in ΔDR5:nls GFP, Students t-test for statistical comparison to wt, n>4 hypocotyls with at least 5 cells per group, **** = p < 0.0001, *** = p < 0.001, ** = p < 0.01, * = p < 0.05*

Local accumulation of auxin during hAT response in the hypocotyl triggers auxin signaling pathway to activate expression of certain auxin responsive genes such as *Aux/IAAs* and *SAURs* (Bellstaedt et al., 2019). *SAURs* represent one of the largest family of early auxin response genes (Stortenbeker & Bemer, 2019). They inhibit PP2C.D phosphatases to activate plasma membrane (PM) H+-ATPases and subsequently promote cell expansion (Ren & Gray, 2015). During hAT response, *IAA29* and as well as *SAUR19* and *SAUR20* are significantly induced after few hours of incubation at hAT compared to oAT in the hypocotyl (Bellstaedt et al., 2019).

In our experimental set up, we exposed 5 day old seedlings to oAT or hAT for 6 hours, dissected the hypocotyl, removed the shoot apical meristem and conducted RT-qPCR analysis. Exposure to hAT triggered significant enhancement of IAA29 and SAUR20 expression in wt hypocotyl, while other *SAURs* remained unaffected compared to oAT (Figure 33F,G). In *zf* triple mutant, elevated levels of *IAA29* and *SAUR20* was detected at oAT compared to wt (Figure 33F,G). At hAT, *IAA29* expression level was significantly higher in *zf* triple mutant compared to wt (Figure 33G), whereas increase in *SAU20* expression triggered by hAT in wt and *zf triple* mutant was largely comparable (Figure 33F).

In summary, *zf* triple mutant exhibited lower overall auxin signaling response in hypocotyl epidermal cells under oAT compared to wt. However after 5h and 8h of hAT we observed a

significant increase in *ΔDR5:nlsGFP* in the hypocotyl epidermis of *zf t*riple mutant compared to wt. In later time points we found *ΔDR5:nlsGFP* significantly reduced in *zf* triple mutant versus wt. On the other hand, we did not detect any dramatic alterations in thermo-responsiveness of *SAUR* genes in *zf* triple mutant when compared to wt. However further, spatio-temporal analyses are required for final conclusion.

Impact of ZFs on auxin metabolism at hAT

Overall, our analyses of ZF role in regulation of thermomorphogenesis support the model in which ZFs through negative regulation of PIN expression restrain exaggerated hypocotyl elongation when ambient temperature increases. This is supported by phenotype of *zf* triple mutant such as enhanced hypocotyl elongation in response to hAT (Figure 24), over-sensitivity to auxin applied on cotyledons (Figure 27), NPA inhibitory effect on elongation at hAT (Figure 27), and loss of thermo-responsive *PIN* expression (Figure 30, Figure 28). However, analyses of *zf* triple mutant resulted in two unexpected observations: Expression of *PIN3* is enhanced when compared to wt already at oAT, but hypocotyl elongation in *zf* triple mutant is not significantly accelerated when compared to wt, unless ambient temperature increases. This suggests that ZFs mediated regulation of *PIN* expression provides control over thermo-regulation of auxin transport machinery, but it does not interfere with all components of the thermo-regulatory network. Thus, we tested, whether ZFs are involved in adjustment of auxin metabolism to hAT.

It has been shown that expression of *YUC8* increase at hAT is a direct target of PIF4, a master regulator of thermo-sensing (J. Sun et al., 2012). Hence, we tested whether expression of this auxin biosynthesis gene is affected in *zf* triple mutant. We found that 6 hours and 1 day after transfer, overall expression of *YUC8* is reduced and increased respectively in *zf* triple mutant compared to wt at oAT, presumably due to interaction of ZFs with components of circadian-clock machinery (Figure 33D-E). However, in response to hAT *YUC8* expression in *zf* triple mutant increased comparably to wt (Figure 33E).

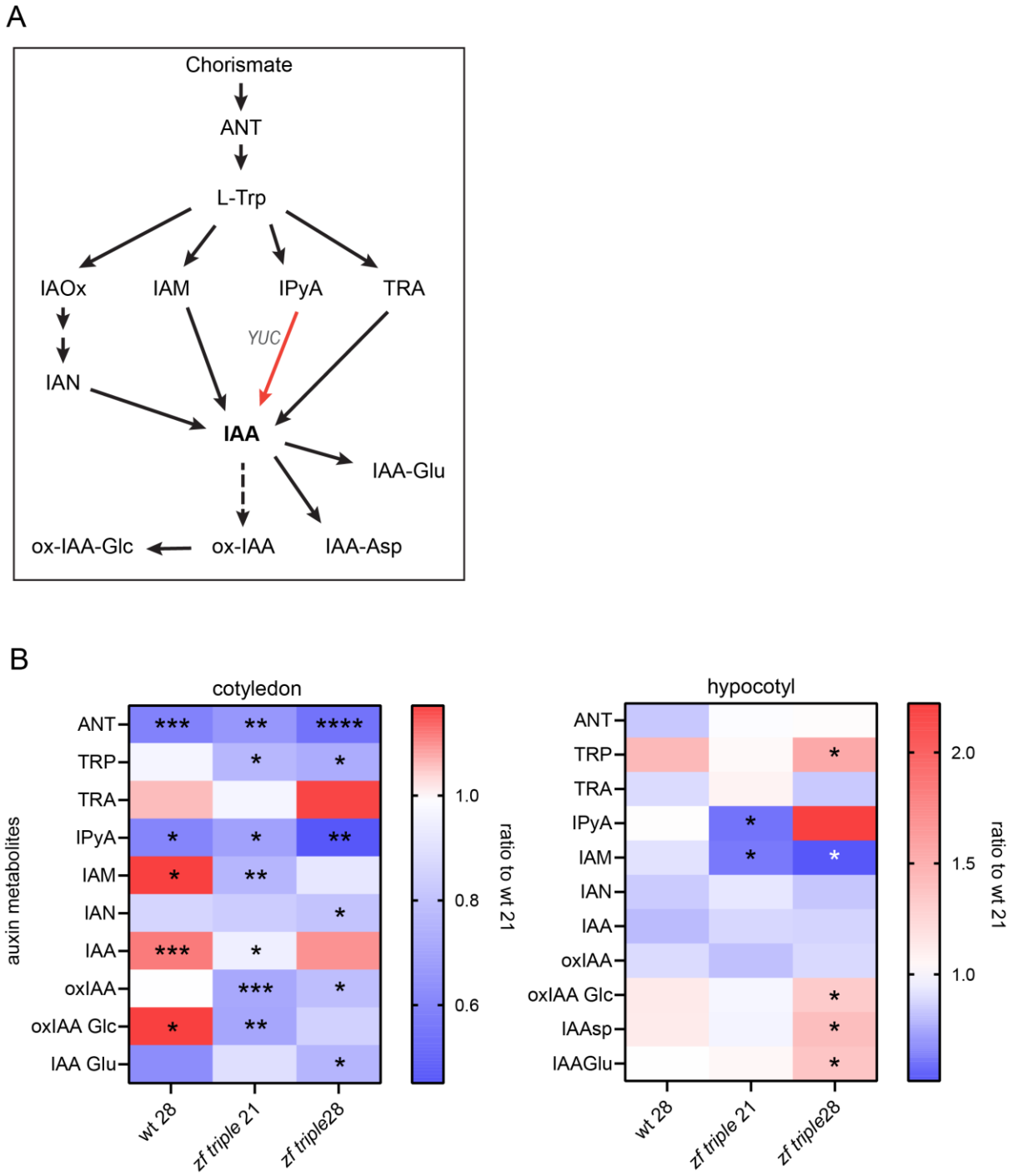

Figure 36: ***Adjustment of Auxin metabolites in zf triple at oAT and hAT. (A)*** *Schematic representation of auxin synthesis pathway. Anthranilate (ANT),L-tryptophane (L-Trp), indole-3-acetaldoxime (IAOx), indole-3-acetamide (IAM), indole-3-pyruvic acid (IPyA), tryptophan aminotransferases (TRA), indole-3-acetonitrile (IAN), indole-3-acetic acid (IAA), IAA-glutamate (IAA-Glu), IAA-aspartic acid (IAA-Asp), oxidized IAA (ox-IAA), ox-IAA with attached glucose (ox-IAA-Glc)* ***(B)*** *Seedlings were grown for 6 days prior transfer to oAT versus hAT. After 1 day of treatment, cotyledons and hypocotyls were dissected and their auxin metabolites were analyzed separately. Ratio of fmol/tissue of the sample to wt sample at oAT was calculated and their mean was visualized by heat map. Students t-test to oAT samples for statistics, **** = p < 0.0001, *** = p < 0.001, ** = p < 0.01, * = p < 0.05*

To further explore whether ZFs contribute to regulation of auxin metabolic pathways at hAT, we analyzed auxin metabolites. Our preliminary measurements hint at overall lower levels of auxin metabolites in cotyledons of *zf* triple mutant versus wt at oAT (Figure 36B). However, transfer to hAT, similarly like in wt, resulted in increase of auxin accompanied with decrease of auxin biosynthesis precursors (Figure 36B). Thus, thermo-regulation of auxin metabolic pathways does not seem to be dramatically affected by loss of ZFs. Due to general low levels of most of the metabolites in the hypocotyl (Figure 5), analyses require further optimization. While additional analyses are needed to corroborate these results, it seems that ZFs do not significantly interfere with thermo-regulation of auxin metabolism.

Discussion

Modulation of auxin synthesis and PIN–dependent transport is essential for hAT responses including hyponastic leaf movement and hypocotyl growth (Keuskamp et al., 2010; Michaud et al., 2017; Park et al., 2019)

ZF proteins directly bind and inhibit *PIN* expression

Our Y1H screen for direct upstream regulators of *PIN* gene transcription revealed three ZF proteins, namely ZF1, ZF2 and ZAT10, which directly bind to *PCRE1* and *PCRE7* elements in PIN1 and PIN7 promoter (Šimášková et al., 2015, unpublished data, Figure 20A). We confirmed binding ability of these transcriptional regulators to the *PIN1* and *PIN7* promoters and found that they also interact with promoters of *PIN3* and *PIN4* (Figure 20C-E). Analysis of *PIN1* and *PIN7* promoter deletion constructs indicate additional ZF binding sites in the respective *PIN1* and *PIN7* promoter outside of the *PCRE1* and *PCRE7* domains (Figure 20B-E). In accordance with published negative regulatory function of ZF1, ZF2 and ZAT10 (Kodaira et al., 2011; Ohta et al., 2001; Sakamoto et al., 2004, 2000), we found the expression of *PIN1*, *PIN4* and *PIN7* repressed by all three ZF proteins in protoplast assay (Figure 20B) and expression of *PIN3*, *PIN4* and *PIN7* significantly reduced upon ZAT10 induction in root and shoot *in planta* (Figure 21).

To evaluate the presence of other potential ZF binding sites in *PIN* promoters, we prepared *PIN* promoter deletion constructs fused to LUCIFERASE and tested ZF inhibitory effect on the reporter activity in protoplast assay. In addition to the already revealed ZF binding sites within the *PCRE1* and *PCRE7* of *PIN1* and *PIN7* promoter we found additional potential binding areas downstream of *PCRE1* and *PCRE7* (Figure 22).

EAR motif in ZFs is not necessary for PIN repression

The EAR motif represents a well-known regulatory mechanism in plants (Kagale & Rozwadowski, 2011). It was the first conserved transcriptional repression motif discovered in plants containing either LxLxL or DLNxxP (Kagale & Rozwadowski, 2011). C2H2 Zinc-finger gene family is one of the transcription factor families carrying the EAR domain with the consensus amino acid sequence

(L/F)DLN(L), thus acting as repressors (Ohta et al., 2001). It has been reported, that the EAR-repression motif determines the negative regulatory function of ZF proteins on gene expression (Ohta et al., 2001; Sakamoto et al., 2004). To examine their importance in the ZF dependent *PIN* regulation, we mutated the DLNL sequence and tested the constructs in protoplasts. Interestingly, we could not detect any alterations in *PIN* repression by ZF proteins carrying mutated EAR motif compared to wt ZF protein (Figure 22A). In contrast to so far performed analysis of simple EAR motif deletions (Sakamoto et al., 2004), our mutation strategy enabled the functional analysis of the EAR motif in ZF proteins on *PIN* expression by minimizing the risk of reducing protein stability and functionality. Based on our results we assume that either the mutation of DLNL to AAAA is not efficient enough to inactivate the repressive function of the EAR motif suggesting a larger consensus sequence of the EAR domain, or ZF proteins carry other yet unknown domains responsible for its negative regulatory transcription factor activity. Interestingly, it has been reported, that the EAR motif of ZAT10 was not involved in the osmotic stress tolerance in planta (Nguyen et al., 2016), supporting our hypothesis, that ZF repressive function on *PIN* transcription is potentially independent of the presence of EAR motif .

Modulation of *ZF* expression pattern during hAT response

After identification of ZF proteins as negative regulators of *PIN* expression, we asked about the relevance of this regulatory mechanism in a developmental context *in planta*. First, we tested different ZF reporter lines to determine ZF expression pattern in different plant organs. Histochemical analysis of *ZF1:GUS* reporter line revealed *ZF1* expression in the cotyledon, but not in the hypocotyl under oAT (Figure 23A). *ZAT10:GUS* expression was found in the cotyledons, petioles, root-shoot junction and in the collumella cells of the primary root at oAT (Figure 23C, expression in the root not shown). Even though we found ZFs as PIN transcriptional repressors (Figure 20), their expression profile can be either overlapping or complementing dependent on the biological activity level of ZF proteins in different plant tissues and environmental conditions. In our case, ZF expression mostly overlap with the typical expression found for *PIN3, PIN4* and *PIN7* in shoot and root tissue (Figure 11-16) (Michniewicz et al., 2007).

Since ZF1, ZF2 and ZAT10 belong to a family of transcription factors involved in regulation of stress responses in plants (Han et al., 2020; Sakamoto et al., 2004), we further monitored *ZF* expression pattern adjustment under hAT.

Upon hAT, we observed visible enhancement of ZF1 expression in the cotyledon vasculature within 1 day compared to oAT (Figure 23A). After 8h of hAT we observed increased patchy expression of *ZAT10:GUS* in the cotyledon (Figure 23C). In accordance, RT-qPCR analysis of cotyledon tissue confirmed significant enhancement of *ZF1* and *ZAT10* after 1 day of hAT versus oAT (Figure 23E). Within the hypocotyl, *ZAT10* expression visibly increased in the vasculature and outer cell layers in the middle part of the hypocotyl after 8h till 1 day of hAT compared to oAT (Figure 23B). Analysis of hAT induced adjustment of overall transcript levels in the hypocotyl by RT-qPCR revealed no significant change of ZFs compared to oAT (Figure 23F-G). Microscopic analysis of *ZAT10:GFP* transcriptional reporter line showed *ZAT10* expression in the vasculature and epidermal cell layer close to the hypocotyl base under oAT (Figure 23H). Upon 8h of hAT, we observed visible increase in *ZAT10:GFP* signal in the hypocotyl vasculature at the hypocotyl base and epidermal cells close to the hypocotyl apex compared to oAT (Figure 23H). Based on qPCR data and analysis of transcriptional reporter lines, we hypothesize that hAT rather affects *ZAT10* expression in a spatial way than in total transcript level compared to oAT in the hypocotyl. Due to almost no signal detection in *ZAT10:ZAT10:GFP* translational reporter line, we hypothesize that low ZAT10 protein abundance is enough to perform its regulatory transcription factor function, or it undergoes quick turnover. Thus, small adjustments of *ZAT10* expression upon hAT will be more difficult to detect.

In conclusion, *ZF1* in the cotyledon vasculature and *ZAT10* in cotyledon epidermis are significantly enhanced upon hAT compared to oAT. While *ZF1* transcription is generally very low in the hypocotyl and was not affected by hAT, *ZAT10* expression pattern was changed after hAT treatment compared to oAT. With increasing temperature, *ZAT10* transcription is enhanced in the hypocotyl vasculature and outer cell layers while decreased in the hypocotyl base compared to oAT.

Enhanced hypocotyl growth of *zf triple* mutant upon hAT

Plants respond to hAT by developmental adaptation including hyponastic leaf movement and hypocotyl growth (Casal & Balasubramanian, 2019). For hAT driven hyponastic leaf movement, importance of PIN mediated auxin transport was reported (Park et al., 2019). Since ZF proteins are regulated by hAT (Figure 23) and were in parallel found to directly inhibit *PIN* expression (Figure 20), we asked about their biological function in hAT response.

When 5 day old *zf* triple mutant seedlings were transferred to hAT, they exhibited increased hypocotyl growth compared to wt seedlings already after 1 day (Figure 24A). In addition, they reached increased final hypocotyl length after 7 days of hAT treatment compared to wt (Figure 24A). However, when *ZAT10* or *ZF1* expression was induced in the hypocotyl and seedlings were transferred to hAT, we observed significant decline in hypocotyl growth compared to DMSO (Figure 24C). Thus, locally enhanced presence of *ZF1* and ZAT10 in the hypocotyl negatively affect hAT induced hypocotyl growth. Noteworthy, *zf* triple mutant did not exhibit differences in hypocotyl growth under oAT compared to wt (Figure 24A), suggesting their specific importance during hAT triggered stress response. In contrast to hAT driven enhanced hypocotyl growth, we found significantly reduced primary root growth in hAT treated *zf* triple mutant compared to wt (Figure 24F). In parallel, we observed larger cotyledon size in *zf* triple at oAT and under hAT when compared to wt oAT and hAT respectively (Figure 24G). In addition to enhanced hypocotyl growth, hyponastic leaf movement represents one of the hallmarks of hAT response in plants, where PIN proteins play an important role (Dornbusch et al., 2014; Park et al., 2019). Continuous monitoring of *zf* triple mutant grown on soil at 22°C revealed enhanced hyponastic leaf movement compared to wt (Figurev 26). Consequently, *zf* triple mutant exhibited longer true leaf petioles compared to wt at 22°C (Figure 26).

In conclusion, ZF proteins are involved in different hAT triggered physiological responses including enhanced hypocotyl growth, primary root growth and hyponastic leaf movement. Interestingly, *zf* triple mutant showed opposite growth response in the hypocotyl and primary root during hAT response. Auxin itself has opposite effect on shoot and root growth. While auxin treatment induce cell growth in the hypocotyl it inhibit cell elongation in the root (Bonner &

Koepfli, 1939; Rayle & Cleland, 1992). We assume that loss of *PIN* downregulation in *zf* triple mutant cause alteration in auxin transport during hAT response leading to opposite phenotype in root and shoot.

Epidermal cell elongation pattern in *zf triple* at hAT

Enhanced hypocotyl growth response in hAT treated *zf* triple mutant compared to wt raised the question, whether increased cell division or cell elongation are responsible for this phenotype. Analysis of epidermal cell length revealed similar cell elongation pattern in *zf* triple when compared to wt after 1 day of hAT treatment. Even though *zf* triple cell epidermal cell elongation pattern was similar to that of wt, we noticed significantly longer cells in the middle hypocotyl after 1 day of hAT (Figure 25, red asterisk). After 2 days when hAT trigger cell growth mostly around the hypocotyl apex in wt compared to oAT (Figure 25A, black asterisk), we observed enhanced elongation in the middle part of *zf* triple hypocotyl compared to wt at hAT (Figure 25C, red asterisk). Thus, hAT driven cell growth in *zf* triple mutant followed different pattern compared to wt. In addition, we detected increased number of epidermal cells after 1 and 2 days of hAT in *zf triple* when compared to wt (Figure 25E).

Since hypocotyl elongation upon hAT is mainly driven by local auxin signaling in the epidermis (S. Kim et al., 2020), modulation of auxin transport and distribution to and in hypocotyl epidermis facilitate hAT induced epidermal cell elongation. We assume, that the transcriptional inhibitory effect of ZFs on *PIN* expression adjust auxin transport and distribution during hAT, thus regulating strength and position of epidermal cell elongation. To understand how ZFs directly affect this process, we need to investigate the ZF dependent adjustment of PIN-facilitated auxin distribution at oAT and hAT.

ZF dependent adjustment of PINs at oAT and hAT

To determine whether ZF dependent adaptation of auxin distribution at oAT and hAT is due to their negative regulatory role on *PIN* expression, we investigated *PIN:PIN:GFP* translational reporter lines in the *zf* triple versus wt background at oAT and hAT.

Confocal analysis revealed enhanced PIN3:GFP abundance homogenously distributed in cotyledon pavement cells of *zf* triple mutant and wt (Figure 28G). In accordance with the repressive ZFs function on *PINs* (Figure 20), RT-qPCR analysis showed elevated *PIN3*, *PIN4* and *PIN7* expression in *zf* triple cotyledon versus wt at oAT (Figure 28B). Due to microscopic limitations, cotyledon vasculature localized PIN3:GFP was not detected. While exposure to hAT repressed PIN3:GFP expression in wt cotyledon epidermis, no significant change was observed on the transcript and protein level in *zf* triple upon hAT treatment (Figure 28A-D). Thus, modulation of PIN3 expression in cotyledon during the first phase of hAT response is facilitated by ZF proteins.

PIN7 expression and protein level were reduced in hAT treated wt cotyledon when compared to oAT (Figure 29). In *zf* triple mutant, *PIN7* transcript was enhanced at oAT when compared to wt, however response to hAT was downregulated (Figure 29B), hinting at presence of additional temperature sensitive factors targeting *PIN7*. Intriguingly, in *zf* triple mutant, we observed a patchy expression pattern with island of cells exhibiting enhanced PIN7-GFP signal, surrounded by cells lacking the expression. We speculate that, while ZFs inhibit *PIN7* expression, there might be additional, thermo-sensitive yet unknown factor that in concert with ZF contribute to regulation of *PIN7* expression in this tissue.

In conclusion, we suggest that hAT driven reduction of *PIN3* expression in cotyledon epidermis is ZF dependent. How pattern of *PIN7* expression is controlled by ZFs during hAT response and whether there are any additional factors requires additional experiments.

In the hypocotyl, *PIN3:PIN3:GFP* was detected in epidermal and endodermal cell layers in both wt and *zf* triple mutant (Figure 30E). In wt endodermis, PIN3:GFP localized to the basal membrane at oAT (Figure 30C,E). In *zf* triple mutant, we noticed significantly enhanced PIN3:GFP protein abundance on the basal membrane when compared to wt already at oAT (Figure 30). Upon hAT, PIN3 protein accumulation on the basal and lateral endodermal membrane of *zf* triple mutant was enhanced compared to wt at hAT (Figure 30C-E). Taking into consideration that hAT promoted alteration of *ZAT10* expression in hypocotyls (Figure 30B,H), we suggest, that ZAT10

could directly restrain PIN3 expression in the endodermis, thus fin-tuning levels of PIN3 during hAT response. To redirect PIN3 protein from the basal towards the lateral endodermal membrane, modulation of *PIN3* transcription via ZFs is not sufficient. Thus, involvement of additional regulatory factors are suggested. Different kinases and phosphatases have been implicated in lateralization of auxin flow via affecting posttranslational modification of PIN proteins leading to lateralization of PIN proteins in different developmental processes (Armengot, Marquès-Bueno, & Jaillais, 2016; Michniewicz et al., 2007). During SAR, PIN3 lateralization was reported, however the regulatory mechanism remain unclear (Keuskamp et al., 2010). Upon hAT response in petioles,PIF4 dependent induction of *PID* expression results in PIN3 lateralization in the abaxial endodermis towards the cortex leading to auxin accumulation in the abaxial epidermal cell layer (Park et al., 2019). Hence, general change of PIN3 polarization towards the lateral endodermal membrane during hAT treatment is presumably ZF independent. However, we noticed that, while hAT driven PIN3 lateralization in wt endodermis declined after 1 day, it remained profound in *zf* triple mutant (Figure 30C,E). Thus, ZFs activity seems to contribute to temporal control of PIN3 protein abundance on the lateral membranes of endodermal cells during hAT response. If ZFs adapt PIN3 polarity by direct modulating the expression of certain kinases e.g. PID or D6PK awaits further analysis.

In hypocotyl epidermal cells, PIN3:GFP exhibited gradual expression with maxima at apex localized to the basal and radial membrane (Figure 31E). Exposure to hAT resulted in enhanced PIN3:GFP signal in wt (Figure 31A,C). Over time, PIN3-GFP expression in epidermis decayed at both oAT and hAT (Figure 31A-D). At oAT, *zf* triple mutant exhibited higher PIN3 protein abundance in hypocotyl basal membrane of epidermal cells when compared to wt and it remained comparably high also after transfer to hAT (Figure 31A-D). Over the time, similarly like in wt, PIN3:GFP expression in *zf* triple mutant attenuated at oAT as well as at hAT (Figure 31A-D). However, when compared to wt at hAT, PIN3:GFP signal in *zf* triple mutant remained significantly stronger at all time points (Figure 31A-E).

Taking into consideration the expression pattern of ZFs, in particular that of ZAT10 which expands along epidermal tissue during hAT response, we hypothesize that ZFs play important role in suppressing *PIN3* expression in epidermis after prolonged exposure to hAT. As *ZAT10* expression

is restricted to the base of hypocotyls, and *ZF1* was not detected in this tissue at oAT, we speculate about two potential scenarios of ZF dependent PIN3 adjustment at oAT. In the first scenario, the reporter constructs do not fully recapitulate expression pattern of ZF genes, thus, even not detected low levels of ZFs contribute to attenuation of epidermal PIN3 expression. Analysis of *PIN3* transcript levels by RT-qPCR do not fully correspond to analysis of PIN3:PIN3:GFP reporter. These discrepancies might be results of insufficient sensitivity of RT-qPCR assay to capture very local changes in gene expression or dynamics of transcript and protein turnover might differ at varying temperature. In the second scenario, *PIN3* expression in epidermis is fine-tuned by ZFs indirectly, through yet unknown factors.

Similar to PIN3:GFP, PIN7:GFP protein is localized to the radial and basal epidermal cell membrane in wt hypocotyl (Figure 32C). Even though we could not detect any significant changes in *PIN7* expression in *zf* triple mutant at oAT or hAT (Figure 32A-B), microscopic analysis revealed significantly lower PIN7 protein abundance in *zf* triple at oAT and patchy enhancement during hAT response when compared to wt (Figure 32C). Analysis of *ZAT10oe* lines revealed strong repression of ZF1 transcription (Figure 21). Hence, other ZF proteins are presumably enhanced or repressed in the absence of ZF1, ZF2 and ZAT10 in *zf* triple mutant and could subsequently affect *PIN7* expression. Considering the relatively large ZF protein family and the close relation to certain ZF proteins, as ZAT6, ZF3, and ZAT13 (Xie et al., 2019)., their potential role in *PIN* regulation can be assumed

ZF dependent adaptation of auxin distribution at oAT and hAT

Under oAT, *YUC8* expression and auxin signaling response was slightly elevated in *zf* triple cotyledon compared to wt (Figure 33A-C,E). However, preliminary data on analysis of auxin metabolism revealed significant decline in auxin precursors and conjugates in *zf* triple cotyledon at oAT when compared to wt (Figure 36B). This preliminary data suggest contribution of ZFs in modulation of auxin synthesis, signaling and presumably metabolism at oAT, although further experimentation is needed to corroborate this role of ZFs. With increasing temperature, *YUC8* expression was equally enhanced in both *zf* triple and wt (Figure 33E). Together with the similar trend of auxin metabolite modulation at hAT in both genotypes (Figure 36 B), we assume that

hAT driven modulation of auxin synthesis and metabolism is independent of ZFs. Interestingly, unlike in wt, hAT triggered enhancement of auxin signaling response in cotyledon was not observed in *zf* triple during the first phase of hAT response (Figure 33A-B). Thus, loss of ZFs does not affect hAT driven auxin synthesis or metabolism, but interferes with adjustment of auxin signaling response.

Preliminary expression analyses revealed significant enhancement of *SAUR20* expression, but no alteration in other *SAURs* in *zf* triple hypocotyl compared to wt at oAT (Figure 33F). Exposure to hAT triggered similar *SAUR20* increase in *zf* triple and wt hypocotyl (Figure 33F), thus ZFs presumably do not directly affect hAT triggered *SAUR* expression. However, experiments need to be repeated to obtain reliable results.

Transcription of auxin signaling gene *IAA29* in *zf* triple hypocotyl was slightly increased at oAT and even stronger enhanced upon hAT when compared to wt at oAT and hAT respectively (Figure 33G). Interestingly, spatio-temporal analysis of *DR5:nlsGFP* in the hypocotyl epidermis demonstrated partially reduced auxin response in *zf* triple at oAT (Figure 34).Exposure to hAT triggered earlier, but not stronger enhancement of auxin signaling in *zf* triple when compared to wt (Figure 35). Altogether this data hint towards accelerated auxin transport to hypocotyl tissue in *zf* triple mutant leading to earlier auxin accumulation in hypocotyl epidermis during hAT. Since overall increase of auxin response at hAT when compared to oAT was not higher in the *zf* triple then in wt (Figure 35), we hypothesize that acceleration of hypocotyl growth in *zf* triple mutants might be caused by higher sensitivity to changes in auxin levels than in wt, e.g. by simultaneous deregulation of other pathways, e.g. GA or BR, which were shown to cross-talk with auxin to coordinate hypocotyl growth in response to hAT (Lu et al., 2021).

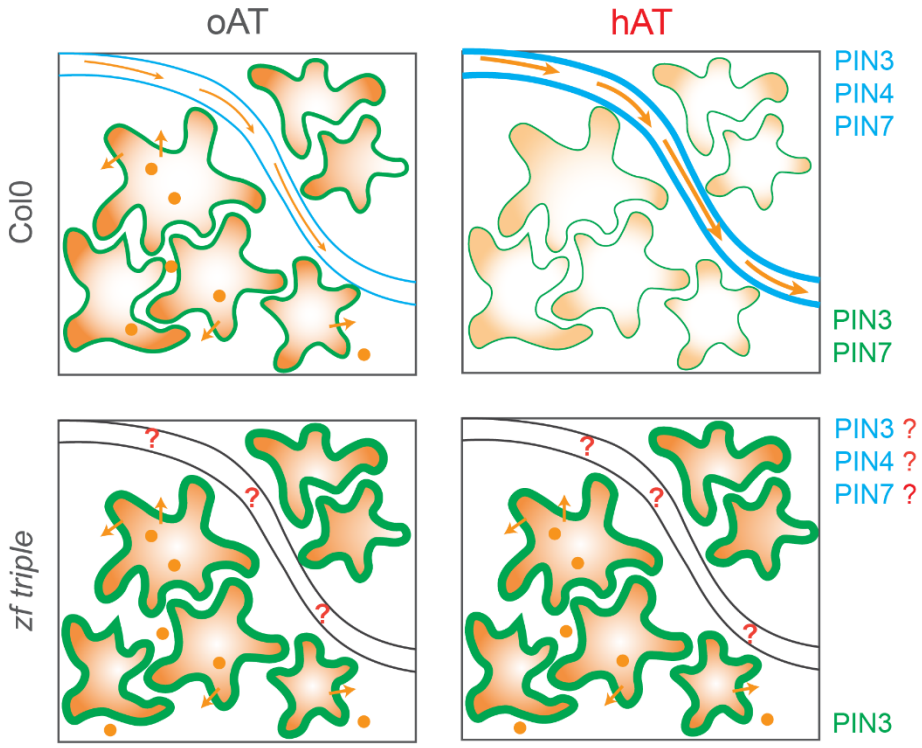

Figure 37: ***Schematic representation of PIN mediated auxin distribution during hAT response in zf triple****. PIN3, PIN4 and PIN7 in blue in cotyledon vasculature. PIN3 and PIN7 in green in cotyledon epidermis, auxin gradient in orange. In wt, PIN3, PIN4 and PIN7 expression is enhanced during hAT response in cotyledon vasculature, while PIN3 and PIN7 in the epidermis decline. In zf triple mutant, cotyledon PIN3 is higher at oAT compared to wt and does not respond to hAT treatment. Red question marks display open questions. 21°C (oAT), 28°C (hAT)*

Conclusion

Understanding the molecular network underlying plant adaptation to hAT is important for the development of effective biotechnologies in agriculture. Whereas mechanisms underlying thermo-sensing and thermo-morphogenesis have been extensively studied, knowledge about counter-balancing mechanisms that preclude risks of trade-offs is rather limited. In our work, we identified unknown molecular components of the thermo-regulatory network, namely ZFs, which through negative regulation of *PIN* transcription, adjust auxin transport to hAT. Our results suggest that the ZF-PIN module might be a part of the negative feedback loop, attenuating activity and output of the thermo-sensing pathways including hypocotyl growth.

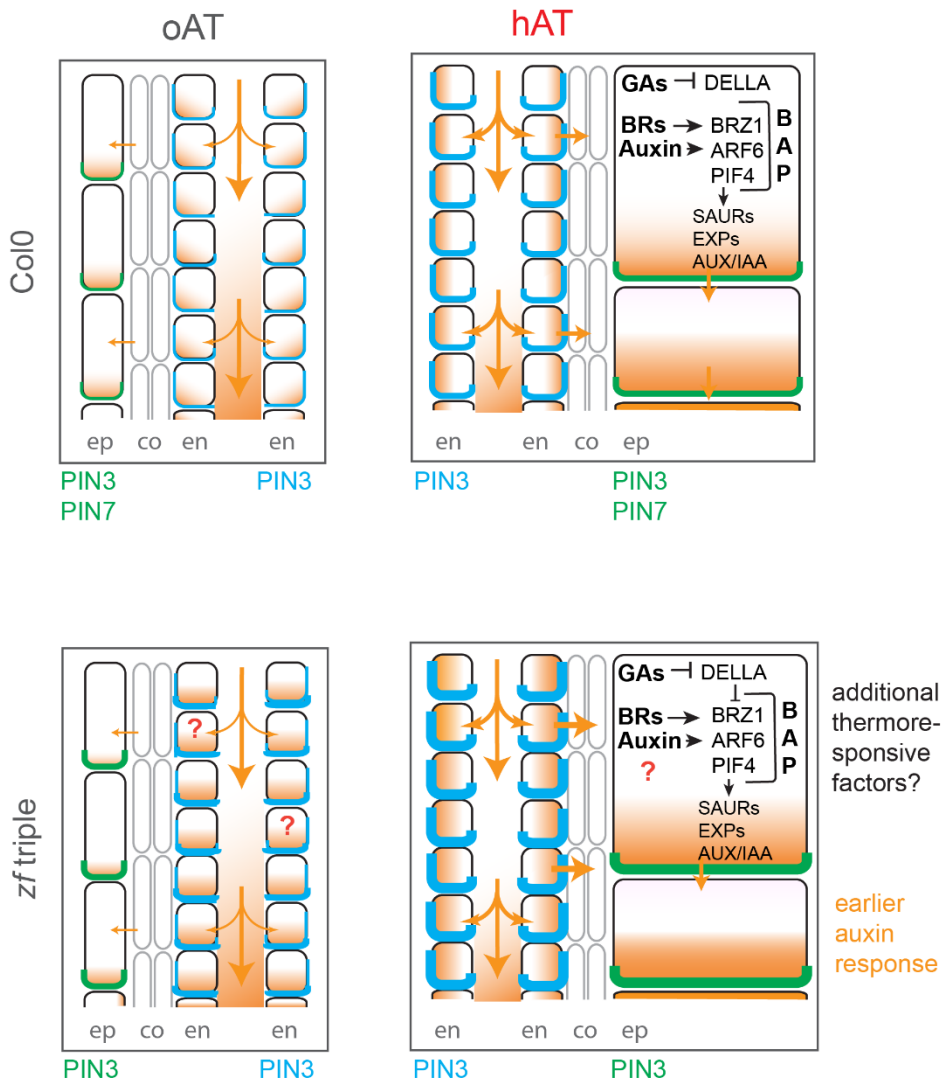

Figure 38: ***Schematic representation of PIN mediated auxin distribution during hAT response in zf triple****. PIN3, PIN4 and PIN7 in blue in hypocotyl endodermis. PIN3 and PIN7 in green in hypocotyl epidermis, auxin gradient in orange. hAT triggered lateralization of endodermal PIN3 drive auxin flow towards the epidermis in wt. zf triple exhibit enhanced PIN3 on basal endodermal membrane already at oAT. Under hAT lateral and basal PIn3:GFP signal increase, which presumably enhancing auxin flow towards epidermis. 21°C (oAT), 28°C (hAT)*

However, how this regulatory module is integrated into known thermo-signalling pathways such as PhyB-PIF4, or recently identified PIF4 independent TOT3-mediated thermo-sensitive phosphorylation cascade, needs further investigation.

Methods

Plant material

Plant material used in this study include *Arabidopsis thaliana* plants, ecotype Col-0. pTCSn::ntdTomato:tNOS-pDR5v2::3nGFP was kindly provided by Ive de Smet (Smet el al 2019). *PIN3:GUS* (Friml et al., 2002), *PIN4:GUS* (Benková et al., 2003) and *PIN7:PIN7:GUS* (Benková et al., 2003) , *PIN3:PIN3:GFP* (Žádníková et al., 2010), *PIN7:PIN7:GFP* (Blilou et al., 2005). The transcriptional reporter line *ZAT10:GFP* was generated by Jose A. O'Brien (Unpublished). *Zf* mutants *zf1* (SALK_133011), *zf2* (SALK_008107), *zat10* (SALK_132562) were obtained from the Salk institute. *Zf* single mutants were crossed with each other and selected by Jose A. O'Brien to obtain *zf* triple and different double mutant variations. To determine the effect of ZF proteins on PIN proteins *zf* triple mutant was crossed with *PIN3:PIN3:GFP* and *PIN7:PIN7:GFP* and further select for homozygous lines for the reporter and all three mutant alleles. In addition *zf* triple was crossed with *pTCSn::ntdTomato:tNOS-pDR5v2::3nGFP* and selected for homozygous lines for the reporter and all three mutant alleles to observe effect of ZFs on auxin response.

Cloning and generation of transgenic lines

All constructs were cloned with Gateway™ (Invitrogen) technology; where the sequences of all used vectors are available online (https://gateway.psb.ugent.be/). For analysis of ZF binding activity in the whole PIN1 and PIN7 promoter we cloned PIN1 and PIN7 promoter deletion constructs for protoplast assay. As control the full 2098bp PIN1 promoter and 1423bp PIN7 promoter was used for protoplast assay. The Δ1pPIN1 deletion construct was obtained by PCR amplification of the 795bp sequence upstream of PIN1 ATG and introduced into the *pDONRP4-P1R* entry vector. Together with *pEN-L1-L+-L2,0* carrying Luciferase sequence it was finally introduced into *pm42GW7,0*. PIN1:LUC, PIN7:LUC, ΔpPIN1:LUC and ΔpPIN7:LUC were cloned by Candela Cuesta Moliner. The Δ1pPIN7 deletion construct was obtained by PCR amplification of the 608bp sequence upstream of PIN7 ATG. After introduction to *pDONRP4-P1R* entry vector Δ1pPIN7 was together with *pEN-L1-L+-L2,0* introduced into *pm42GW7,0.*

To test the EAR motif activity of ZF proteins, we prepared EAR mutated ZF constructs for protoplast assay and for generation of transgenic lines. ZF genomic sequence consist of one exon without any introns. To obtain fully functional control constructs we amplified ZF sequences (ZF1=, ZF2=ZAT10=681bp) by PCR and introduced them into *pDONR221* and sub cloned via LR reaction to *p2GW7,0* (p35S:ZF) for protoplast assay and to *pmDC7,0* for generation of estradiol inducible ZF overexpression lines (ZF ind. OE lines) . For preparation of EAR mutant ZF constructs we changed the corresponding DLN/L nucleotide sequence of ZF sequence in *pDONR221* to AAA/A by site directed mutagenesis with Q5 Site-Directed Mutagenesis Kit (NEB) and introduced to *p2GW7,0* (p35S:ZFm) and *pmDC7,0* (ZFm ind. OE lines).

On soil phenotyping:

Seeds were ethanol sterilized with 70% ethanol for 20 minutes and 100% ethanol for one minute and subsequently stratified for 2 days in ddH2O at 4°C. Afterwards they were transferred to soil (one seed per pot) and grown in the growth chambers equipped with LED Philips GreenPower Production module DR/B/FR plus DR/W (PPFD=165µmol/m²/s) under long day conditions (07:00-23:00 light) at 22°C for 2 weeks until seedlings fully developed their first and second true leaves. For further analysis of periodic leaf movement they were placed in front of an AXION webcam (Axis Companion Cube L Webcam) and monitored for one whole day. From the resulting video (1 picture per second) measurements every 30 minutes were done. To monitor the leaf up and down movement two different values were quantified including the angle between the leaf tips of the first true leaf and the angle between the first true leaf petioles. For further visualization the corresponding angle was used (360°minus quantified angel).

Growth conditions

Seeds were surface sterilized with 70% ethanol for 30 minutes and 1 minute with 100% ethanol, air-dried, plated on half strength Murashige and Skoog (MS) media (Duchefa) with 1%(w/v) sucrose and 1% (w/v) agar (pH=5.9) and stratified for 2 days at 4°C in the dark. Seedlings were grown vertical for 5 days in the mini incubators (Model: Panasonic MIR-154) at oAT in long day conditions (07:00 light on/23:00 light off) with LED Fluence Ray22 (PPFD 195 µmol/m²/s).

RNA extraction, RT and qPCR analysis

For quantitative analysis of gene transcription we harvested cotyledons and hypocotyl separately and kept them at -80°C. We particularly removed the shoot apical meristem from the hypocotyl samples during the harvesting process. Plant material was grinded by (machine) with metal beads in liquid nitrogen for 2 minutes in total prior RNA extraction with Monarch Total RNA Miniprep Kit (NEB). 1ug of RNA was used to generate cDNA using the iScript™ cDNA Synthesis Kit (BioRad). For further analysis 5 µL reaction containing 2.5 µL 2xLuna® Universal qPCR Master Mix (New England BioLabs), 1.5uL 1uM primer and 1uL of diluted (usually 1:5-1:10) cDNA were loaded to 384-well plates (Roche) using a JANUS Automated Workstation (PerkinElmer) or Biomek i5-Series Automated Workstations (Beckmann Coulter). qPCRs were performed using the LightCycler 480 (Roche). Samples ($n \geq 3$) were measured in technical triplicates. PP2A and UBC9 were used as reference genes.

Histochemical and histological analysis

We analyzed different GUS-reporter constructs including pZF1:GUS, pZAT10:GUS, pPIN1:GUS, pPIN3:GUS, pPIN4:GUS and pPIN7:PIN7:GUS. For detection of GUS activity we incubated seedlings in reaction buffer containing 0.1 M sodium phosphate buffer (pH 7), 1 mM ferricyanide, 1 mM ferrocyanide, 0.1% Triton X-100, and 1 mg mL−1 X-Gluc for in dark at 37 °C for different time frames dependent on the reporter-construct. After removal of chlorophyll by incubation in 70% ethanol for 1-2 days, seedlings were cleared in 4% HCl 20% methanol solution for 2-5 minutes at 65 °C and further washed in 7% NaOH/60% ethanol for 20 minutes at room temperature. Afterwards seedlings were rehydrated by subsequent incubation in 60, 40, 20, 10% ethanol for 20 minutes followed by incubation in 25% glycerol and 5% ethanol-solution for at least 30 minutes. For further microscopic analysis we mounted on glass slides in 50% glycerol and monitored with Olympus VS120 Slide Scanner.

Hypocotyl phenotyping

5 day old seedlings were treated according to the experimental setup. For temperature phenotyping assays seedlings were transferred at ZTG2 (ZTG2=09:00) to hAT versus oAT

incubators for additional 3-4 days with daily scanning at ZTG6. For NAA and estradiol experiments NAA-lanolin and/or estradiol-lanolin versus DMSO-lanolin (as negative control) was locally applied at ZTG2-4 on cotyledons and/or hypocotyls of 5day old seedlings at ZTG2 with a toothpick followed by incubated at oAT or hAT in the Mini Percival incubator for additional 3-4 days with daily scanning at ZTG6.

Protoplast assay

Protoplasts were isolated from 4-day old Arabidopsis root suspension culture in enzyme solution (1% cellulose and 0.2% Macerozyme (Yakult)) dissolved in B5 0.34M glucose-mannitol solution(2.2 g MS with vitamins, 15.25 g glucose, 15.25 g mannitol, pH to 5.5 with KOH) with slight shaking for 4 h in the dark. Cells were collected by centrifugation at 800 x g for 5 minutes (acceleration=9 deacceleration=5) and resuspended in B5 glucose-mannitol solution to a final concentration of 4 × 106 protoplasts/mL. 50uL of cell suspension were transiently co-transfected with 1ug of normalization plasmid expressing the Renilla luciferase (rLUC) under the control of the 35Spromoter, 1ug of reporter plasmid expressing fLUC driven by PIN promoter (pPIN1.LUC, pPIN4:LUC, pPIN7:LUC, p35S:LUC) and 1ug of the effector construct with ZF under the control of 35S promoter (p35S:ZF1, p35S:ZF2, p§%S:ZAT10). PEG-mediated transformation was performed by addition of 60 µL of PEG solution (0.1 M Ca(NO3)2, 0.45 M mannitol, 25% PEG 6000) to the cell-cDNA mixture and soft mixing prior incubation for 30 minutes in the dark. Wash out of PEG solution and sedimentation of cells was achieved by addition of 140 µL of 0.275 M Ca(NO3)2 solution. The remaining cells were suspended in 200 µL of B5 glucose-mannitol solution and incubated for 16 h in the dark at room temperature to enable expression of transfected constructs. Next day cells were lysed by addition of 50uL of lysis buffer (info) and fLUC and rLUC activities were determined with the Dual-Luciferase reporter assay system (Promega). Variations in transfection efficiency were corrected by normalization of fLUC by the rLUC activities.

Chromatin Immunoprecipitation (ChIP)

For analyzing the direct binding potential of ZAT10 proteins to PIN1,3,4 and 7 promoters Chromatin Immunoprecipitation was performed. Isolated Protoplasts (see protoplast assay) were

transfected by PEG-mediated transformation with 1-5ug 35S:ZAT10-HA cDNA or with water and incubated for 16 hours in the dark. ChIP assays were performed as described by Lee et al. (2007) and adapted by Krisztina Ötvös. Transformed protoplasts were fixed in 1% Paraformaldehyde and washed in MTSB buffer (50 mM PIPES (pH=6.9), 5 mM MgSO4, 5 mM EGTA) 3 times. Afterwards nuclei were extracted with freshly prepared ice cold Galbraith solution (45 mM MgCl2, 20 mM MOPS, 30 mM Sodium Citrate, 0.1% Triton X-100, pH=7) and pellet was re-suspended in EB2 (0.25 M sucrose, 10mM Tris-Hcl pH=8, 0.15 % Triton X100, 5mM beta-mercapto-ethanol, 1mM PMSF, protease inhibitor complex tablet) and centrifuged at 14000g 10 minutes at 4°C. After removal of supernatant pellet was re-suspended with EB3 (1.75 M sucrose, 10mM Tris-HCl pH=8, 0.15 % Triton X-100, 2mM MgCl2, 5mM beta-mercapto-ethanol, 1mM PMSF, protease inhibitor complex tablet) and layerd on top of fresh EB3 prior centrifugation for 1h top speed at 4°C. After removal of supernatant the resulting pellet was re-suspended in IP buffer (50 mM Hepes pH=7.8, 140 mM NaCl, 1 % Triton X-100, 0.1 % Sodium-deoxycholate, protease inhibitor complex tablet and phosphatase inhibitor complex tablet) and sonicated in ice water for 10 times 30 seconds off 30 seconds on with Sonicator Bioruptor Plus (diagenode) to obtain chromatin fragments of sizes between 100-500bp. Samples were shortly centrifuged for 5 minutes at 14000g at 4°C to remove pellet and supernatant was used for Immuno-precipitation with Anti-HA monoclonal antibody bound to protein G–coated magnetic beads (Dynabeads Protein G Immunoprecipitation kit; Invitrogen) to immunoprecipitate the genomic DNA fragments bound to ZAT10-HA. Semiquantitative PCR was performed with immunoprecipitated genomic DNA using primer pairs corresponding to fragments of R2R3 promoter (F2 and F5). Primers specific for Actin () was used to amplify a negative control.

Microscopic analysis

For all microscopy experiments 5 day old seedlings grown in the mini Percival incubator oAT were used as starting material for different time frames of various treatments. Temperature, hormonal and chemical treatments (NAA-lanolin/estradiol-lanolin vs DMSO-lanolin) were done at Zeitgeber 2-5. Microscopy analysis of cotyledons on glass slides (info) were performed with Leica SP8 inverted (WLL, FALCON) confocal microscope with 10x or 20x dry objective using time gating to

exclude auto-fluorescence. Hypocotyl analysis on glass slides (info) was mostly performed with Leica TCS SP8 DIVE CS (DeepSee dual, FALCON) multiphoton microscope with 20x water immersion objective. Fluorescence markers were excited at 488 nm. For analysis of the epidermal cell length pattern in hypocotyls we performed propidium iodid staining for 20 minutes and confocal pictures were obtained by Leica SP8 inverted (WLL, FALCON) confocal microscope with 10x or 20x dry objective. PI was excited at 488nm.

Auxin metabolite measurement

Analysis of auxin metabolites was performed by Pěnčík lab in Olomouc following the methods described by Pěnčík et al. (2018). Samples of hypocotyls and cotyledons were extracted with 0.5 ml of 50 mM phosphate buffer (pH 7.0) containing 0.1% sodium diethyldithiocarbamate and mixture of stable isotope-labelled internal standards. 200 µl of the extract was acidified with HCl to pH 2.7 and processed by in-tip micro solid phase extraction (in-tip µSPE). Another 200 µl portion was derivatized by cysteamine, acidified with HCl to pH 2.7 and purified using in-tip µSPE in order to determine IPyA. After evaporation under reduced pressure, samples were analyzed using HPLC system 1260 Infinity II (Agilent Technologies, USA) equipped with Kinetex C18 column (50 mmx2.1 mm, 1.7 µm; Phenomenex) and linked to 6495 Triple Quad detector (Agilent Technologies, USA).

Yeast-1-Hybrid (Y1H) assay

The Y1H screen was performed as described by Simaskova (Šimášková et al., 2015). The yeast strain YM4271 and destination vectors pDEST-MW1 and pDEST- MW2 have been previously described. Yeast reporter strains were designed as described before (Deplancke, Dupuy, Vidal, & Walhout, 2004). The 200 bp promoter fragment of PCRE1 and PCRE7 were cloned into the destination vectors pDEST-MW1 and pDEST- MW2 by Gateway cloning for the Y1H cDNA library screen. The DNA PCRE1 and PCRE7 baits were transformed to yeast following the Yeast Protocol Handbook from Clontech except that we used 1ug of linearized plasmid DNA for yeast transformation, the heat shock period at 42 °C was extended to 20 min and the cells were resuspended in 150 µl TE buffer (Šimášková et al., 2015). The cDNA Y1H library screen was

performed with a REGIA and REGULATORS collection. For every transcription factor 20 µl of competent yeast was mixed with 2 µl of carrier DNA, 100 ng plasmid (transcription factor) DNA and 100 µl of TE/LiAC/PEG. Yeast cells were resuspended in 20 µl TE buffer and transferred to SD-His-Ura-Trp medium. After 3 days of growing, positive clones were selected 6 to 8 days after incubation at 30°C on replica plates with with 0, 15 and 30 mM 3-aminotriazole.

Data analysis

Data were analyzed using ImagJ software (National Institute of Health, http://rsb.info.nih.gov/ij), GraphPad Prism 8, and Microsoft PowerPoint programs. All data were analyzed using Student's t test or 2-way ANOVA

References

Abas, L., Kolb, M., Stadlmann, J., Janacek, D. P., Lukic, K., Schwechheimer, C., … Hammes, U. Z. (2021). Naphthylphthalamic acid associates with and inhibits PIN auxin transporters. *Proceedings of the National Academy of Sciences of the United States of America*, *118*(1), e2020857118. https://doi.org/10.1073/pnas.2020857118

Adamowski, M., & Friml, J. (2015). PIN-dependent auxin transport: action, regulation, and evolution. *The Plant Cell*, *27*(1), 20–32. https://doi.org/10.1105/tpc.114.134874

Armengot, L., Marquès-Bueno, M. M., & Jaillais, Y. (2016). Regulation of polar auxin transport by protein and lipid kinases. *Journal of Experimental Botany*, *67*(14), 4015–4037. https://doi.org/10.1093/jxb/erw216

Bai, F., & DeMason, D. A. (2008). Hormone interactions and regulation of PsPK2::GUS compared with DR5::GUS and PID::GUS in Arabidopsis thaliana. *American Journal of Botany*, *95*(2), 133–145. https://doi.org/https://doi.org/10.3732/ajb.95.2.133

Balcerowicz, M. (2020). PHYTOCHROME-INTERACTING FACTORS at the interface of light and temperature signalling. *Physiologia Plantarum*, *169*(3), 347–356. https://doi.org/https://doi.org/10.1111/ppl.13092

Bellstaedt, J., Trenner, J., Lippmann, R., Poeschl, Y., Zhang, X., Friml, J., … Delker, C. (2019). A Mobile Auxin Signal Connects Temperature Sensing in Cotyledons with Growth Responses in Hypocotyls. *Plant Physiology*, *180*(2), 757–766. https://doi.org/10.1104/pp.18.01377

Benková, E., Michniewicz, M., Sauer, M., Teichmann, T., Seifertová, D., Jürgens, G., & Friml, J. (2003). Local, Efflux-Dependent Auxin Gradients as a Common Module for Plant Organ Formation. *Cell*, *115*(5), 591–602. https://doi.org/https://doi.org/10.1016/S0092-8674(03)00924-3

Blilou, I., Xu, J., Wildwater, M., Willemsen, V., Paponov, I., Friml, J., … Scheres, B. (2005). The PIN auxin efflux facilitator network controls growth and patterning in Arabidopsis roots. *Nature*, *433*(7021), 39–44. https://doi.org/10.1038/nature03184

Bonner, J., & Koepfli, J. B. (1939). The Inhibition of Root Growth by Auxins. *American Journal of Botany*, *26*(7), 557–566. https://doi.org/10.2307/2436583

Bouré, N., Kumar, S. V., & Arnaud, N. (2019). The BAP Module: A Multisignal Integrator Orchestrating Growth. *Trends in Plant Science*, *24*(7), 602–610. https://doi.org/https://doi.org/10.1016/j.tplants.2019.04.002

Box, M. S., Huang, B. E., Domijan, M., Jaeger, K. E., Khattak, A. K., Yoo, S. J., … Wigge, P. A. (2015). ELF3 Controls Thermoresponsive Growth in Arabidopsis. *Current Biology*, *25*(2), 194–199. https://doi.org/10.1016/j.cub.2014.10.076

Casal, J. J., & Balasubramanian, S. (2019). Thermomorphogenesis. *Annual Review of Plant Biology*, *70*(1), 321–346. https://doi.org/10.1146/annurev-arplant-050718-095919

Casanova-Sáez, R., & Voß, U. (2019). Auxin Metabolism Controls Developmental Decisions in Land Plants. *Trends in Plant Science*, *24*(8), 741–754. https://doi.org/10.1016/j.tplants.2019.05.006

Chapman, E. J., Greenham, K., Castillejo, C., Sartor, R., Bialy, A., Sun, T., & Estelle, M. (2012). Hypocotyl Transcriptome Reveals Auxin Regulation of Growth-Promoting Genes through GA-Dependent and -Independent Pathways. *PLOS ONE*, *7*(5), e36210. Retrieved from https://doi.org/10.1371/journal.pone.0036210

Chuang, Z., Bing, L., Shilong, P., Xuhui, W., B., L. D., Yao, H., … Senthold, A. (2017). Temperature increase reduces global yields of major crops in four independent estimates. *Proceedings of the National Academy of Sciences*, *114*(35), 9326–9331. https://doi.org/10.1073/pnas.1701762114

Chung, B. Y. W., Balcerowicz, M., Di Antonio, M., Jaeger, K. E., Geng, F., Franaszek, K., … Wigge, P. A. (2020). An RNA thermoswitch regulates daytime growth in Arabidopsis. *Nature Plants*, *6*(5), 522–532. https://doi.org/10.1038/s41477-020-0633-3

Ciftci-Yilmaz, S., & Mittler, R. (2008). The zinc finger network of plants. *Cellular and Molecular Life Sciences*, *65*(7), 1150–1160. https://doi.org/10.1007/s00018-007-7473-4

Cortijo, S., Charoensawan, V., Brestovitsky, A., Buning, R., Ravarani, C., Rhodes, D., … Wigge, P. A. (2017). Transcriptional Regulation of the Ambient Temperature Response by H2A.Z Nucleosomes and HSF1 Transcription Factors in Arabidopsis. *Molecular Plant*, *10*(10), 1258–1273. https://doi.org/10.1016/j.molp.2017.08.014

Crawford, A. J., McLachlan, D. H., Hetherington, A. M., & Franklin, K. A. (2012). High temperature exposure increases plant cooling capacity. *Current Biology*, *22*(10), R396–R397. https://doi.org/https://doi.org/10.1016/j.cub.2012.03.044

Das, D., St Onge, K. R., Voesenek, L. A. C. J., Pierik, R., & Sasidharan, R. (2016). Ethylene- and Shade-Induced Hypocotyl Elongation Share Transcriptome Patterns and Functional Regulators. *Plant Physiology*, *172*(2), 718–733. https://doi.org/10.1104/pp.16.00725

de Lucas, M., & Prat, S. (2014). PIFs get BRright: PHYTOCHROME INTERACTING FACTORs as integrators of light and hormonal signals. *New Phytologist*, *202*(4), 1126–1141. https://doi.org/https://doi.org/10.1111/nph.12725

De Schepper, V., De Swaef, T., Bauweraerts, I., & Steppe, K. (2013). Phloem transport: a review of mechanisms and controls. *Journal of Experimental Botany*, *64*(16), 4839–4850. https://doi.org/10.1093/jxb/ert302

Deepika, Ankit, Sagar, S., & Singh, A. (2020). Dark-Induced Hormonal Regulation of Plant Growth and Development . *Frontiers in Plant Science* . Retrieved from https://www.frontiersin.org/article/10.3389/fpls.2020.581666

Deplancke, B., Dupuy, D., Vidal, M., & Walhout, A. J. M. (2004). A gateway-compatible yeast one-hybrid system. *Genome Research*, *14*(10B), 2093–2101. https://doi.org/10.1101/gr.2445504

Di, D.-W., Zhang, C., Luo, P., An, C.-W., & Guo, G.-Q. (2016). The biosynthesis of auxin: how many paths truly lead to IAA? *Plant Growth Regulation*, *78*(3), 275–285. https://doi.org/10.1007/s10725-015-0103-5

Dornbusch, T., Michaud, O., Xenarios, I., & Fankhauser, C. (2014). Differentially phased leaf

growth and movements in Arabidopsis depend on coordinated circadian and light regulation. *The Plant Cell*, *26*(10), 3911–3921. https://doi.org/10.1105/tpc.114.129031

Drechsel, G., Raab, S., & Hoth, S. (2010). Arabidopsis zinc-finger protein 2 is a negative regulator of ABA signaling during seed germination. *Journal of Plant Physiology*, *167*(16), 1418–1421. https://doi.org/https://doi.org/10.1016/j.jplph.2010.05.010

Du, J., Jiang, H., Sun, X., Li, Y., Liu, Y., Sun, M., … Yang, W. (2018). Auxin and Gibberellins Are Required for the Receptor-Like Kinase ERECTA Regulated Hypocotyl Elongation in Shade Avoidance in Arabidopsis . *Frontiers in Plant Science* . Retrieved from https://www.frontiersin.org/article/10.3389/fpls.2018.00124

Englbrecht, C. C., Schoof, H., & Böhm, S. (2004). Conservation, diversification and expansion of C2H2 zinc finger proteins in the Arabidopsis thaliana genome. *BMC Genomics*, *5*, 1–17. https://doi.org/10.1186/1471-2164-5-39

Fiorucci, A.-S., Galvão, V. C., Ince, Y. Ç., Boccaccini, A., Goyal, A., Allenbach Petrolati, L., … Fankhauser, C. (2020). PHYTOCHROME INTERACTING FACTOR 7 is important for early responses to elevated temperature in Arabidopsis seedlings. *New Phytologist*, *226*(1), 50–58. https://doi.org/https://doi.org/10.1111/nph.16316

Franklin, K. A., Lee, S. H., Patel, D., Kumar, S. V., Spartz, A. K., Gu, C., … Gray, W. M. (2011). Phytochrome-Interacting Factor 4 (PIF4) regulates auxin biosynthesis at high temperature. *Proceedings of the National Academy of Sciences of the United States of America*, *108*(50), 20231–20235. https://doi.org/10.1073/pnas.1110682108

Franklin, K. A., Toledo-Ortiz, G., Pyott, D. E., & Halliday, K. J. (2014). Interaction of light and temperature signalling. *Journal of Experimental Botany*, *65*(11), 2859–2871. https://doi.org/10.1093/jxb/eru059

Friml, J., Wiśniewska, J., Benková, E., Mendgen, K., & Palme, K. (2002). Lateral relocation of auxin efflux regulator PIN3 mediates tropism in Arabidopsis. *Nature*, *415*(6873), 806–809. https://doi.org/10.1038/415806a

Gao, C., Liu, X., De Storme, N., Jensen, K. H., Xu, Q., Yang, J., … Liesche, J. (2020). Directionality of Plasmodesmata-Mediated Transport in Arabidopsis Leaves Supports Auxin Channeling. *Current Biology*, *30*(10), 1970–1977.e4. https://doi.org/10.1016/j.cub.2020.03.014

Gray, W. M., Östin, A., Sandberg, G., Romano, C. P., & Estelle, M. (1998). High temperature promotes auxin-mediated hypocotyl elongation in Arabidopsis *Proceedings of the National Academy of Sciences*, *95*(12), 7197 LP-7202. https://doi.org/10.1073/pnas.95.12.7197

Gull, A. (2019). Biotic and Abiotic Stresses in Plants. In A. A. Lone (Ed.) (p. Ch. 1). Rijeka: IntechOpen. https://doi.org/10.5772/intechopen.85832

Han, G., Lu, C., Guo, J., Qiao, Z., Sui, N., Qiu, N., & Wang, B. (2020). C2H2 Zinc Finger Proteins: Master Regulators of Abiotic Stress Responses in Plants . *Frontiers in Plant Science* . Retrieved from https://www.frontiersin.org/article/10.3389/fpls.2020.00115

Hart, J. E., & Gardner, K. H. (2021). Lighting the way: Recent insights into the structure and regulation of phototropin blue light receptors. *Journal of Biological Chemistry*, *296*, 100594. https://doi.org/https://doi.org/10.1016/j.jbc.2021.100594

Hayes, S., Sharma, A., Fraser, D. P., Trevisan, M., Cragg-Barber, C. K., Tavridou, E., … Franklin, K. A. (2017). UV-B Perceived by the UVR8 Photoreceptor Inhibits Plant Thermomorphogenesis. *Current Biology : CB*, *27*(1), 120–127. https://doi.org/10.1016/j.cub.2016.11.004

Hošek, P., Kubeš, M., Laňková, M., Dobrev, P. I., Klíma, P., Kohoutová, M., … Zažímalová, E. (2012). Auxin transport at cellular level: new insights supported by mathematical modelling. *Journal of Experimental Botany*, *63*(10), 3815–3827. https://doi.org/10.1093/jxb/ers074

Huq, E., Al-Sady, B., & Quail, P. H. (2003). Nuclear translocation of the photoreceptor phytochrome B is necessary for its biological function in seedling photomorphogenesis. *The Plant Journal*, *35*(5), 660–664. https://doi.org/https://doi.org/10.1046/j.1365-313X.2003.01836.x

Jae-Hoon, J., Mirela, D., Cornelia, K., Surojit, B., Daphne, E., Mingjun, G., … A., W. P. (2016).

Phytochromes function as thermosensors in Arabidopsis. *Science*, *354*(6314), 886–889. https://doi.org/10.1126/science.aaf6005

Kagale, S., & Rozwadowski, K. (2011). EAR motif-mediated transcriptional repression in plants: An underlying mechanism for epigenetic regulation of gene expression. *Epigenetics*, *6*(2), 141–146. https://doi.org/10.4161/epi.6.2.13627

Keuskamp, D. H., Pollmann, S., Voesenek, L. A. C. J., Peeters, A. J. M., & Pierik, R. (2010). Auxin transport through PIN-FORMED 3 (PIN3) controls shade avoidance and fitness during competition. *Proceedings of the National Academy of Sciences*, *107*(52), 22740 LP-22744. https://doi.org/10.1073/pnas.1013457108

Kim, S., Hwang, G., Kim, S., Thi, T. N., Kim, H., Jeong, J., … Oh, E. (2020). The epidermis coordinates thermoresponsive growth through the phyB-PIF4-auxin pathway. *Nature Communications*, *11*(1), 1053. https://doi.org/10.1038/s41467-020-14905-w

Kim, T.-W., Guan, S., Sun, Y., Deng, Z., Tang, W., Shang, J.-X., … Wang, Z.-Y. (2009). Brassinosteroid signal transduction from cell-surface receptor kinases to nuclear transcription factors. *Nature Cell Biology*, *11*(10), 1254–1260. https://doi.org/10.1038/ncb1970

Kodaira, K.-S., Qin, F., Tran, L.-S. P., Maruyama, K., Kidokoro, S., Fujita, Y., … Yamaguchi-Shinozaki, K. (2011). Arabidopsis Cys2/His2 Zinc-Finger Proteins AZF1 and AZF2 Negatively Regulate Abscisic Acid-Repressive and Auxin-Inducible Genes under Abiotic Stress Conditions . *Plant Physiology*, *157*(2), 742–756. https://doi.org/10.1104/pp.111.182683

Kohnen, M. V, Schmid-Siegert, E., Trevisan, M., Petrolati, L. A., Sénéchal, F., Müller-Moulé, P., … Fankhauser, C. (2016). Neighbor Detection Induces Organ-Specific Transcriptomes, Revealing Patterns Underlying Hypocotyl-Specific Growth. *The Plant Cell*, *28*(12), 2889 LP-2904. https://doi.org/10.1105/tpc.16.00463

Koini, M. A., Alvey, L., Allen, T., Tilley, C. A., Harberd, N. P., Whitelam, G. C., & Franklin, K. A. (2009). High Temperature-Mediated Adaptations in Plant Architecture Require the bHLH Transcription Factor PIF4. *Current Biology*, *19*(5), 408–413. https://doi.org/https://doi.org/10.1016/j.cub.2009.01.046

Křeček, P., Skůpa, P., Libus, J., Naramoto, S., Tejos, R., Friml, J., & Zažímalová, E. (2009). The PIN-FORMED (PIN) protein family of auxin transporters. *Genome Biology*, *10*(12), 249. https://doi.org/10.1186/gb-2009-10-12-249

Le, J., Liu, X.-G., Yang, K.-Z., Chen, X.-L., Zou, J.-J., Wang, H.-Z., … Sack, F. (2014). Auxin transport and activity regulate stomatal patterning and development. *Nature Communications*, *5*(1), 3090. https://doi.org/10.1038/ncomms4090

Leivar, P., & Quail, P. H. (2011). PIFs: pivotal components in a cellular signaling hub. *Trends in Plant Science*, *16*(1), 19–28. https://doi.org/10.1016/j.tplants.2010.08.003

Lewis, D. R., Wu, G., Ljung, K., & Spalding, E. P. (2009). Auxin transport into cotyledons and cotyledon growth depend similarly on the ABCB19 Multidrug Resistance-like transporter. *The Plant Journal*, *60*(1), 91–101. https://doi.org/https://doi.org/10.1111/j.1365-313X.2009.03941.x

Leyser, O. (2018). Auxin Signaling. *Plant Physiology*, *176*(1), 465–479. https://doi.org/10.1104/pp.17.00765

Liscum, E., Askinosie, S. K., Leuchtman, D. L., Morrow, J., Willenburg, K. T., & Coats, D. R. (2014). Phototropism: Growing towards an Understanding of Plant Movement. *The Plant Cell*, *26*(1), 38–55. https://doi.org/10.1105/tpc.113.119727

Ljung, K., Bhalerao, R. P., & Sandberg, G. (2001). Sites and homeostatic control of auxin biosynthesis in Arabidopsis during vegetative growth. *The Plant Journal*, *28*(4), 465–474. https://doi.org/https://doi.org/10.1046/j.1365-313X.2001.01173.x

Lu, H.-P., Wang, J.-J., Wang, M.-J., & Liu, J.-X. (2021). Roles of plant hormones in thermomorphogenesis. *Stress Biology*, *1*(1), 20. https://doi.org/10.1007/s44154-021-00022-1

Ludwig-Müller, J. (2011). Auxin conjugates: their role for plant development and in the evolution of land plants. *Journal of Experimental Botany*, *62*(6), 1757–1773. https://doi.org/10.1093/jxb/erq412

Ma, D., Li, X., Guo, Y., Chu, J., Fang, S., Yan, C., … Liu, H. (2016). Cryptochrome 1 interacts with PIF4 to regulate high temperature-mediated hypocotyl elongation in response to blue light. *Proceedings of the National Academy of Sciences of the United States of America*, *113*(1), 224–229. https://doi.org/10.1073/pnas.1511437113

Ma, L., & Li, G. (2019). Auxin-Dependent Cell Elongation During the Shade Avoidance Response . *Frontiers in Plant Science* . Retrieved from https://www.frontiersin.org/article/10.3389/fpls.2019.00914

Majda, M., & Robert, S. (2018). The Role of Auxin in Cell Wall Expansion. *International Journal of Molecular Sciences*, *19*(4), 951. https://doi.org/10.3390/ijms19040951

McClung, C. R. (2006). Plant circadian rhythms. *The Plant Cell*, *18*(4), 792–803. https://doi.org/10.1105/tpc.106.040980

McClung, C. R. (2019). The Plant Circadian Oscillator. *Biology* . https://doi.org/10.3390/biology8010014

Michaud, O., Fiorucci, A.-S., Xenarios, I., & Fankhauser, C. (2017). Local auxin production underlies a spatially restricted neighbor-detection response in Arabidopsis *Proceedings of the National Academy of Sciences*, *114*(28), 7444 LP-7449. https://doi.org/10.1073/pnas.1702276114

Michniewicz, M., Brewer, P. B., & Friml, J. (2007). Polar Auxin Transport and Asymmetric Auxin Distribution. *The Arabidopsis Book*, *2007*(5). https://doi.org/10.1199/tab.0108

Mittler, R., Kim, Y., Song, L., Coutu, J., Coutu, A., Ciftci-Yilmaz, S., … Zhu, J.-K. (2006). Gain- and Loss-of-Function Mutations in Zat10 Enhance the Tolerance of Plants to Abiotic Stress. *FEBS Letters*, *580*(28–29), 6537–6542. https://doi.org/10.1016/j.febslet.2006.11.002

Müller-Moulé, P., Nozue, K., Pytlak, M. L., Palmer, C. M., Covington, M. F., Wallace, A. D., … Maloof, J. N. (2016). YUCCA auxin biosynthetic genes are required for Arabidopsis shade avoidance. *PeerJ*, *4*, e2574–e2574. https://doi.org/10.7717/peerj.2574

Munguía-Rodríguez, A. G., López-Bucio, J. S., Ruiz-Herrera, L. F., Ortiz-Castro, R., Guevara-García,

Á. A., Marsch-Martínez, N., … Martínez-Trujillo, M. (2020). YUCCA4 overexpression modulates auxin biosynthesis and transport and influences plant growth and development via crosstalk with abscisic acid in Arabidopsis thaliana. *Genetics and Molecular Biology*, *43*(1). https://doi.org/10.1590/1678-4685-gmb-2019-0221

Nguyen, X. C., Kim, S. H., Hussain, S., An, J., Yoo, Y., Han, H. J., … Chung, W. S. (2016). A positive transcription factor in osmotic stress tolerance, ZAT10, is regulated by MAP kinases in Arabidopsis. *Journal of Plant Biology*, *59*(1), 55–61. https://doi.org/10.1007/s12374-016-0442-4

Nguyen, X. C., Kim, S. H., Lee, K., Kim, K. E., Liu, X.-M., Han, H. J., … Chung, W. S. (2012). Identification of a C2H2-type zinc finger transcription factor (ZAT10) from Arabidopsis as a substrate of MAP kinase. *Plant Cell Reports*, *31*(4), 737–745. https://doi.org/10.1007/s00299-011-1192-x

Oh, E., Zhu, J.-Y., Bai, M.-Y., Arenhart, R. A., Sun, Y., & Wang, Z.-Y. (2014). Cell elongation is regulated through a central circuit of interacting transcription factors in the Arabidopsis hypocotyl. *eLife*, *3*, e03031. https://doi.org/10.7554/eLife.03031

Oh, E., Zhu, J.-Y., & Wang, Z.-Y. (2012). Interaction between BZR1 and PIF4 integrates brassinosteroid and environmental responses. *Nature Cell Biology*, *14*(8), 802–809. https://doi.org/10.1038/ncb2545

Ohta, M., Matsui, K., Hiratsu, K., Shinshi, H., & Ohme-Takagi, M. (2001). Repression Domains of Class II ERF Transcriptional Repressors Share an Essential Motif for Active Repression. *The Plant Cell*, *13*(8), 1959. https://doi.org/10.2307/3871331

Park, Y.-J., Kim, J. Y., Lee, J.-H., Han, S.-H., & Park, C.-M. (2021). External and Internal Reshaping of Plant Thermomorphogenesis. *Trends in Plant Science*, *26*(8), 810–821. https://doi.org/https://doi.org/10.1016/j.tplants.2021.01.002

Park, Y.-J., Lee, H.-J., Gil, K.-E., Kim, J. Y., Lee, J.-H., Lee, H., … Park, C.-M. (2019). Developmental Programming of Thermonastic Leaf Movement. *Plant Physiology*, *180*(2), 1185 LP-1197. https://doi.org/10.1104/pp.19.00139

Pham, V. N., Kathare, P. K., & Huq, E. (2018). Phytochromes and Phytochrome Interacting Factors. *Plant Physiology*, *176*(2), 1025–1038. https://doi.org/10.1104/pp.17.01384

Procko, C., Burko, Y., Jaillais, Y., Ljung, K., Long, J. A., & Chory, J. (2016). The epidermis coordinates auxin-induced stem growth in response to shade. *Genes & Development*, *30*(13), 1529–1541. https://doi.org/10.1101/gad.283234.116

Procko, C., Crenshaw, C. M., Ljung, K., Noel, J. P., & Chory, J. (2014). Cotyledon-Generated Auxin Is Required for Shade-Induced Hypocotyl Growth in Brassica rapa. *Plant Physiology*, *165*(3), 1285–1301. https://doi.org/10.1104/pp.114.241844

Rayle, D. L., & Cleland, R. E. (1992). The Acid Growth Theory of auxin-induced cell elongation is alive and well. *Plant Physiology*, *99*(4), 1271–1274. https://doi.org/10.1104/pp.99.4.1271

Ren, H., & Gray, W. M. (2015). SAUR Proteins as Effectors of Hormonal and Environmental Signals in Plant Growth. *Molecular Plant*, *8*(8), 1153–1164. https://doi.org/https://doi.org/10.1016/j.molp.2015.05.003

Rivero, L., Scholl, R., Holomuzki, N., Crist, D., Grotewold, E., & Brkljacic, J. (2014). Chapter 1 Handling Arabidopsis Plants : Growth , Preservation of Seeds , Transformation , and Genetic Crosses, *1062*, 3–25. https://doi.org/10.1007/978-1-62703-580-4

Rockwell, N. C., & Lagarias, J. C. (2006). The structure of phytochrome: a picture is worth a thousand spectra. *The Plant Cell*, *18*(1), 4–14. https://doi.org/10.1105/tpc.105.038513

Rossel, J. B., Wilson, P. B., Hussain, D., Woo, N. S., Gordon, M. J., Mewett, O. P., … Pogson, B. J. (2007). Systemic and Intracellular Responses to Photooxidative Stress in Arabidopsis. *The Plant Cell*, *19*(12), 4091–4110. https://doi.org/10.1105/tpc.106.045898

Sakamoto, H., Araki, T., Meshi, T., & Iwabuchi, M. (2000). Expression of a subset of the Arabidopsis Cys2/His2-type zinc-finger protein gene family under water stress. *Gene*, *248*(1–2), 23–32. https://doi.org/https://doi.org/10.1016/S0378-1119(00)00133-5

Sakamoto, H., Maruyama, K., Sakuma, Y., Meshi, T., Iwabuchi, M., Shinozaki, K., & Yamaguchi-Shinozaki, K. (2004). Arabidopsis Cys2/His2-Type Zinc-Finger Proteins Function as

Transcription Repressors under Drought, Cold, and High-Salinity Stress Conditions. *Plant Physiology*, *136*(1), 2734–2746. https://doi.org/10.1104/pp.104.046599

Sassi, M., Lu, Y., Zhang, Y., Wang, J., Dhonukshe, P., Blilou, I., … Xu, J. (2012). COP1 mediates the coordination of root and shoot growth by light through modulation of PIN1- and PIN2-dependent auxin transport in Arabidopsis. *Development*, *139*(18), 3402–3412. https://doi.org/10.1242/dev.078212

Šimášková, M., O'Brien, J. A., Khan, M., Van Noorden, G., Ötvös, K., Vieten, A., … Benková, E. (2015). Cytokinin response factors regulate PIN-FORMED auxin transporters, *6*, 8717.

Stavang, J. A., Gallego-Bartolomé, J., Gómez, M. D., Yoshida, S., Asami, T., Olsen, J. E., … Blázquez, M. A. (2009). Hormonal regulation of temperature-induced growth in Arabidopsis. *The Plant Journal*, *60*(4), 589–601. https://doi.org/https://doi.org/10.1111/j.1365-313X.2009.03983.x

Stortenbeker, N., & Bemer, M. (2019). The SAUR gene family: the plant's toolbox for adaptation of growth and development. *Journal of Experimental Botany*, *70*(1), 17–27. https://doi.org/10.1093/jxb/ery332

Sun, J., Qi, L., Li, Y., Chu, J., & Li, C. (2012). PIF4-mediated activation of YUCCA8 expression integrates temperature into the auxin pathway in regulating arabidopsis hypocotyl growth. *PLoS Genetics*, *8*(3), e1002594–e1002594. https://doi.org/10.1371/journal.pgen.1002594

Sun, Q., Wang, S., Xu, G., Kang, X., Zhang, M., & Ni, M. (2019). SHB1 and CCA1 interaction desensitizes light responses and enhances thermomorphogenesis. *Nature Communications*, *10*(1), 3110. https://doi.org/10.1038/s41467-019-11071-6

Sun, T., & Gubler, F. (2004). MOLECULAR MECHANISM OF GIBBERELLIN SIGNALING IN PLANTS. *Annual Review of Plant Biology*, *55*(1), 197–223. https://doi.org/10.1146/annurev.arplant.55.031903.141753

Takatsuji, H. (1999). *Zinc-finger proteins: The classical zinc finger emerges in contemporary plant science*. *Plant molecular biology* (Vol. 39). https://doi.org/10.1023/A:1006184519697

Tao, Y., Ferrer, J.-L., Ljung, K., Pojer, F., Hong, F., Long, J. A., … Chory, J. (2008). Rapid synthesis of auxin via a new tryptophan-dependent pathway is required for shade avoidance in plants. *Cell*, *133*(1), 164–176. https://doi.org/10.1016/j.cell.2008.01.049

Teale, W. D., Paponov, I. A., & Palme, K. (2006). Auxin in action: signalling, transport and the control of plant growth and development. *Nature Reviews Molecular Cell Biology*, *7*(11), 847–859. https://doi.org/10.1038/nrm2020

van Zanten, M., Pons, T. L., Janssen, J. A. M., Voesenek, L. A. C. J., & Peeters, A. J. M. (2010). On the Relevance and Control of Leaf Angle. *Critical Reviews in Plant Sciences*, *29*(5), 300–316. https://doi.org/10.1080/07352689.2010.502086

Vu, L. D., Xu, X., Zhu, T., Pan, L., van Zanten, M., de Jong, D., … De Smet, I. (2021). The membrane-localized protein kinase MAP4K4/TOT3 regulates thermomorphogenesis. *Nature Communications*, *12*(1), 2842. https://doi.org/10.1038/s41467-021-23112-0

Wang, R., Zhang, Y., Kieffer, M., Yu, H., Kepinski, S., & Estelle, M. (2016). HSP90 regulates temperature-dependent seedling growth in Arabidopsis by stabilizing the auxin co-receptor F-box protein TIR1. *Nature Communications*, *7*(1), 10269. https://doi.org/10.1038/ncomms10269

Xie, M., Sun, J., Gong, D., & Kong, Y. (2019). The Roles of Arabidopsis C1-2i Subclass of C2H2-type Zinc-Finger Transcription Factors. *Genes*, *10*(9), 653. https://doi.org/10.3390/genes10090653

Xu, H., Chen, P., & Tao, Y. (2021). Understanding the Shade Tolerance Responses Through Hints From Phytochrome A-Mediated Negative Feedback Regulation in Shade Avoiding Plants . *Frontiers in Plant Science* . Retrieved from https://www.frontiersin.org/article/10.3389/fpls.2021.813092

Yang, C., & Li, L. (2017). Hormonal Regulation in Shade Avoidance . *Frontiers in Plant Science* . Retrieved from https://www.frontiersin.org/article/10.3389/fpls.2017.01527

Yuta, F., Hiroyuki, T., Naotake, K., Yuka, O., Noriko, H., Saori, T., … Yutaka, K. (2017). Phototropin

perceives temperature based on the lifetime of its photoactivated state. *Proceedings of the National Academy of Sciences*, *114*(34), 9206–9211. https://doi.org/10.1073/pnas.1704462114

Žádníková, P., Petrášek, J., Marhavý, P., Raz, V., Vandenbussche, F., Ding, Z., … Benková, E. (2010). Role of PIN-mediated auxin efflux in apical hook development of Arabidopsis thaliana. *Development*, *137*(4), 607–617. https://doi.org/10.1242/dev.041277

Zhang, L.-L., Luo, A., Davis, S. J., & Liu, J.-X. (2021). Timing to grow: roles of clock in thermomorphogenesis. *Trends in Plant Science*, *26*(12), 1248–1257. https://doi.org/https://doi.org/10.1016/j.tplants.2021.07.020

Zhao, J., Lu, Z., Wang, L., & Jin, B. (2020). Plant Responses to Heat Stress: Physiology, Transcription, Noncoding RNAs, and Epigenetics. *International Journal of Molecular Sciences*, *22*(1), 117. https://doi.org/10.3390/ijms22010117

Zheng, Z., Guo, Y., Novák, O., Chen, W., Ljung, K., Noel, J. P., & Chory, J. (2016). Local auxin metabolism regulates environment-induced hypocotyl elongation. *Nature Plants*, *2*(4), 16025. https://doi.org/10.1038/nplants.2016.25

Zhou, M. Q., Shen, C., Wu, L. H., Tang, K. X., & Lin, J. (2011). CBF-dependent signaling pathway: A key responder to low temperature stress in plants. *Critical Reviews in Biotechnology*, *31*(2), 186–192. https://doi.org/10.3109/07388551.2010.505910

Zhu, J.-Y., Oh, E., Wang, T., & Wang, Z.-Y. (2016). TOC1–PIF4 interaction mediates the circadian gating of thermoresponsive growth in Arabidopsis. *Nature Communications*, *7*(1), 13692. https://doi.org/10.1038/ncomms13692